THE UNIVERSITY OF CHICAGO

# THE ROLES OF EVOLUTIONARY HISTORY AND ECOLOGICAL INTERACTIONS IN THE MAINTENANCE OF A HIGH-DIVERSITY MACROALGAL ASSEMBLAGE

A DISSERTATION SUBMITTED TO
THE FACULTY OF THE DIVISION OF THE BIOLOGICAL SCIENCES
AND THE PRITZKER SCHOOL OF MEDICINE
IN CANDIDACY FOR THE DEGREE OF
DOCTOR OF PHILOSOPHY

COMMITTEE ON EVOLUTIONARY BIOLOGY

BY

COURTNEY CRUISE STEPIEN

CHICAGO, ILLINOIS

JUNE 2016

## DEDICATION

For my husband, who decided that my particular flavor of crazy was acceptable, came with me to Chicago and embraced it all. Thank you.

## TABLE OF CONTENTS

## LIST OF TABLES

## LIST OF FIGURES

## LIST OF PLATES

## ACKNOWLEDGEMENTS

I'd like to thank my advisor Cathy Pfister, who had higher expectations of me than I did myself, and who helped me see I was capable of meeting them. Thanks also to Tim Wootton, who always entertained my research questions. Cathy and Tim have been generous with their time and their advice, and I am grateful for their mentorship. Thanks to committee members Trevor Price and Rick Ree, who happily dove into the world of seawater chemistry when my interests took me there. Trevor has provided unwavering support during my time here, and his passion for research comes through in all topics. Rick has always given balanced advice and guidance as my evolutionary interests expanded.

Out in Washington, thanks to the Makah Tribal Nation for providing access to Tatoosh Island and Shi Shi Beach. Thanks to my Aunt Susan, who took me to Shi Shi six years before I would return there as a grad student doing a pilot project. Thanks also to Dave and Martha Hurd for providing their rental house and garage in Sekiu, WA for Sara Jackrel and I to conduct experiments in. Thanks also to Bob Paine and his daughter Anne Paine for spending time with me on Tatoosh.

My cohort has been a wonderful source of support and inspiration. I am fortunate to have been in the Pfister-Wootton lab and have had the pleasure of a diverse, supportive lab group. My lab mates – Sophie McCoy, Orissa Moulton, Sara Jackrel, Amy Henry, Will Tyburczy, Aaron Kandur, Katherine Silliman, Liz Sander, Nicole Bitler, and Simon Lax, Sebastian Heilpern, Kristen Voorhies, Dylan Maddox, Matt Helmus, Gregor-Fausto Siegmund, Sam Betcher, Lyda Harris and Peter Zaykoski have been integral in their support both in the lab and in the field.

Special thanks to our newest lab members Mark Bitter and John Park, for reinvigorating this end-stage grad student with their optimism and making her smile.

I am grateful to Gerry Olack for technical expertise with isotope analyses, Special thanks also to the two Amys, Amy Zanne and Amy Austin, who invited me to contribute to a special issue that has opened a whole new line of research for me.

Many people in the Ecology & Evolution Department, the Committee on Evolutionary Biology and the Division of Biological Sciences provided support that made the day-to-day work possible: Josh Berg, Dave Tooley, Bonnie Brown, Connie Homan, Libby Eakin, Carolyn Johnson, Noami Perez, Julie Steffen, Melissa Lindberg, Jeff Wisniewski, Mary Johnson, Sandra Akbar and Alexa Bontrager. And thanks to Dave Steele, for delivering the package that allowed me to get the work done and always making sure we had Girl Scout cookies.

I'm thankful to members of my Academic Writing Club research support group: nicolita, SarahJW, Diane Folan, SP, Beth S, westendpond and Pam K. We've cheered each other on for nearly a year now, and it's been a great source of support, happiness and motivation.

Thanks to my counselor, Dr. Charles (Chuck) Berry.

Andrea Sequeira, Emily Buchholtz and Martina Koniger mentored me as an undergrad at Wellesley College, took me along on their research adventures and later became close friends. Thanks to them for inviting me back to give a seminar at Wellesley, a wonderful experience and

a pleasure to be on the other side of my old lecture hall.

My mother, with a PhD in Oceanography, and my father, with a MS in Fisheries Management, have shown me through their own lives that the degree is just the beginning. Their unwavering support of family and friends is an example that I try to live by every day, though I am not always successful.

# CHAPTER I

# INTRODUCTION

Communities comprise a non-random sample of regional species pools, whether in phenotypic or phylogenetic terms (Weiher and Keddy 1995, Kraft et al. 2007). With increasing acknowledgment that community diversity influences ecosystem function and stability (Harmon et al. 2009, Hector 2011, Cadotte et al. 2012), a major focus of community ecology has been to determine the relative contributions of environmental and organismal variables to species interactions and community assembly. As ecological communities are increasingly subjected to the effects of climate change and intensifying environmental disturbance, researchers have focused on the question of how to use these variables to predict community responses to environmental change (Agrawal et al. 2007, Wood et al. 2010). Two competing mechanisms - environmental filtering and competition – may determine community structure; both are evident in the phylogenetic signature of communities. Environmental filtering, where the physiological demands of a habitat limit colonization and establishment of species to a subset of adapted lineages, yields a phylogenetically clustered pattern (Weiher and Keddy 1995, Webb et al. 2002). In contrast, since related species are likely to need similar resources, competitive exclusion may prevent close relatives from co-occurring, resulting in a pattern where community members are phylogenetically overdispersed.

While phylogenetic community structure is a powerful tool to evaluate the generation and maintenance of diversity, ecological mechanisms of community assembly cannot be inferred

from patterns of phylogenetic structure alone; one also needs to know whether phenotypes are clustered or overdispersed (Cavender-Bares et al. 2006, Losos 2008). Many studies have successfully integrated phylogenetic and phenotypic community metrics into evaluations of competition and environmental filtering (Cavender-Bares et al. 2004, Kembel and Hubbell 2006, Graham et al. 2009, Kraft and Ackerly 2011). However, few studies take into account additional dynamic ecological processes such as herbivory, disturbance or colonization, or fine-scale environmental patterns such as temperature gradients or habitat heterogeneity (Verdú and Pausas 2007, Helmus et al. 2010, Cadotte and Strauss 2011). Disturbance is widely acknowledged to contribute to species diversity (Connell 1978, Huston 1979, Sousa 1979), but is less rarely evaluated as a driver of phylogenetic community structure.

Where it has been evaluated, pulse habitat-clearing disturbances have been demonstrated to be a driver of phylogenetic clustering, as in woody plant communities (Cavender-Bares and Reich 2012, Norden et al. 2012) and in zooplankton communities (Helmus et al. 2010). Herbivory is an additional form of biotic disturbance that strongly structures communities.

In this thesis, I expand studies of drivers of community structure to a species-rich system that experiences strong local abiotic and biotic disturbance gradients: the sessile marine macroalgal community of the temperate marine rocky intertidal zone. In this system I measure both physical environmental variables and functional traits of species to determine the relative importance of environmental filtering traits on community structure. Three natural treatments are apparent: 1) a distinct temperature, wave and light stress gradient; 2) major habitat-generating

disturbances; and 3) grazer disturbance. I manipulated herbivory intensity and physical disturbance regimes to determine how these additional processes influence community structure along an environmental gradient. I focus on a key trait in this system: resource acquisition in the form of inorganic carbon acquisition by macrophytes for photosynthesis.

## DISSERTATION OVERVIEW

In this dissertation, I use laboratory studies, field experiments and phylogenetics to understand the assembly and maintenance of high-diversity macroalgal assemblages from local to global scales. In *Chapter II: Functional traits for carbon access*, I perform laboratory studies and phylogenetic analyses to investigate species' abilities to access dissolved carbon and the evolutionary history of this trait. I used pH* drift assays to identify Northeast Pacific intertidal algal species that can access not only dissolved $CO_2$, but can also additionally concentrate and use $HCO_3^-$. I then assessed a subset of species for their ability to change the Total Alkalinity (TA) of seawater. Thirty-two of 40 macrophyte species deplete $HCO_3^-$, indicating they have a CCM. Fifteen of 23 species tested also changed seawater TA, shifting local carbon concentrations towards increasing $CO_2$ and $HCO_3^-$ an advantage. My phylogenetic analyses of published pH* data in the Rhodophyta and Phaeophyta show that CCM presence is more phylogenetically divergent than expected at the macroalgal Family level, and is largely conserved within Families.

While pH drift assays represent a snap-shot assessment of CCMs in macrophytes, tissue C isotope ratios ($\delta^{13}C$) provide a more time-integrated assessment of CCM presence due to differing isotopic signals of $CO_2$ and $HCO_3^-$. In *Chapter III: Impacts of geography, taxonomy*

*and functional group on inorganic carbon use patterns in marine macrophytes*, I compare these two methods of investigating CCM presence in macrophytes and perform a meta-analysis of local to global-scale trends in carbon acquisition. I show that species pH* and $\delta^{13}C$ measurements are not independent of each other, and that globally, seaweed tissue $\delta^{13}C$ decreases with increasing distance from the equator and also differs between intertidal and subtidal habitats. Macrophytes rely more on $CO_2$ further from the equator, but have increased use of $HCO_3^-$ at sites with high temperature variance. These patterns appear to be driven by species turnover rather than intraspecific variation.

To understand the factors that drive local macroalgal assemblage structure, I used a combination of field experiments and phylogenetic techniques. In *Chapter IV: Phylogenetic, richness and abundance responses to disturbance*, I observe intertidal macroalgal assemblages across four years under differential abiotic and biotic disturbance regimes. By establishing plots that have been cleared to mimic pulse disturbances and either including herbivores or excluding them from the plot, I investigate the effects of each of these processes. Having created a phylogeny of all Rhodophyta observed in experimental plots, I show that while the mid intertidal zone has intermediate species richness, it has the highest phylogenetic diversity. Contrary to expectations, macroalgal assemblages are not increasing phylogenetically clustered with increasing environmental stress. Reducing grazers in disturbance plots in the mid zones reduce phylogenetic diversity.

This dissertation provides data supporting an integrated understanding of how assemblages are

structured by pulse abiotic and press biotic disturbances, and how environmental gradients and resource acquisition moderate this response. While I have focused on marine macrophyte assemblages, results here are applicable to marine invertebrates and terrestrial plants.

# CHAPTER II

# FUNCTIONAL TRAITS FOR CARBON ACCESS IN MACROPHYTES


## ABSTRACT

Understanding functional trait distributions among organisms can inform impacts on and responses to environmental change. In marine systems, only 1% of dissolved inorganic carbon in seawater exists as $CO_2$. Thus the majority of marine macrophytes not only passively access $CO_2$ for photosynthesis, but also actively transport $CO_2$ and the more common bicarbonate ($HCO_3^-$, 92% of seawater dissolved inorganic carbon) into their cells. Because species with these carbon concentrating mechanisms (CCMs) are non-randomly distributed in ecosystems, we ask whether there is a phylogenetic pattern to the distribution of CCMs among algal species. To determine macrophyte traits that influence carbon uptake, we assessed 40 common macrophyte species from the rocky intertidal community of the Northeast Pacific Ocean to a) query whether macrophytes have a CCM and b) determine the evolutionary history of CCMs, using ancestral state reconstructions and stochastic character mapping based on previously published data. Thirty-two species not only depleted $CO_2$, but also concentrated and depleted $HCO_3^-$, indicative of a CCM. While analysis of CCMs as a continuous trait in 30 families within Phylum Rhodophyta and 18 Ochrophyta families showed a significant phylogenetic signal under a Brownian motion model, analysis of CCMs as a discrete trait indicated that families are more divergent than expected in their CCM presence or absence. The trait of CCM presence or absence was largely conserved within Families, but more phylogenetically divergent than expected among macrophyte Families. Fifteen of 23 species tested also changed the seawater

buffering capacity, or Total Alkalinity (TA), shifting DIC composition towards increasing concentrations of $HCO_3^-$ and $CO_2$ for photosynthesis. Manipulating the external TA of the local environment may influence carbon availability in boundary layers and areas of low water mixing, offering an additional mechanism to increase $CO_2$ availability.

## INTRODUCTION

Traits determine both the environmental impacts on, and environmental effects of, organisms, processes which ultimately shape evolution through natural selection. Hence, understanding trait distributions among species can help to anticipate ecological effects of environmental change. Most studies focus on morphological traits, or other traits that are readily measured in museum collections or laboratories. Though often more difficult to measure than morphological traits, functional traits offer direct insight into ecologically important differences among species that may control both evolutionary history and the scope for future adaptation.

Changes in the global carbon cycle arising from anthropogenic $CO_2$ release to the atmosphere may both affect, and be affected by, many species within ecosystems (Wootton et al. 2008, Kroeker et al. 2010, McCoy and Pfister 2014). Unlike terrestrial situations, where plants interact with inorganic carbon solely as $CO_2$, which has a high diffusion rate in air, aquatic plants exist in a medium with low $CO_2$ diffusion and in which dissolved inorganic carbon (DIC) occurs in several forms. In some marine environments, photosynthesis can be carbon-limited owing to low diffusion of $CO_2$ in water, local depletion of dissolved inorganic carbon (DIC), and pH-dependent shifts in the concentrations of DIC forms in seawater. As phototrophs deplete DIC, the relative equilibrium concentrations of DIC remaining (bicarbonate: $HCO_3^-$, carbon dioxide: $CO_2$,

and carbonate: $CO_3^{2-}$) change and drive seawater to higher pH. Alternately, as dissolved inorganic carbon increases in seawater, $CO_2$ and $HCO_3^-$ increase in concentration, while $CO_3^{2-}$ declines and pH drops (Figure 2.A.1). Thus, pH provides a proxy for DIC proportions. At ambient seawater pH of roughly 8.0, $HCO_3^-$ comprises 92% of DIC in the surface ocean, with $CO_2$ concentration at 1%. At pH > 9.0, however, $CO_2$ concentration approaches zero. In addition to relying on passive diffusion of $CO_2$, the majority of marine macroalgal species can utilize a carbon concentrating mechanism (CCM). Plants with CCMs can actively transport $HCO_3^-$ or $CO_2$ into plant cells, thereby increasing photosynthetic rates under high competition for DIC (Giordano et al. 2005). CCMs are hypothesized to have evolved in response to historically carbon-limited environments (Meyer and Griffiths 2013) and occur over taxonomically and spatially diverse species (Raven 1997, Hepburn et al. 2011) with differing underlying physiological mechanisms (Reinfelder 2011).

Marine and terrestrial phototrophs alike employ CCMs to increase inorganic carbon availability (for example, C4 and CAM plants in terrestrial ecosystems), but they do so under different conditions. In coastal marine systems, variation in upwelling, temperature, pH, salinity variation, and terrestrial inputs can all influence local seawater DIC availability and relative proportions of dissolved $CO_2$, $HCO_3^-$ and $CO_3^{2-}$ (Maberly et al. 1992), while intertidal macroalgae experience the added complexity of daily exposure to atmospheric $CO_2$. Because $CO_2$ diffuses more slowly in water, DIC availability in boundary layers surrounding macrophytes may become locally depleted as organisms take up $CO_2$ (Hurd 2000, Cornwall et al. 2013), increasing pH during hours of peak photosynthesis (Wootton et al. 2008). Taken together, environmental variation and biotic interactions create variable $CO_2$ concentrations in coastal

marine systems.

Marine macrophytes with CCMs are distributed non-randomly along global and local environmental gradients. Species sampled in warmer climates have tissue $\delta^{13}C$ values more indicative of bicarbonate use than those in cooler environments, implying potential carbon-limiting environments in the tropics (Marconi et al. 2011). There also appears to be a latitudinal trend in CCM prevalence based on $\delta^{13}C$ trends, where a greater proportion of species near the poles have isotope signatures indicative of CCM absence (Stepien 2015). Vertical depth trends have also been observed along the coastal emersion gradient from the intertidal to the subtidal, with decreasing CCM frequency at lower depths (Cornwall et al. 2015, Stepien 2015) potentially caused by light limitation (Raven et al. 2002b). Macroalgae that depend on passive diffusion of $CO_2$ may directly benefit from elevated $CO_2$ arising from anthropogenic activities (Kübler et al. 1999), whereas those that use $HCO_3^-$ or create conditions that favor increased $CO_2$ diffusion may be at a disadvantage because these mechanisms can carry energetic costs (Raven 1997). In phytoplankton for example, elevated $CO_2$ conditions may shift dominance among species due to differential abilities of species to concentrate DIC for photosynthesis (Low-Décarie et al. 2014). Here we evaluate the functional trait of carbon access, as well as how this macrophyte trait may result in a positive effect on further carbon acquisition.

In addition to affecting seawater pH through changes in DIC arising from photosynthesis and respiration, there is evidence that organisms alter the expected pH-DIC relationship by changing the buffering capacity of seawater (Axelsson and Uusitalo 1988), which may further feed back to local DIC availability. Total alkalinity (TA) reflects the acid buffering capacity of water and comprises all compounds that minimize seawater pH change. While DIC makes up the

majority of ambient seawater total alkalinity, other compounds such as borates and organic compounds comprise the rest (Morel et al. 1993). Under the expected relationship between DIC and pH – in which TA is held constant – pH increases as DIC decreases. Whereas photosynthesis and respiration do not change TA (Morel et al. 1993), a net uptake of negative ions by algae, such as $OH^-$ (Lobban and Harrison 1994), or a release of positively charged compounds that bind to proton acceptors may result in drops in TA. As TA decreases, more $H^+$ remains in solution causing pH decline, and the proportions of photosynthetically useful $HCO_3^-$ and $CO_2$ increase. Spatio-temporal variation in TA occurs in reefs from coral calcification (Anthony et al. 2011, Andersson et al. 2014). Nutrient exchange by phytoplankton, microbes and microalgae can also affect TA (Brewer and Goldman 1976, Fabregas et al. 1987, Morel et al. 1993). By influencing seawater pH without directly acting on DIC, TA shifts present a distinct pathway from active carbon transport or proton pumps for modifying DIC availability.

Here we use pH drift assays to assess the status and variability of marine macrophyte CCMs from the Northeast Pacific. These assays measure DIC depletion in sealed containers under continuous photosynthesis. We supplement pH assays with TA measurements and show that macrophytes vary in $HCO_3^-$ use, with some species unexpectedly altering TA to a degree not fully accounted for by $HCO_3^-$ uptake or calcification. Macrophytes may lower total alkalinity through means other than DIC depletion or calcification, increasing access to DIC for photosynthesis in the process, and potentially influencing species' local access to DIC. We then use phylogenetic analyses of CCMs to ask how CCM presence has evolved in the red and brown algal lineages.

## MATERIALS AND METHODS

### pH and total alkalinity assays

We assayed how 39 species of marine macroalgae (Rhodophyta: Florideophyceae and Bangiaceae, Chlorophyta: Ulvophyceae and Ochrophyta: Phaeophyceae) and one surfgrass species (Tracheophyta: Monocots) alter seawater pH through DIC depletion using a pH drift assay (modified from (Maberly 1990, Murru and Sandgren 2004, Hepburn et al. 2011)). Assays included five coralline red algal species (three upright and two crustose species), which may affect water chemistry through calcification. Species represented conspicuous taxa from the near-subtidal to high intertidal on emergent rocky benches at Shi Shi Beach, Olympic National Park, Washington, USA (48.28°N, 124.68°W) and Slip Point, Clallam Bay, Washington, USA (48.26°N, 124.25°W), collected from 21 June – 13 July 2013. Local vertical range (low, mid or high intertidal zone) was noted; when species spanned multiple zones, specimens were collected across their full vertical range to determine within-species variance. Based on specimen availability, 2-13 replicates per species were assayed. Specimens were rinsed, cleaned of visible epiphytes and stored at 7ºC for 12-48 hours, then rinsed twice in sterilized seawater, patted dry and separated into 4 g amounts (wet mass). Due to differing individual mass among and within species, some replicates contained multiple individuals, some contained a single individual, and some contained a partial individual. Where cut individuals were used, we always used a mix of whole individuals and partial individual replicates to ensure that exudates from cut individuals did not overwhelm the signal of whole individuals, which the exception of one larger kelp species (*Alaria marginata*) for which small specimens were unavailable. A ratio of 4 g macrophyte to 125 mL seawater (0.032 g/mL) in our assay fell within the range of biomass-to-

seawater-volume ratios previously reported in pH assay studies (0.007 – 0.143 g/mL) (Axelsson and Uusitalo 1988, Hepburn et al. 2011, Cornwall et al. 2012), while allowing us to use entire individuals and minimize self-shading. Although calcifying species differ in their photosynthetic biomass to total biomass ratios due to their calcium carbonate skeletons (75-80% inorganic content, versus 10-50% for fleshy species (Paine 1966)), we applied the same 4 g mass treatment to investigate if calcifying species raise pH* > 9.0 and how they might influence seawater TA.

We collected seawater 150 m off Sekiu, Washington, USA (48.26°N, -124.30°W), and measured seawater salinity, temperature and pH. To minimize the influence of microbes on pH, we filtered seawater through a polypropylene filter net (Aquatic Ecosystems) and a Whatman GF/C filter (1.2 µm pore size), and then UV treated water (TMC V2 8 Watt) for 24 hours at a 450 lph flow rate. Water was allowed to equilibrate to outdoor atmospheric conditions and used within 48 hours of sterilization. Because fresh seawater was collected and processed for each assay, we tested whether 5 of the 11 seawater batches differed in nutrient profiles. Phosphate, silica, nitrate, nitrite and ammonium concentrations were quantified at the University of Washington Marine Chemistry Lab following filtration and UV treatment. One seawater batch was also assayed for initial TA.

Macrophytes were placed with sterilized seawater in 125 mL sealed clear polystyrene containers and incubated under full-spectrum light alongside seawater controls in a 12ºC water bath, a temperature reflecting mean June-July sea surface temperature near collection sites (Wootton et al. 2008). Macrophytes were exposed to 286 ± 5 µmol/$m^2$s photosynthetically active radiation under full-spectrum Marine White Lights (TMC Aquaray Aquabeam 1000 HD Ultra) for 24 hours, an incubation length comparable to other pH assay studies, which ensured ample

time for macrophytes to reach a steady-state pH* (Hepburn et al. 2011, Cornwall et al. 2012). Jars were placed on an 18 rpm shaker rack to disrupt boundary layer formation. Five species, typically in six replicate containers, were run with six seawater controls without macroalgae in each trial. Specimens and controls were randomized in water bath position and consequently also randomized in measurement order for pH and TA, minimizing potential effects of machine drift. Species replicates were also run across multiple trials using different seawater batches to determine if different seawater stocks significantly influenced the assay.

We recorded seawater pH of each jar at 0, 12 and 24 hours using an IntelliCAL pH probe (PCH101) and HACH meter (HQ40d) calibrated with NBS pH 7.0 and 10.0 standards before each incubation (Thermo-Fisher Scientific). As species deplete dissolved $CO_2$, DIC decreases, which causes an increase in pH. At pH = 9.0, $CO_2$ concentration is too low (< 1 μmol/kg seawater) to be biologically accessible for the majority of macroalgae and DIC depletion stops. However, if species have a CCM and can access $HCO_3^-$, DIC is further depleted and pH increases beyond 9.0 (Maberly 1990). The upper boundary of pH drift – pH* – reflects the minimum DIC concentration that a species can access (sensu (Tilman 1981)). Whether a result of DIC-independent physiological limitations due to too-high pH (Middelboe and Hansen 2007) or of DIC-dependent limitations due to too-low DIC, pH* represents a concentration beyond which a species cannot further deplete DIC (Cornwall et al. 2012). In preliminary 32-hour assays, 11 of 12 species reached pH* within 12-24 hours, indicating that 24 hours was a sufficient incubation length. While *Neorhodomela larix* pH* did not stabilize within 32 hours of incubation, seawater pH reached 9.63 by 24 hours, so the CCM categorization of *N. larix* was unaffected. The rank order of pH of seawater incubated with different macrophyte species after 12 hours mirrored

their order after 24 hours, indicating that any incubation effects accumulating in the last 12 hours did not alter the relative effects of species on seawater.

To determine if macrophytes had a lasting effect on seawater pH beyond depleting DIC, we unsealed containers post-incubation, removed macrophytes and waited a further 24 hours for 40 mL of seawater to re-equilibrate with outdoor atmospheric $CO_2$ in the 12ºC water bath. pH was then remeasured as the pH of equilibration with the atmosphere ($pH_e$). To make $pH_e$ values comparable across assays from different seawater batches and to control for variations in ambient atmospheric $pCO_2$ through time, $pH_e$ was reported as the relative change from seawater controls: macrophyte-incubated seawater $pH_e$ minus control seawater $pH_e$, post-equilibration. If changes in seawater pH during incubation were due exclusively to decreases in $CO_2$ and $HCO_3^-$ concentrations via macrophyte photosynthesis, then $pH_e$ of macrophyte-incubated seawater should equal $pH_e$ of control seawater after atmospheric re-equilibration, and $pH_e$ shift would be 0. Alternatively, a difference in $pH_e$ between macrophyte-incubated seawater and controls indicates macrophytes affected seawater chemistry other than through simple DIC depletion.

To test whether total alkalinity changed with macrophyte presence, TA was measured immediately after the 24-hour pH assay on 15 ml using an Alkalinity Titrator (Apollo SciTech Model AS-Alk2 SeaWATER gran titration) sample with 0.1 N HCl at 25ºC calibrated with a TA standard (Batch 128, Andrew Dickson CO2QC Laboratory, Scripps Institute Oceanography). Specimens were randomized in water bath position and consequently also randomized in measurement order for TA, minimizing potential effects of machine drift. TA was measured as the concentration of titratable weak bases present relative to a reference pH at which DIC is 100% $CO_2$. These measures had a measurement uncertainty (s.d.) of $\pm$ 45 μmol/kg (1.9%) based

on multiple assays of the standard. To make total alkalinity values comparable across assays from different seawater batches, TA was reported as change from seawater controls: macrophyte-incubated seawater TA minus control seawater TA, post incubation. If a TA shift is 0 μmol/kg, macrophytes did not change seawater at all during the incubation. Negative changes to TA indicate macrophyte-associated TA declines, while increased TA was indicated by positive values. To test whether pH*, $pH_e$ or TA shifts were significantly different from seawater controls, we applied a two-tailed t-test by species.

**Evolution of CCMs using discrete CCM status and continuous pH***

We asked whether CCMs evolved differentially among families within the red and brown algae (Rhodophyta and Ochrophyta), by mapping pH* results and the incidence of CCMs to family-level phylogenies. We did not investigate evolutionary patterns in the Chlorophyta because of the limited number of green algae species prevalent in our flora. An ultrametric Bayesian phylogeny for Rhodophyta was adapted from the literature (Verbruggen et al. 2010) with a best-fit $\lambda = 10$. An ultrametric maximum likelihood phylogeny for Ochrophyta was digitized (Laubach et al. 2012) and adapted from (Silberfeld et al. 2010) with $\lambda = 1000$. Experimental pH* data were compiled from a review of 25 pH* studies, including this one ((Stepien 2015), Tables 2.C.1 and 2.C.2).

pH* was mapped as a continuous trait onto family-level trees using family averages. One hundred eleven Rhodophyta species were categorized into 30 families and subfamilies according to taxonomy in AlgaeBase (Guiry and Guiry 2012) and 51 Ochrophyta species were similarly categorized into 18 families. We also examined CCMs as a discrete trait, by scoring CCM

presence for species with mean pH* > 9.05 to account for potential artifacts in the assay (Stepien 2015). CCM presence was assigned to a family if at least one family member had a CCM. Evidence for CCMs from short-term pH* assay data largely correlate with time-integrated measurements of bicarbonate use and CCM presence using macrophyte tissue carbon stable isotopes (Stepien 2015).

We performed ancestral state reconstruction and stochastic character mapping (Huelsenbeck et al. 2003) on CCM presence/absence using the R packages “ape” (Paradis et al. 2014) and “phytools” (Revell 2012) and an equal rates model for each Phylum as in (Litsios et al. 2012). Stochastic character mapping was performed 1000 times to obtain the average number of transitions between CCM presence and absence (Lapiedra et al. 2013).

To test whether CCMs exhibited more or less divergence than expected if they were evolving under a null Brownian motion model of evolution, we calculated Blomberg's K for the continuous pH* trait (Blomberg et al. 2003) and Pagel's $\lambda$ for the discrete CCM status trait (Pagel 1999) within Rhodophyta and Ochrophyta. In a Brownian motion evolutionary model, the observed difference in traits between a pair of taxa is directly proportional to the estimated branch length since their lineages diverged. K ranges from 0 to infinity, where $K = 0$ indicates trait evolution is completely independent of phylogeny, $K = 1$ indicates Brownian motion evolution, $K > 1$ indicates that close relatives are more similar than expected, and $K < 1$ (the majority of values reported) indicates that close relatives are more divergent than expected (Blomberg et al. 2003). We tested whether K was different from 1, indicating a departure from a Brownian motion model, by comparing our observed K values to a null distribution of $K = 1$ generated from our phylogenies using the R package “phytools”. For the discrete trait of CCM

presence or absence by family, we calculated Pagel's λ using "phytools". Pagel's λ varies from 0, where each phylogeny branch tip is independently derived (trait relationships are best represented by an unresolved 'star' phylogeny), to 1, where the internal, non-tip phylogenetic branches explain some of the shared ancestry of the traits and there is significant phylogenetic structure. To test for significance of λ, we used a likelihood ratio test to compare the calculated λ to $\lambda = 1$.

We tested for an effect of macroalgal Phylum membership (Chlorophyta, Rhodophyta, Phaeophyta) on seawater pH* and TA with an ANOVA, followed by a Kruskal-Wallis test if residuals were not normally distributed. To test whether families with CCMs had more species than families lacking CCMs, we obtained family richness data from AlgaeBase and applied a one-tailed t-test.

**Species-specific effects on the dissolved inorganic carbon (DIC) system**

pH*, temperature, salinity and TA data were used to calculate DIC at 12ºC as the sum of $HCO_3^-$, $CO_3^{2-}$ and $CO_2$, as well as calcium and aragonite saturation states in final control and macrophyte-incubated seawater. We used the CO2sys_v2.1 Excel macro (Pierrot and Wallace 2006) under default constants (Dickson and Millero 1987), with pH scale set to NBS. We regressed pH* on TA to test whether they were related. To determine whether TA or pH* influenced the pH of equilibration with atmosphere ($pH_e$), $pH_e$ was regressed against TA and pH* in a multiple regression.

To compare how changes in TA and pH alter $CO_2$, $HCO_3^-$ and $CO_3^{2-}$ availability, we compared observed proportions of these three DIC forms to expected proportions if TA remained

Plate 2.1. Range expansion of an urban husband on a research cruise in the Strait of Juan de Fuca.

constant. Using macrophyte-incubated seawater pH* and control seawater TA, we calculated the expected concentration of each DIC form over a range of pH* values. We then compared these expected values to the concentrations of $CO_2$, $HCO_3^-$ and $CO_3^{2-}$ observed at the pH* and corresponding TA of macrophyte-incubated seawater (Figure 2.A.1).

## RESULTS

### Assay repeatability and seawater variation in within-species trials

Seawater nutrient concentrations varied among batches (Table 2.B.1), however this did not strongly affect assay results of CCM presence or absence. Of 10 species assayed with multiple seawater batches, three had different pH* between batches (two-tailed t test, *C. pikeanum* $t_5 = 6.5$, $p = 0.001$; *C. ruprechtiana* $t_8 = 5.9$, $p < 0.001$; *A. coalita* $t_8 = 4.6$, $p = 0.002$). Although pH* differed among trials in these three species, all trials consistently indicated pH* > 9.0 (*A. coalita*) or < 9.0 (*C. pikeanum, C. ruprechtiana*) within species. Some of the highest pH* values observed *(Ulva intestinalis*, 10.16 ± 0.06 standard error[s.e.]; *Urospora sp.*, 10.23 ± 0.02 s.e.) were from assays in comparatively low-nutrient seawater (Table 2.B.1), suggesting that seawater nutrients were not limiting to DIC depletion. Therefore, replicates from different seawater batches were pooled for species-level analyses.

### Carbon concentrating mechanisms and pH*

pH* levels ranged from 8.48-10.39 (Table 2.A.1). Thirty-two of 39 species increased seawater pH* > 9.0, indicating these species use $HCO_3^-$ and have active CCMs (Figure 2.1), consistent with other studies (Maberly 1990, Murru and Sandgren 2004, Giordano et al. 2005, Hepburn et

al. 2011). The angiosperm species *Phyllospadix scouleri* also had pH* indicative of a CCM. Species with CCMs showed differential efficiency in depleting dissolved inorganic carbon, based on a range of pH* from 9.08-10.39. All Phyla assayed (Chlorophyta, Rhodophyta and Phaeophyta) contained both species with and without active CCMs. pH* differed among Phyla ($F_{2, 36} = 3.8$, $p = 0.032$), with Chlorophyta driving pH* higher than Rhodophyta (Tukey HSD, $p = 0.026$). While seawater incubated with crustose calcifying species had pH* < 9.0, upright calcifying species increased seawater pH* > 9.0, indicating $HCO_3^-$ usage. Within-species pH* standard error ranged from 0.00-0.11 pH units (Figure 2.1, Table 2.A.1), indicating that independent replicates of the same species produced consistent results and that the minority of partial individuals used in some replicates did not drive observed patterns. *Mastocarpus jardiini* (± 0.20 pH units) was a notable exception to low within-species variation, but may comprise a multi-species complex (Lindstrom et al. 2011).

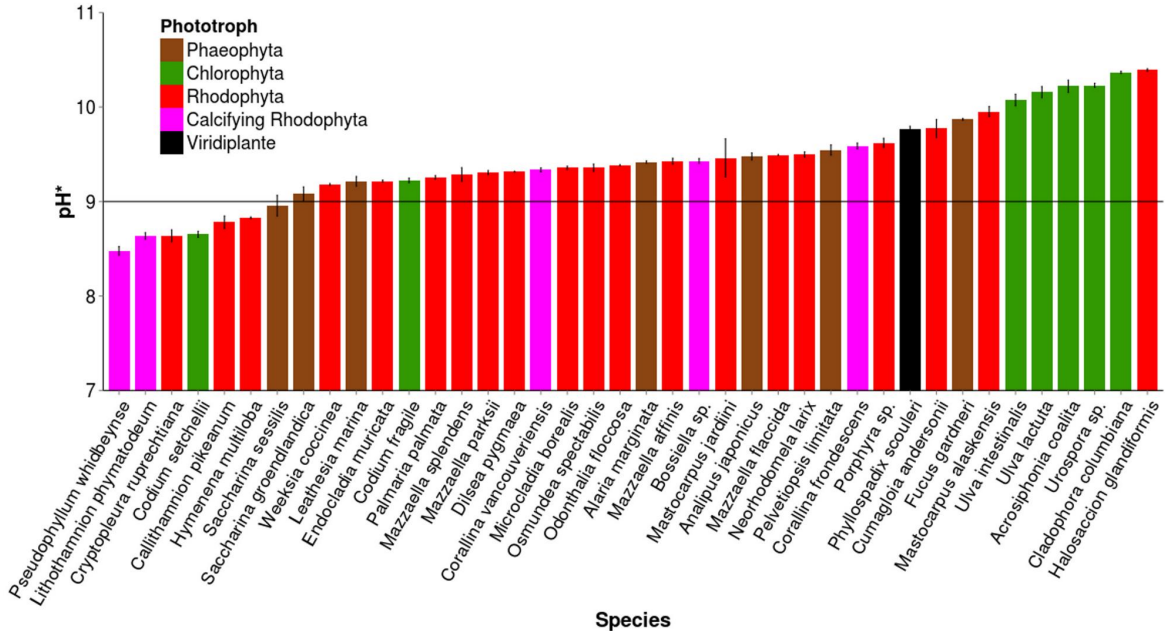


**Figure 2.1.** Mean pH* ± standard error (s.e.) for 39 species of intertidal seaweed and one surfgrass. Species with pH* > 9.0 (line) can utilize $HCO_3^-$. Calcifying Rhodophyta species with pH* < 9.0 are crustose species, while calcifying Rhodophytes with pH* > 9.0 are articulated species.

### Predictors and patterns of pH at equilibrium ($pH_e$)

After re-equilibration to atmospheric $CO_2$ levels and thus initial seawater DIC values, the pH value at this equilibrium ($pH_e$) of both control and treatment replicates was compared to initial seawater pH prior to incubation (time 0). Control $pH_e$ did not differ from control initial pH (two-tailed paired t test, $t_{53} = -1.0$, $p = 0.324$). However, macrophyte-incubated seawater $pH_e$ deviated from initial seawater controls by -0.35 ± 0.12 to +0.28 ± 0.03 s.e. pH units (Table 2.A.1), but was unrelated to pH* ($R^2 = 0.102$, $F_{1, 36} = 4.1$, $p = 0.051$). Values differed by Phylum ($F_{3, 35} = 3.3$, $p = 0.032$), with Chlorophyta having lower $pH_e$ than Rhodophyta (Tukey HSD, $p = 0.024$). $pH_e$

differences in macrophyte-incubated seawater compared to initial conditions suggest that macroalgae influence seawater chemistry in ways other than depleting DIC for photosynthesis.

**Evolutionary history of CCMs**

Our phylogenetic analysis of Ochrophyta: Phaeophyceae comprised species from 18 of 59 families (31%). In Rhodophyta: Florideophyceae, we analyzed 29 of 95 families (31%), excluding Bangiaceae (1 family). In both clades, species showed little variation in CCM status within-family (Table 2.C.1, Table 2.C.2). In 10 of 20 Rhodophyta families in which there were data for multiple species, 100% of member species shared the same CCM designation (i.e. all species in the family had CCMs, or all lacked them; n = 2-7 species per family, Table 2.C.1). This was also the case in 6 of 10 Ochrophyta families with more than one family member (n = 2-12 species per family, Table 2.C.2). Ancestral state reconstruction indicated that CCMs are likely ancestral in Ochrophyta (0.87 probability), but are near-equally likely to be ancestral or not in Rhodophyta (0.52 probability of CCM presence). Families with CCMs did not have higher species richness than families lacking CCMs in Rhodophyta (one-tailed t test, $t_{22.1} = -1.48$, $p = 0.076$) or Ochrophyta (one-tailed t test, $t_{14.9} = -1.39$, $p = 0.092$).

Stochastic character mapping of CCM status revealed that CCMs have been lost and gained an equal number of times in Rhodophyta, but lost more often than gained in Ochrophyta (Figures 2.2*a* and 2.2*b*). In Rhodophyta, an average of 34.6 transitions (mode = 34) were observed between discrete CCM states in stochastic trait mapping (Figure 2.2*a*), with 17.4 transitions from CCM absence to presence (mode = 19), and 17.2 from CCM presence to absence (mode = 20). In Ochrophyta, there were an average of 4.7 transitions (mode = 3)

observed in stochastic trait mapping (Figure 2.2*b*), with 1.1 transitions from CCM absence to presence (mode = 0), and the majority of transitions (3.6) from CCM presence to absence (mode = 3).

Blomberg's K for Rhodophyta for the continuous pH* trait did not differ from K =1 (K = 0.80, p = 0.455), suggesting that evolution of pH* or CCM efficiency in Rhodophyta exhibited significant phylogenetic signal consistent with the expectations of a Brownian motion model. However, Pagel's λ for the discrete trait CCM presence differed from 1 ($\lambda = 4.10 \times 10^{-5}$, p = 0.021), and was comparable to λ = 0 (p = 1.000), i.e., a star phylogeny. Similarly, in Ochrophyta, Blomberg's K for pH* also did not differ from K =1 (K = 0.82, p = 0.627), and λ was significantly different from 1 for the discrete CCM trait ($\lambda = 7.56 \times 10^{-5}$, p = 0.0005) and effectively no different from 0 (p = 1.000), again indicating that families' discrete CCM status are largely independently derived.

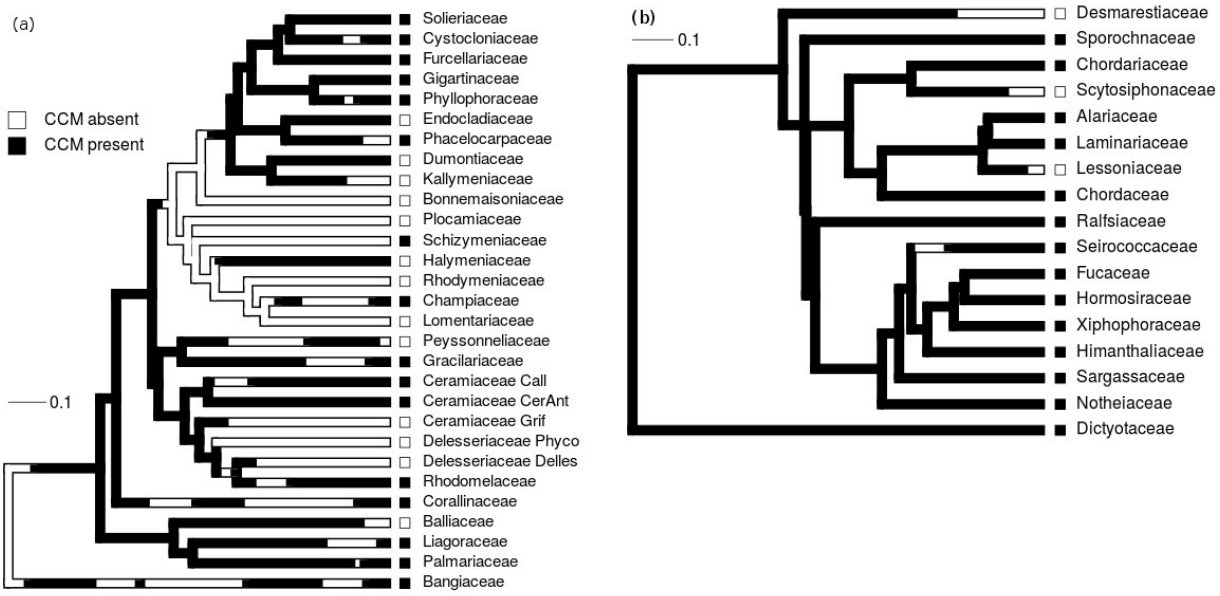


**Figure 2.2.** Stochastic character mapping of the CCM trait. One of 1000 phylogenies generated depicting one possible trait reconstruction for CCM presence and absence in (*a*) 30 families from Phylum Rhodophyta in a phylogeny adapted from Verbruggen et al. (2010), Pagel's $\lambda = 4.10 \times 10^{-5}$, $p = 0.021$; and (*b*) 18 families from Phylum Ochrophyta in a phylogeny adapted from (Silberfeld *et al.* 2010), Pagel's $\lambda = 7.56 \times 10^{-5}$, $p = 0.0005$. Trait reconstructions were generated through stochastic character mapping (Revell 2012). Changes may occur within branches because reconstructions depict not only the states at nodes but also the states at all points between nodes. Taxa with two phrases indicate Family and Subfamily.

**Species-specific shifts in seawater TA**

Although pH* indicated 2 groups of species, where a CCM was either indicated or not, seawater alkalinity patterns differed among species in unexpected ways. Shifts in TA differed among species as pH increased: at high pH, some species depleted TA while others increased it (Figure 2.3*a*). TA shifts ranged from depletions of up to 1170 µmol/kg seawater, to increases of up to 255 µmol/kg seawater and differed significantly from controls in 16 of 24 species evaluated (Figure 2.3*a*, Table 2.A.1); only *Porphyra sp.* increased TA. Although four of five green algal species

decreased TA more than any other fleshy macroalgal species (Figure 2.3*a*), TA did not vary by Phylum (Kruskal-Wallis $\chi^2 = 3.09$, df = 2, p = 0.213). Initial seawater TA on a collected batch was 2192 µmol/kg seawater, compared to 2198 µmol/kg post-incubation for that batch, indicating that seawater TA in controls changed little during incubation. Calcium and aragonite saturation also varied among species (Table 2.A.2).

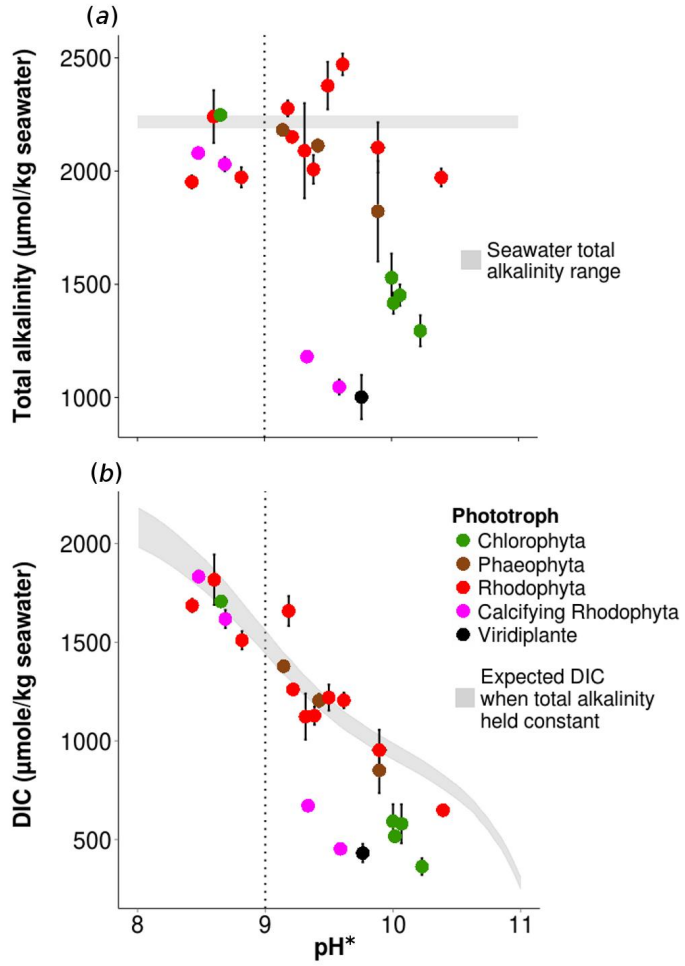


**Figure 2.3.** Seawater total alkalinity and DIC concentrations post macrophyte incubation. The 24-hour incubation was done under light with 23 seaweed species and one surfgrass species (2-6 reps). (*a*) Mean seawater TA ± standard error (s.e.) versus pH*. Gray envelope indicates control seawater TA. Dotted line indicates break point for $HCO_3^-$ use (pH > 9.0). (*b*) Mean calculated DIC ± s.e. versus pH*. Gray envelope indicates expected DIC-pH relationship if TA is held constant at ambient seawater levels.

Deviation in seawater $pH_e$ from initial conditions was positively related to TA, but not to pH* (Figure 2.A.2; multiple regression, $R^2 = 0.466$, $F_{1,21} = 8.3$ , $p = 0.012$, and $p = 0.168$, respectively), supporting the hypothesis that changes in water chemistry by macrophytes via change in TA, rather than incomplete re-equilibration, caused shifts in $pH_e$. TA was negatively related to pH* ($R^2 = 0.203$, $F_{1,21} = 5.4$, $p = 0.031$, Figure 3*a*).

**DIC depletion by macrophytes**

Thirteen species depleted significantly more DIC than expected if TA had remained constant, while only *Porphyra sp.* increased DIC (149 ± 28 s.e. μmol/kg seawater, $t_6 = 2.8$, $p = 0.029$, Figure 2.3*b*, Table 2.A.2). Deviation from expected DIC was greater for articulated calcifying Rhodophytes than crustose species (-711 ± 30 μmol/kg seawater versus -139 ± 23 μmol/kg seawater, respectively). Chlorophytes also showed strong depletion in DIC up to -524 ± 38 μmol/kg seawater, and the one angiosperm species surveyed showed the greatest observed depletion of DIC relative to the expected DIC value (*P. scouleri,* -757 ± 72 μmol/kg seawater).

**TA-induced changes in carbon availability**

Macrophyte-driven changes in TA can change $HCO_3^-$, $CO_2$ and $CO_3^{2-}$ concentrations relative to the concentrations if TA was unchanged. Through decreasing TA and thus decreasing pH, 13 species significantly increased $HCO_3^-$ concentrations and 12 species significantly increased $CO_2$ concentrations (Figure 2.4, Table 2.A.2) at the expense of $CO_3^{2-}$. Increases in $HCO_3^-$ ranged from 14.29 ± 0.85 to 357.59 ± 7.59 s.e. more μmol/kg seawater, corresponding to 144-1571% of

expected values (Figure 2.4*a*). Increases in $CO_2$ ranged from 0.09 ± 0.01 to 4.73 ± 0.28 μmol/kg, reflecting proportionately large changes (141-83000%) owing to its negligible concentration at higher pH. The single species that increased TA (*Porphyra sp.*) led to a $CO_2$ loss of 0.17 ± 0.02 μmol/kg seawater, 40% of expected values under constant TA (Figure 2.4*b*, Table 2.A.2). Because $[CO_3^{2-}]$ is inversely proportional to $[CO_2] + [HCO_3^-]$ (Figure 2.A.1), decreases in $CO_3^{2-}$ approximately mirrored increases in $HCO_3^-$ (Figure 2.A.3).

The majority of macrophytes with CCMs (pH* > 9.0) that shifted seawater TA showed small but significant changes in $CO_2$ (Figure 2.4*b*). Because $HCO_3^-$ users raised seawater pH* well above 9.0 – after which $[CO_2] < 1$ μmol/kg seawater – TA-induced changes to $[CO_2]$ were largely negligible (Figure 2.A.1). Six species did not appear to access bicarbonate based on their pH* value, however they significantly decreased total alkalinity (Table 2.A.1). For these species, TA-induced decreases in pH* quickly fall within a pH range with non-negligible $CO_2$ concentrations (Figure 2.A.1), causing increases in $[HCO_3^-]$ and driving $[CO_2]$ to the highest levels observed in the study (Figures 2.4*c*, 2.4*d*).

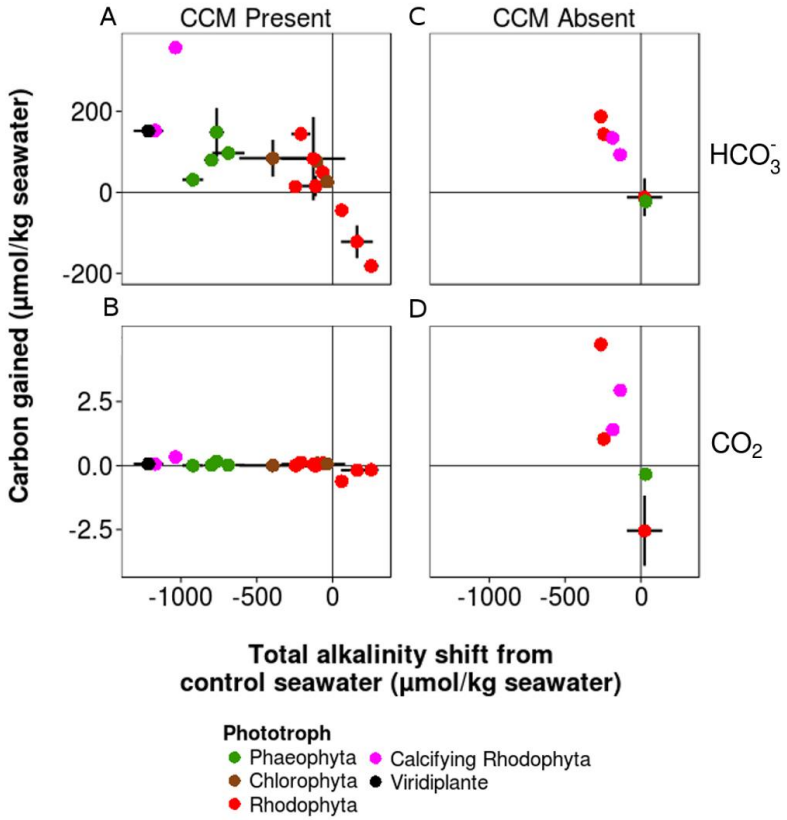


**Figure 2.4**. Carbon gained through total alkalinity shifts. (*a*) Mean $HCO_3^-$ ± standard error (s.e.) gained versus mean TA shift ± s.e. in seawater incubated with CCM-present macrophytes. (*b*) $CO_2$ gained versus TA shift in seawater incubated with CCM-present macrophytes. (*c*) $HCO_3^-$ gained versus TA shift in seawater incubated with CCM-absent macrophytes. (*d*) $CO_2$ gained versus TA shift in seawater incubated with CCM-absent macrophytes. Solid lines indicate control seawater axes for all panels.

## DISCUSSION

### CCM evolution in Rhodophyta and Ochrophyta

Our analysis of 31% of families in each of Rhodophyta and Ochrophyta showed consistent patterns of CCM evolution between red and brown algal lineages but differing patterns between categorization of CCMs as a continuous versus discrete trait. Evolution of the

continuous trait pH*, to an extent a measure of CCM efficiency, exhibited a phylogenetic signal similar to a Brownian motion model of evolution in Rhodophyta and Ochrophyta, where phenotypic differences between taxa are directly proportional to the branch lengths characterizing their independent evolutionary history (Figure 2.2a). In contrast, the discrete trait of CCM presence was not significantly different from a star phylogeny, indicating that phylogenetic signal in CCM presence was much weaker, and suggests that different lineages experienced different rates of CCM evolution in response to their environment (Blomberg et al. 2003).

While we inferred many losses of CCMs in the marine algal lineages investigated, loss of CCMs is rare in terrestrial plant lineages. CCMs have evolved as $C_4$ photosynthesis more than 62 times independently in flowering plants and are considered highly convergent in flowering plants (Sage et al. 2011). In the grass family Poaceae alone (100 million years old (Prasad et al. 2011)) there are 22-24 inferred origins of $C_4$ photosynthesis, and 1 potential loss (Aliscioni et al. 2012), in contrast to the 35 transitions observed in Rhodophyta. The high number of CCM losses in Rhodophyta (17) mirrors the number of transitions observed in some behavioral traits, such as foraging behavior in pigeons and doves (Lapiedra et al. 2013), although clade age and size varied among these traits.

Loss of CCMs in Rhodophytes and Ochrophytes and gain of CCMs in Rhodophytes indicate that selection for CCMs may depend upon environmental parameters, including local and global habitat features, and source inorganic carbon availability that are far more variable in marine systems than terrestrial ones. In the poles, where temperatures are low, $CO_2$ is more easily absorbed from the atmosphere into the oceans, and in the low-light subtidal zone, where

macrophytes are constantly submerged compared to the intertidal zone, CCMs are less common (Cornwall et al. 2015, Stepien 2015). This may explain why the Ochrophyta: Phaeophyceae, one of the few lineages that largely originated and diversified in temperate latitudes (Chin et al. 1991), and are proportionately more prevalent at lower tidal levels, shows less phylogenetic structure than expected (Figure 2.2*b*) and many more losses than gains in our analysis. Clade age may also contribute to the large number of transitions and low phylogenetic signal observed in red algae, a 500-600 million year old clade (Yoon et al. 2004), compared to 150-200 myo Phaeophyceae (Silberfeld et al. 2010).

CCMs in marine macrophytes have demonstrated plasticity in functionality by depth (Cornwall et al. 2015), and pyrenoids, chloroplast components of CCMs in some taxa, have been lost and gained multiple times in Chlorophyta (Meyer and Griffiths 2013). In contrast, CCM evolution in terrestrial plants is strongly linked to the proportion of vascular bundle sheath tissue (Christin et al. 2013). As a complex physiological trait without assignment to a single morphological structure, it is difficult to determine the mechanism by which a marine lineage loses or gains a CCM. CCMs can be costly to utilize (Raven 1997), and local and long-term patterns in carbon supply may change their selective advantage. Whether increasing seawater DIC leads to a selective disadvantage for CCMs is an important area of future research.

**Macrophytes exert species-specific effects on seawater chemistry**

Most macroalgal species tested increased pH > 9.0, though their effects on seawater TA varied greatly (Figures 2.1 and 2.3). Overall, 92% of species had either a CCM or the ability to shift TA, with Chlorophytes having significantly higher pH* than Rhodophytes; excluding *C. setchellii*,

Chlorophytes assayed here are characterized as fast-growing, early successional species (Sousa 1984) that may benefit from bicarbonate access. Of 6 possible combinations of CCMs and TA shifts – CCM presence or absence with TA increase, decrease, or no effect – 5 were observed. We never observed species that lacked CCMs increase TA, and few species lacking CCMs decreased TA. Several species of red (*E. muricata*, *D. pygmaea*, *M. alaskensis*) and brown seaweeds (*A. marginata*) with CCMs had no effect on seawater TA. The only species with a CCM that increased TA (*Porphyra sp.*) also decreased $CO_2$ ($t_3 = -3.6$, $p = 0.038$), however the change was small (-0.17 μmol/kg seawater $CO_2$). Among the remaining CCM-TA trait combinations, we focus on the groups that decreased TA and thus increased DIC: 1) species with CCMs that decreased TA (the majority of species surveyed), and 2) species lacking CCMs that decreased TA.

Species with CCMs that decreased TA were represented across all three algal phyla and the angiosperm assayed. TA decreases likely resulted from macrophyte-facilitated proton addition to seawater. Biological uptake and transformation of cations such as positively-charged ammonium generates $H^+$ and decreases TA, while uptake of anions like negatively-charged nitrate and sulfate generates OH-, which increases TA (Goldman and Brewer 1980). In previous studies, the brown alga *Ascophyllum* decreased TA through cation generation (Axelsson and Uusitalo 1988). However, these effects are relatively small and do not fully explain the large TA declines observed.

Calcifying algae interact with the ocean carbon system to form a $CaCO_3$ skeleton, which may further alter local seawater chemistry. In the proposed 'trans' model of calcification, active transport of $Ca^{2+}$ and passive diffusion of $CO_2$ forms $CaCO_3$ and releases H+ ions extracellularly

(McConnaughey and Whelan 1997), possibly decreasing pH locally and further increasing $CO_2$ for photosynthesis. In calcifying freshwater green algae, $Ca^{2+}$ and $HCO_3^-$ uptake leads to precipitation of $CaCO_3$ and production of $CO_2$ (Raven 1997). In our study, articulated corallines (*C. frondescens*, *C. vancouveriensis*) increased pH* > 9.0 and strongly decreased TA. Crustose corallines (*P. whidbeyense* and *L. phymatodeum*), in contrast, had little effect on either pH or TA, perhaps because their comparatively slower metabolism (Adey and Vassar 1975) prevented detection of the influence of photosynthesis or calcification on seawater chemistry. Calcium carbonate skeletons in macroalgae are usually assumed to function as a defense against enemies (Padilla 1989). Our results support an alternative hypothesis: that macroalgal calcium carbonate skeletons are a byproduct of manipulating TA to facilitate photosynthesis in environments where DIC may be depleted, a mechanism proposed for calcification in coccolithophores (Leonardos et al. 2009) and macrophytes (McConnaughey and Whelan 1997).

**Macrophyte-driven shifts in total alkalinity may serve as a carbon concentrating mechanism**

Species lacking CCMs that decreased TA (such as *C. ruprechtiana*, *H. multiloba*) likely released or took up other ionic components independent of the carbonate system. Decreased TA benefits these $CO_2$-dependent species because $CO_2$ becomes relatively more available (Figure 2.3*d*). An intriguing consideration is that TA reduction may be a mechanism beyond active carbon transport to locally increase $CO_2$ access. For species that cannot otherwise access $HCO_3^-$; TA reductions increased $CO_2$ up to 4 μmol/kg seawater. For those that have a recognized CCM, a reduction in TA may present another means for concentrating carbon and thus may too be considered a CCM.

Just as some CCMs create external 'acid zones' to convert $HCO_3^-$ to $CO_2$ by pumping H+ into the boundary layer (Hellblom and Axelsson 2003), decreased TA may create local 'low TA zones' that generate lower pH regions to adjust the buffering capacity of the water. Organic bases can have significant impacts on seawater TA in cultures of marine macroalgae and in marine sites characterized by high biological activity and restricted water mixing (Hernández-Ayon et al. 2007). Regardless of the mechanism of a decrease in TA, there is growing evidence that photosynthetic carbon uptake extends beyond the dynamics of $CO_2$ (Andersson et al. 2014). The net result of a reduction in alkalinity is increased availability of DIC, both as $HCO_3^-$ and $CO_2$, for photosynthesis (Figure 2.4), and carbon capture via photosynthesis may be higher than expected on the basis of $CO_2$ dynamics alone. That both the angiosperm *P. scouleri* and calcifying algae had large TA decreases but no significant change in $pH_e$ from controls may point to the diversity of mechanisms by which macrophytes – angiosperms, calcifying and non-calcifying macroalgae – interact with seawater. Carbon acquisition thus likely has multiple underlying mechanisms that deserve further study.

**Potential alternative drivers of macrophyte-associated pH* and TA shifts**

Although macrophytes were rinsed and assayed in sterilized seawater, macrophytes likely hosted microbial populations that may have affected pH* and TA. To generate the range of observed pH* values and TA shifts however, microbial communities would need to be remarkably distinct among macroalgal species to cause shifts ranging from 0-2.4 pH units, or decreases in TA of up to half that of control seawater. Ascribing the range of pH* and TA shifts observed among species to the relatively high algal biomass, rather than microbial communities,

seems more parsimonious. Dissolved organic carbon, though possibly an exudate in the algae in our experiments, also is unlikely to differ by amounts that would drive such large changes in TA. Further, there is strong concordance among the assayed species between phototroph tissue $\delta^{13}C$ – a strong indicator of CCM status – and pH assay results (Stepien 2015).

Calcium and aragonite saturation states were higher in seawater incubated with macrophytes (Table 2.A.1) and may have led to some spontaneous $CaCO_3$ precipitation at high pH*, which could drastically lower total alkalinity. However, if a purely abiotic pH-dependent reaction was behind some of the large TA drops observed, it would not lead to consistent differences among species with similar pH* across multiple independent replicates (Figure 2.3*a*). If observed TA reductions were generated by spontaneous external calcification, then the consistent species-specific responses imply that some macroalgae possess traits that promote the process, such as morphologies or chemical exudates that promote $CaCO_3$ enucleation, whereas others do not. Such external calcium carbonate precipitation would be distinct from carbon concentrating mechanisms, an interesting finding worth further investigation. Overall, both total alkalinity shifts and pH* values were consistent within species among intra-study replicates, inter-study replicates, and seawater batches, indicating that findings were due to macrophyte species identity rather than methodological artifacts.

**Potential implications of CCMs for macrophyte communities**

While macrophyte-induced shifts in TA may be non-linear, not occurring until the surrounding seawater approaches the species' pH* (Axelsson and Uusitalo 1988), the size of the boundary layer and effects of water mixing may create conditions in nearshore environments

where these mechanisms become locally important in carbon cycling. In our study, 4 g of macrophyte shifted TA in 125 mL of water (32 g/L). Comparable studies with biomass-to-seawater proportions as low as 0.007 g/mL in 700 mL chambers report similar TA shifts (Axelsson and Uusitalo 1988). The boundary layer can be very small in communities dominated by crust-forming species, but may be much thicker in more structurally diverse communities (Cornwall et al. 2013), indicating that observed TA effects could be far-reaching in areas of low water motion. Furthermore, although the experiments are small-scale, the algal biomass to volume ratio used is actually very similar to those calculated at a typical high tide (the most dilute conditions) from field data (3-30 g/L; (Leigh et al. 1987)).

While current techniques cannot probe TA changes at boundary layer scales, pH shifts of more than 2 units have been observed in boundary layers of algal species and biofilms under realistic flow and pH regimes (Larkum et al. 2003, Hurd et al. 2011). Macrophyte-driven elevated pH at larger scales along shoreline waters indicates species may compete for DIC (Björk et al. 2004, Wootton et al. 2008). CCMs may allow macroalgae to be more productive in slow-moving seawater, where rates of $CO_2$ supply can be reduced (Hurd 2000). Excluding *C. setchellii*, Chlorophytes assayed here are characterized as fast-growing, early successional species (Sousa 1984) that may benefit from bicarbonate access. Chlorophytes such as species in the cosmopolitan genus *Ulva* can dominate areas of periodic low flow including tidepools (Björk et al. 2004), and embayments where it blooms in high densities (Guidone et al. 2012, Alstyne et al. 2015).

Macrophytes with CCMs have extremely variable community abundances, from 0-100% coverage in communities surveyed thus far (Hepburn et al. 2011, Cornwall et al. 2015). The

great interspecies differences in carbon uptake demonstrated in our study and others suggests that carbon use and its local seawater effects may be important to intra-and interspecific interactions in marine macrophyte communities.

**ACKNOWLEDGEMENTS**

We thank the National Park Service (Olympic NP) for access to Shi Shi Beach, and the Makah Tribal Nation for access to Tatoosh Island, D. and M. Hurd for providing research facilities, and T. Price and R. Ree for helpful comments. Research was supported in part by the National Science Foundation (DGE1144082 to CCS, DEB1311286 to CAP and CCS, OCE0928232 to CAP and DEB0919240 to JTW), and the National Institutes of Health (T32 GM007197).

## APPENDIX 2A: CALCULATED CHANGES OF $PH_E$ AND $[CO_3^{2-}]$ AS A FUNCTION OF TOTAL ALKALINITY SHIFTS

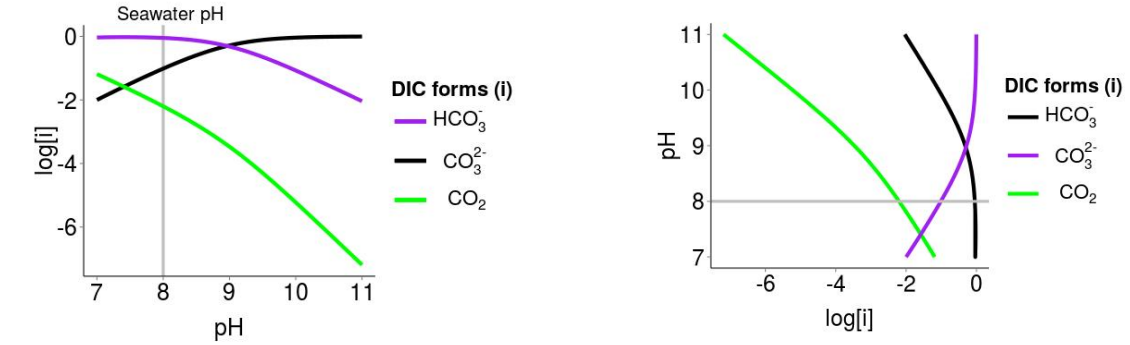


*A* *B*

**Figure 2.A.1**. Bjerrum plots of the dissolved inorganic carbon system. *A*) Log of $[HCO_3^-]$, $[CO_3^{2-}]$ and $[CO_2]$ as a function of pH. Grey line indicates concentrations at control seawater pH. While pH is an emergent property of dissolved inorganic carbon concentrations (*B*), it is often depicted on the x axis, as these values are somewhat interdependent.

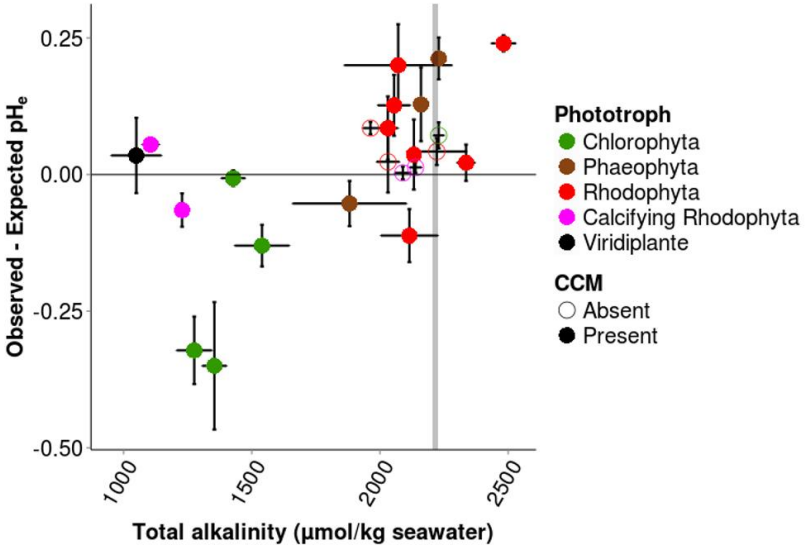


**Figure 2.A.2.** Mean change ± SEM in observed versus expected $pH_e$ vs total alkalinity in 39 species of seaweed and 1 surfgrass. All units in µmol/kg seawater. Filled circles depict species with CCMs present, open circles CCMs are absent. N = 111.

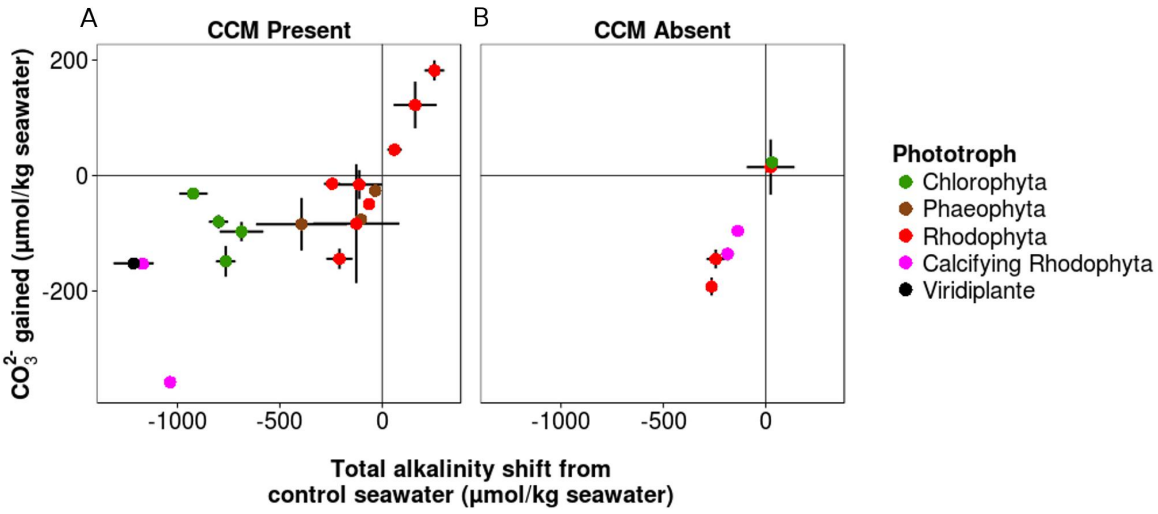


**Figure 2.A.3.** Carbonate gained through total alkalinity shifts. Mean change ± SEM in observed versus expected [$CO_3^{2-}$] vs total alkalinity shift in µmol/kg seawater for (*A*) 17 species of seaweed and one species of surfgrass with CCMs, and (*B*) 6 species of seaweed without CCMs. N = 111.

**2.A.1. pH* and ΔpHe ± standard error (s.e.) for 39 species of intertidal seaweed and 1 species of surfgrass**. Total alkalinity (TA) ± s.e. for 24 species. ΔpHe is calculated as observed pHe of macrophyte-incubated seawater minus pHe of seawater with ed absent, post incubation and requilibrium. † indicates calcifying species. ‡ indicates crust-forming calcifying species. N indicates number of individuals per species. p is p value for a one-tailed t test for shift in total alkalinity. Bolding indicates p value less .050. Ω Ar and Ω Ca indicates the saturation state of aragonite and calcium, repsectively. *Corallina frondescens* has only 1 replicate for pHe. CCM present indicates pH* > 9.0 if 'yes' and pH* < 9.0 if 'no.' TA shifts are reported as the TA of macrophyte-ated seawater minus the TA of control seawater, post incubation. If a TA shift is 0, macrophytes did not change seawater at all during the incubation. TA shifts indicate whether changes in total alkalinity were significantly higher than 0 ('increase' relative to l seawater), lower than 0 ('decrease' relative to control seawater) or not different from 0 (not significant, 'n.s.', no effect of macrophyte incubation). Where multiple seawater batches are listed, this indicates species replicates were run across multiple trials, a some specimens were run with batch x and others with batch y.

| on | Taxa | CCM present | TA shift | pH* (s.e) | N | $\Delta pH_e$ (s.e.) | p $\Delta pH_e$ | TA (s.e.) µmol/kg SW | N | ΔTA (s.e) µmol/kg SW | p ΔTA | Ω Ca(s.e.) | Ω Ar (s.e.) | Ω Ca (s.e.) control | Ω Ar (s.e.) control | Seawater batch |
|---|---|---|---|---|---|---|---|---|---|---|---|---|---|---|---|---|
| phyta | *Acrosiphonia coalita* | yes | decrease | 10.22 (0.07) | 10 | -0.01 (0.01) | 0.662 | 1427.75 (46.66) | 4 | -799.50 (53.50) | **< 0.001** | 10.20 (0.46) | 6.47 (0.29) | 3.03 (0.19) | 1.92 (0.12) | 4, 14 |
| | *Cladophora columbiana* | yes | - | 10.37 (0.01) | 6 | -0.02 (0.05) | 0.700 | - | - | - | - | - | - | - | - | 8 |
| | *Codium fragile* | yes | - | 9.22 (0.02) | 6 | 0.19 (0.09) | 0.097 | - | - | - | - | - | - | - | - | 9 |
| | *Codium setchellii* | no | n.s. | 8.65 (0.03) | 6 | 0.07 (0.02) | **0.030** | 2229.00 (21.00) | 6 | 31.33 (30.06) | 0.214 | 8.68 (0.36) | 5.51 (0.23) | 3.21 (0.11) | 2.04 (0.07) | 11 |
| | *Ulva intestinalis* | yes | decrease | 10.08 (0.06) | 6 | -0.35 (0.12) | **0.030** | 1354.20 (47.34) | 5 | -764.30 (57.85) | **< 0.001** | 9.25 (0.65) | 5.82 (0.41) | 2.64 (0.07) | 1.66 (0.04) | 10 |
| | *Ulva lactuta* | yes | decrease | 10.16 (0.06) | 10 | -0.13 (0.04) | **0.019** | 1540.00 (106.42) | 4 | -687.25 (113.26) | **0.007** | 11.35 (1.31) | 7.20 (0.83) | 3.03 (0.19) | 1.92 (0.12) | 4, 14 |
| | *Urospora sp.* | yes | decrease | 10.23 (0.02) | 3 | -0.32 (0.06) | **0.035** | 1275.67 (68.67) | 3 | -922.00 (77.73) | **0.005** | 7.82 (0.88) | 4.96 (0.56) | 3.21 (0.11) | 2.04 (0.07) | 11 |
| phyta | *Alaria marginata* | yes | decrease | 9.42 (0.01) | 6 | 0.13 (0.07) | 0.115 | 2160.00 (27.69) | 5 | -103.83 (53.50) | **0.018** | 15.47 (0.24) | 9.81 (0.15) | 2.75 (0.07) | 1.74 (0.04) | 12 |
| | *Analipus japonicus* | yes | - | 9.48 (0.04) | 6 | 0.10 (0.03) | **0.013** | - | - | - | - | - | - | - | - | 5, 6 |
| | *Fucus gardneri* | yes | n.s. | 9.87 (0.01) | 10 | -0.05 (0.04) | 0.232 | 1881.50 (221.93) | 4 | -394.00 (229.53) | 0.174 | 14.90 (2.37) | 9.47 (1.51) | 2.57 (0.07) | 1.64 (0.04) | 4, 13 |
| | *Leathesia marina* | yes | - | 9.21 (0.05) | 6 | 0.23 (0.02) | **< 0.001** | - | - | - | - | - | - | - | - | 8 |
| | *Pelvetiopsis limitata* | yes | - | 9.55 (0.05) | 6 | 0.14 (0.02) | **< 0.001** | - | - | - | - | - | - | - | - | 5, 6 |
| | *Saccharina groendlandica* | yes | n.s. | 9.08 (0.07) | 12 | 0.21 (0.04) | **< 0.001** | 2229.17 (17.37) | 6 | -34.67 (23.08) | 0.106 | 14.05 (0.33) | 8.92 (0.21) | 2.75 (0.07) | 1.74 (0.04) | 8, 12 |
| | *Saccharina sessilis* | no | - | 8.96 (0.11) | 5 | -0.09 (0.09) | 0.404 | - | - | - | - | - | - | - | - | 9 |
| phyta | *Bossiella sp.*† | yes | - | 9.43 (0.03) | 6 | -0.07 (0.04) | 0.144 | - | - | - | - | - | - | - | - | 7 |
| | *Callithamnion pikeanum* | no | n.s. | 8.78 (0.07) | 7 | 0.04 (0.02) | 0.141 | 2221.67 (116.36) | 3 | 24.00 (125.42) | 0.856 | 6.74 (0.48) | 4.28 (0.31) | 3.21 (0.11) | 2.04 (0.07) | 8, 11 |
| | *Corallina frondescens*† | yes | decrease | 9.59 (0.03) | 5 | 0.06 (NA) | - | 1105.60 (33.23) | 5 | -1169.90 (40.07) | **< 0.001** | 6.96 (0.35) | 4.42 (0.22) | 2.57 (0.07) | 1.64 (0.04) | 13, 14 |
| | *Corallina vancouveriensis*† | yes | decrease | 9.34 (0.02) | 6 | -0.07 (0.03) | 0.086 | 1228.17 (23.18) | 6 | -1035.67 (28.89) | **< 0.001** | 6.88 (0.36) | 4.37 (0.23) | 2.75 (0.07) | 1.74 (0.04) | 12 |
| | *Cryptopleura ruprechtiana* | no | decrease | 8.64 (0.06) | 10 | 0.09 (0.01) | **< 0.001** | 1963.00 (28.68) | 3 | -34.67 (23.08) | **0.002** | 4.32 (0.24) | 2.74 (0.15) | 3.03 (0.19) | 1.92 (0.12) | 8, 14 |
| | *Cumagloia andersonii* | yes | - | 9.77 (0.10) | 6 | 0.21 (0.03) | **< 0.001** | - | - | - | - | - | - | - | - | 5, 6 |
| | *Dilsea pygmaea* | yes | n.s. | 9.32 (0.01) | 2 | 0.20 (0.08) | 0.228 | 2071.00 (210.00) | 2 | -126.67 (219.06) | 0.654 | 15.08 (2.08) | 9.57 (1.32) | 3.21 (0.11) | 2.04 (0.07) | 11 |
| | *Endocladia muricata* | yes | decrease | 9.22 (0.01) | 6 | 0.04 (0.06) | 0.592 | 2132.17 (14.29) | 6 | -65.50 (23.35) | **0.004** | 14.12 (0.25) | 8.96 (0.16) | 3.21 (0.11) | 2.04 (0.07) | 11 |
| | *Halosaccion glandiformis* | yes | decrease | 10.39 (0.01) | 6 | 0.09 (0.06) | 0.202 | 2030.67 (39.45) | 6 | -244.83 (47.05) | **0.001** | 14.63 (0.50) | 9.30 (0.32) | 2.57 (0.07) | 1.64 (0.04) | 13 |
| | *Hymenena multiloba* | no | decrease | 8.83 (0.01) | 10 | 0.02 (0.06) | 0.696 | 2031.25 (44.48) | 4 | -244.25 (51.32) | **0.020** | 8.37 (0.43) | 5.31 (0.27) | 3.03 (0.19) | 1.92 (0.12) | 4, 14 |
| | *Lithothamnion phymatodeum*‡ | no | decrease | 8.64 (0.03) | 10 | 0.00 (0.01) | 0.803 | 2089.25 (30.86) | 4 | -186.25 (38.46) | **0.007** | 7.57 (0.40) | 4.81 (0.51) | 2.57 (0.07) | 1.64 (0.04) | 10, 13 |
| | *Mastocarpus alaskensis* | yes | n.s. | 9.95 (0.05) | 10 | -0.11 (0.05) | 0.069 | 2114.75 (111.21) | 4 | -112.50 (118.05) | 0.387 | 17.40 (1.02) | 11.04 (0.65) | 3.03 (0.19) | 1.92 (0.12) | 7, 14 |
| | *Mastocarpus jardiini* | yes | - | 9.46 (0.20) | 6 | 0.13 (0.05) | 0.059 | - | - | - | - | - | - | - | - | 9 |
| | *Mazzaella affinis* | yes | - | 9.43 (0.03) | 6 | 0.07 (0.03) | 0.092 | - | - | - | - | - | - | - | - | 9 |
| | *Mazzaella flaccida* | yes | - | 9.49 (0.00) | 6 | 0.27 (0.04) | **< 0.001** | - | - | - | - | - | - | - | - | 5, 6 |
| | *Mazzaella parksii* | yes | - | 9.31 (0.02) | 6 | 0.10 (0.04) | 0.054 | - | - | - | - | - | - | - | - | 7 |
| | *Mazzaella splendens* | yes | - | 9.29 (0.07) | 6 | 0.03 (0.02) | 0.165 | - | - | - | - | - | - | - | - | 9 |
| | *Microcladia borealis* | yes | - | 9.36 (0.02) | 6 | 0.21 (0.03) | **0.001** | - | - | - | - | - | - | - | - | 8 |
| | *Neorhodomela larix* | yes | n.s. | 9.50 (0.03) | 6 | - | - | 2388.00 (104.96) | 4 | 160.75 (111.80) | 0.223 | 19.37 (1.01) | 12.29 (0.64) | 3.03 (0.19) | 1.92 (0.12) | 14 |
| | *Odonthalia floccosa* | yes | decrease | 9.39 (0.01) | 4 | 0.13 (0.06) | 0.072 | 2054.83 (63.40) | 6 | -209.00 (69.11) | **0.021** | 14.70 (0.49) | 9.33 (0.31) | 2.75 (0.07) | 1.74 (0.04) | 12 |
| | *Osmundea spectabilis* | yes | - | 9.36 (0.04) | 6 | 0.28 (0.03) | **< 0.001** | - | - | - | - | - | - | - | - | 5, 6 |
| | *Palmaria palmata* | yes | - | 9.26 (0.02) | 6 | 0.09 (0.07) | 0.216 | - | - | - | - | - | - | - | - | 7 |
| | *Porphyra sp.* | yes | increase | 9.62 (0.05) | 10 | 0.24 (0.01) | **< 0.001** | 2482.00 (47.87) | 4 | 254.75 (54.71) | **0.012** | 21.07 (0.69) | 13.37 (0.44) | 3.03 (0.19) | 1.92 (0.12) | 4, 14 |
| | *Pseudolithophyllum whidbeyense*‡ | no | decrease | 8.48 (0.05) | 5 | 0.01 (0.01) | 0.271 | 2138.80 (23.61) | 5 | -136.70 (31.21) | **0.003** | 5.03 (0.28) | 3.20 (0.18) | 2.57 (0.07) | 1.64 (0.04) | 13 |
| | *Weeksia coccinea* | yes | n.s. | 9.18 (0.01) | 6 | 0.02 (0.03) | 0.542 | 2335.67 (35.07) | 6 | 60.17 (42.67) | 0.149 | 11.25 (1.21) | 7.16 (0.77) | 2.57 (0.07) | 1.64 (0.04) | 11, 13 |
| lante | *Phyllospadix scouleri* | yes | decrease | 9.76 (0.03) | 6 | 0.04 (0.07) | 0.633 | 1049.67 (97.80) | 6 | -1214.17 (103.51) | **< 0.001** | 6.49 (0.99) | 4.12 (0.63) | 2.75 (0.07) | 1.74 (0.04) | 12 |

**Table 2.A.2**. Changes in seawater carbon concentrations after incubation with 23 species of macroalgae and 1 species of surfgrass. ΔDIC is deviation of Dissolved Inorganic Carbon concentration from expected DIC depletion under control Total Alkalinity conditions. $\Delta HCO_3^{2-}$ and $\Delta CO_2$ are carbon gained due to TA-induced pH shifts driven by macroalgae. N indicates number of individuals per species. p value is for a one-tailed t test for changes in carbon concentrations. † indicates articulated calcifying species. ‡ indicates crust-forming calcifying species. Bolding indicates p value < 0.050.

| Division | Taxa | N | Δ DIC (SEM) µmol/kgSW | p ΔDIC | Δ $HCO_3^{2-}$ (SEM) µmol/kgSW | p Δ$HCO_3^{2-}$ | Δ $CO_2$ (SEM) µmol/kgSW | p Δ$CO_2$ |
|---|---|---|---|---|---|---|---|---|
| Chlorophyta | *Acrosiphonia coalita* | 4 | -458.46 (65.54) | **< 0.001** | 79.99 (11.53) | **0.040** | 0.02 ($4.2x10^{-3}$) | 0.154 |
| | *Codium setchellii* | 6 | -1.06 (17.29) | 0.284 | -22.28 (6.21) | 0.203 | -0.34 (0.08) | 0.157 |
| | *Ulva intestinalis* | 5 | -462.32 (25.05) | **< 0.001** | 148.32 (60.11) | 0.332 | 0.17 (0.08) | 0.367 |
| | *Ulva lactuta* | 4 | -393.06 (54.99) | **0.007** | 97.01 (16.73) | 0.065 | 0.02 (0.01) | 0.190 |
| | *Urospora sp.* | 3 | -523.74 (37.96) | **0.007** | 31.28 (3.42) | **0.034** | $2.9x10^{-3}$ ($4.5x10^{-4}$) | 0.066 |
| Phaeophyta | *Alaria marginata* | 5 | -45.67 (18.24) | **0.012** | 76.01 (9.04) | **0.020** | 0.09 (0.01) | **0.021** |
| | *Fucus gardneri* | 4 | -238.41 (132.44) | 0.170 | 84.32 (45.52) | 0.423 | 0.01 (0.02) | 0.893 |
| | *Saccharina groendlandica* | 6 | -0.85 (12.35) | 0.106 | 26.19 (5.39) | 0.104 | 0.07 (0.01) | 0.091 |
| Rhodophyta | *Callithamnion pikeanum* | 3 | -5.26 (99.82) | 0.864 | -12.14 (46.57) | 0.894 | -2.54 (1.37) | 0.400 |
| | *Corallina frondescens*† | 5 | -711.21 (31.57) | **< 0.001** | 152.71 (7.62) | **< 0.001** | 0.06 (0.01) | **0.010** |
| | *Corallina vancouveriensis*† | 6 | -710.97 (27.99) | **< 0.001** | 357.59 (7.59) | **< 0.001** | 0.33 (0.02) | **0.002** |
| | *Cryptopleura ruprechtiana* | 3 | -250.67 (35.25) | **0.022** | 187.37 (15.40) | **0.020** | 4.73 (0.28) | **0.011** |
| | *Dilsea pygmaea* | 2 | -105.27 (138.03) | 0.671 | 83.18 (102.84) | 0.669 | 0.06 (0.10) | 0.766 |
| | *Endocladia muricata* | 6 | -67.37 (9.97) | **0.008** | 49.41 (4.36) | **0.006** | 0.10 (0.01) | **0.006** |
| | *Halosaccion glandiformis* | 6 | -129.96 (20.95) | 0.001 | 14.29 (0.85) | **< 0.001** | $1.0x10^{-3}$ ($7.2x10^{-5}$) | **0.002** |
| | *Hymenena multiloba* | 4 | -161.70 (36.20) | **0.026** | 143.43 (16.34) | **0.022** | 1.04 (0.12) | **0.023** |
| | *Lithothamnion phymatodeum*‡ | 4 | -155.43 (25.19) | **0.005** | 134.24 (11.29) | **0.009** | 1.41 (0.11) | **0.007** |
| | *Mastocarpus alaskensis* | 4 | -63.42 (63.67) | 0.377 | 15.60 (25.07) | 0.776 | -0.02 (0.02) | 0.680 |
| | *Neorhodomela larix* | 4 | 97.13 (64.44) | 0.232 | -122.07 (40.48) | 0.229 | -0.18 (0.07) | 0.281 |
| | *Odonthalia floccosa* | 6 | -114.65 (41.39) | **0.019** | 144.05 (17.53) | **0.020** | 0.13 (0.02) | **0.038** |
| | *Porphyra sp.* | 4 | 149.00 (27.61) | **0.017** | -181.85 (17.45) | 0.014 | -0.17 (0.02) | **0.038** |
| | *Pseudolithophyllum whidbeyense*‡ | 5 | -122.87 (20.99) | **0.006** | 92.92 (7.50) | **0.005** | 2.94 (0.19) | **0.002** |
| | *Weeksia coccinea* | 6 | 46.57 (28.48) | 0.162 | -44.14 (10.42) | 0.145 | -0.61 (0.20) | 0.275 |
| Viridiplante | *Phyllospadix scouleri* | 6 | -756.59 (72.36) | **< 0.001** | 151.92 (4.60) | **< 0.001** | 0.07 ($4.8x10^{-3}$) | **0.002** |

## APPENDIX 2B: SEAWATER CHARACTERISTICS

**Table 2.B.1**. **Source pH, temperature, salinity and nutrient profile of seawater collected for pH* assays.** All concentrations are in µM.

| seawater batch | date collected | source pH | source temp (ºC) | source salinity | $[PO_4]$ | $[Si(OH)_4]$ | $[NO_3]$ | $[NO_2]$ | $[NH_4]$ |
|---|---|---|---|---|---|---|---|---|---|
| SW04 | 06/19/13 | 8.11 | 12.2 | 35 | - | - | - | - | - |
| SW05 | 06/21/13 | 7.83 | 12.7 | 34 | - | - | - | - | - |
| SW06 | 06/21/13 | 7.83 | 12.7 | 34 | - | - | - | - | - |
| SW07 | 06/24/13 | 7.97 | 12.7 | 34 | - | - | - | - | - |
| SW08 | 06/25/13 | 8.03 | 13.2 | 32 | 1.85 | 46.93 | 20.67 | 0.27 | 0.82 |
| SW09 | 06/29/13 | 8.34 | 18.8 | 30 | - | - | - | - | - |
| SW10 | 06/30/13 | 8.33 | 19.4 | 29 | 0.17 | 8.23 | 0.14 | 0.03 | 0.09 |
| SW11 | 07/06/13 | 8.24 | 14.0 | 32 | 0.65 | 22.08 | 3.49 | 0.18 | 0.09 |
| SW12 | 07/08/13 | 8.08 | 13.2 | 32 | - | - | - | - | - |
| SW13 | 07/09/13 | 8.00 | 14.4 | 33 | 1.73 | 48.89 | 15.44 | 1.06 | 0.62 |
| SW14 | 07/13/13 | 7.91 | 14.5 | 32 | 1.78 | 44.95 | 20.10 | 0.35 | 0.76 |

## APPENDIX 2C: PH* DATA FOR RHODOPHYTA AND PHAEOPHYTA FROM THE LITERATURE

**Table 2.C.1. Mean pH* for each of 111 species from Phylum Rhodophyta.** Species data are compiled and averaged by family membership into 30 families for ancestral state reconstruction and stochastic character mapping. Mean species pH* are taken from a meta analysis of 25 pH* studies (Stepien 2015). † indicates data from this study contributed to the species mean. Families in which at least one member has a CCM were designated as having CCMs. Grey shading indicates families and species that are categorized as having CCMs. The cutoff for CCM presence in individual species was pH* > 9.05.

| family | CCM in at least one taxa | Mean family pH* | n | % of species with CCM | % of species without CCM | species | mean species pH* | species CCM |
|---|---|---|---|---|---|---|---|---|
| Balliaceae | no | 8.76 | 1 | - | - | *Ballia callitricha* | 8.76 | no |
| Bangiaceae | yes | 9.63 | 10 | 90% | 10% | *Porphyra umbilicalis* | 9.91 | yes |
| | | | | | | *Porphyra perforata* | 9.84 | yes |
| | | | | | | *Porphyra fucicola* | 9.80 | yes |
| | | | | | | *Porphyra endiviifolium* | 9.77 | yes |
| | | | | | | *Polysiphonia nigrescens* | 9.70 | yes |
| | | | | | | *Porphyra papenfussii* | 9.69 | yes |
| | | | | | | *Porphyra sp. 3* † | 9.62 | yes |
| | | | | | | *Polysiphonia violaceae* | 9.60 | yes |
| | | | | | | *Porphyra torta* | 9.55 | yes |
| | | | | | | *Polysiphonia sp. 4* | 8.78 | no |
| Bonnemaisoniaceae | no | 8.89 | 1 | - | - | *Bonnemaisonia nootkana* | 8.89 | no |
| Ceramiaceae_Call | yes | 9.03 | 2 | 50% | 50% | *Callithamnion pikeanum* † | 9.21 | yes |
| | | | | | | *Euptilota articulata* | 8.84 | no |
| Ceramiaceae_CerAnt | yes | 9.64 | 4 | 75% | 25% | *Ceramium pacificum* | 10.25 | yes |
| | | | | | | *Ceramium rubrum* | 9.72 | yes |
| | | | | | | *Microcladia borealis* † | 9.60 | yes |
| | | | | | | *Pterothamnion pectinatum* | 8.97 | no |
| Ceramiaceae_Grif | no | 8.96 | 2 | 0% | 100% | *Anotrichium crinitum* | 8.98 | no |
| | | | | | | *Ptilota plumosa* | 8.94 | no |
| Champiaceae | yes | 9.59 | 1 | - | - | *Neogastroclonium subarticulatum* | 9.59 | yes |
| Corallinaceae | yes | 9.05 | 8 | 50% | 50% | *Corallina frondescens* † | 9.59 | yes |
| | | | | | | *Bossiella sp. 1* † | 9.43 | yes |
| | | | | | | *Corallina vancouveriensis* † | 9.34 | yes |
| | | | | | | *Corallina officinalis* | 9.17 | yes |

| Table 2.C.1 continued. Mean pH* for each of 111 species from Phylum Rhodophyta. | | | | | | | | |
|---|---|---|---|---|---|---|---|---|
| **family** | **CCM in at least one taxa** | **Mean family pH*** | **n** | **% of species with CCM** | **% of species without CCM** | **species** | **mean species pH*** | **species CCM** |
| | | | | | | *Jania rosea* | 8.92 | no |
| | | | | | | *Arthrocardia sp. 1* | 8.86 | no |
| | | | | | | *Lithothamnion phymatodeum* † | 8.64 | no |
| | | | | | | *Pseudolithophyllum whidbeyense* † | 8.48 | no |
| Cystocloniaceae | yes | 8.92 | 3 | 33% | 67% | *Cystoclonium purpureum* | 9.40 | yes |
| | | | | | | *Craspedocarpus venosus* | 8.79 | no |
| | | | | | | *Rhodophyllis membranacea* | 8.59 | no |
| Delesseriaceae_Delles | no | 8.75 | 3 | 0% | 100% | *Membranoptera alata* | 8.79 | no |
| | | | | | | *Hemineura frondosa* | 8.76 | no |
| | | | | | | *Delesseria sanguinea* | 8.70 | no |
| Delesseriaceae_Phyco | no | 8.78 | 9 | 0% | 100% | *Polyneura latissima* | 8.98 | no |
| | | | | | | *Hymenena flabelligera* | 8.89 | no |
| | | | | | | *Hymenena durvilleai* | 8.85 | no |
| | | | | | | *Hymenena multiloba* † | 8.83 | no |
| | | | | | | *Myriogramme gunniana* | 8.79 | no |
| | | | | | | *Halicnide similans* | 8.74 | no |
| | | | | | | *Phycodrys rubens* | 8.70 | no |
| | | | | | | *Cryptopleura ruprechtiana* † | 8.64 | no |
| | | | | | | *Schizoseris sp. 1* | 8.59 | no |
| Dumontiaceae | yes | 9.57 | 6 | 100% | 0% | *Dumontia contorta* | 10.00 | yes |
| | | | | | | *Dumontia incrassata* | 9.85 | yes |
| | | | | | | *Constantinea subulifera* | 9.70 | yes |
| | | | | | | *Dilsea carnosa* | 9.40 | yes |
| | | | | | | *Dilsea pygmaea* † | 9.32 | yes |
| | | | | | | *Weeksia coccinea* † | 9.18 | yes |
| Endocladiaceae | yes | 9.43 | 1 | - | - | *Endocladia muricata* † | 9.43 | yes |
| Fryeellaceae | no | 8.85 | 1 | - | - | *Fryeella gardneri* | 8.85 | no |
| Furcellariaceae | yes | 9.12 | 2 | 50% | 50% | *Furcellaria lumbricalis* | 9.20 | yes |
| | | | | | | *Opuntiella californica* | 9.04 | no |
| Gigartinaceae | yes | 9.49 | 7 | 100% | 0% | *Chondracanthus exasperatus* | 9.71 | yes |
| | | | | | | *Iridaea cordata* | 9.60 | yes |
| | | | | | | *Chondrus crispus* | 9.56 | yes |
| | | | | | | *Mazzaella flaccida* † | 9.49 | yes |
| | | | | | | *Mazzaella affinis* † | 9.43 | yes |

| Table 2.C.1 continued. Mean pH* for each of 111 species from Phylum Rhodophyta. | | | | | | | | |
|---|---|---|---|---|---|---|---|---|
| **family** | **CCM in at least one taxa** | **Mean family pH*** | **n** | **% of species with CCM** | **% of species without CCM** | **species** | **mean species pH*** | **species CCM** |
| | | | | | | *Mazzaella splendens* † | 9.36 | yes |
| | | | | | | *Mazzaella parksii* † | 9.31 | yes |
| Gracilariaceae | yes | 9.30 | 6 | 83% | 17% | *Gracilariopsis lemaneiformis* | 9.58 | yes |
| | | | | | | *Gracilaria conferta* | 9.50 | yes |
| | | | | | | *Gracilaria pacifica* | 9.43 | yes |
| | | | | | | *Gracilaria gaditana* | 9.40 | yes |
| | | | | | | *Gracilaria sp. 3* | 9.06 | yes |
| | | | | | | *Curdiea angustata* | 8.81 | no |
| Halymeniaceae | yes | 9.11 | 8 | 50% | 50% | *Prionitis sternbergii* | 9.55 | yes |
| | | | | | | *Prionitis lanceolata* | 9.46 | yes |
| | | | | | | *Halymenia schizymenioides* | 9.38 | yes |
| | | | | | | *Halymenia gardneri* | 9.35 | yes |
| | | | | | | *Polyopes constrictus* | 8.96 | no |
| | | | | | | *Halymenia sp. 2* | 8.94 | no |
| | | | | | | *Thamnoclonium dichotomum* | 8.79 | no |
| | | | | | | *Carpopeltis phyllophora* | 8.49 | no |
| Kallymeniaceae | no | 8.81 | 4 | 0% | 100% | *Euthora cristata* | 8.92 | no |
| | | | | | | *Callophyllis rangiferina* | 8.82 | no |
| | | | | | | *Kallymenia cribrosa* | 8.81 | no |
| | | | | | | *Callophyllis lambertii* | 8.71 | no |
| Liagoraceae | yes | 9.77 | 1 | - | - | *Cumagloia andersonii* † | 9.77 | yes |
| Lomentariaceae | no | 8.98 | 1 | - | - | *Lomentaria articulata* | 8.98 | no |
| Palmariaceae | yes | 10.32 | 3 | 100% | 0% | *Palmaria decipiens* | 10.61 | yes |
| | | | | | | *Halosaccion glandiforme* † | 10.47 | yes |
| | | | | | | *Palmaria palmata* † | 9.87 | yes |
| Peyssonneliaceae | no | 8.88 | 1 | - | - | *Sonderopelta coriacea* | 8.88 | no |
| Phacelocarpaceae | no | 8.82 | 1 | - | - | *Phacelocarpus peperocarpos* | 8.82 | no |
| Phyllophoraceae | yes | 9.84 | 5 | 0% | 100% | *Mastocarpus papillatus* | 10.34 | yes |
| | | | | | | *Mastocarpus alaskensis* † | 9.95 | yes |
| | | | | | | *Mastocarpus stellatus* | 9.90 | yes |
| | | | | | | *Ahnfeltiopsis leptophylla* | 9.56 | yes |
| | | | | | | *Mastocarpus jardiini* † | 9.46 | yes |
| Plocamiaceae | no | 8.69 | 3 | 0% | 100% | *Plocamium cartilagineum* | 8.87 | no |
| | | | | | | *Plocamium dilatatum* | 8.64 | no |

| Table 2.C.1 continued. Mean pH* for each of 111 species from Phylum Rhodophyta. | | | | | | | | |
|---|---|---|---|---|---|---|---|---|
| **family** | **CCM in at least one taxa** | **Mean family pH*** | **n** | **% of species with CCM** | **% of species without CCM** | **species** | **mean species pH*** | **species CCM** |
| | | | | | | *Plocamium sp. 1* | 8.56 | no |
| Rhodomelaceae | yes | 9.52 | 10 | 80% | 20% | *Neorhodomela oregona* | 10.19 | yes |
| | | | | | | *Neorhodomela larix* † | 9.99 | yes |
| | | | | | | *Odonthalia floccosa* † | 9.80 | yes |
| | | | | | | *Polysiphonia lanosa* | 9.77 | yes |
| | | | | | | *Osmundea pinnatifida* | 9.73 | yes |
| | | | | | | *Polysiphonia hendryi gardneri* | 9.54 | yes |
| | | | | | | *Osmundea spectabilis* † | 9.48 | yes |
| | | | | | | *Odonthalia washingtoniensis* | 9.24 | yes |
| | | | | | | *Lenormandia marginata* | 9.01 | no |
| | | | | | | *Laurencia sp. 2* | 8.40 | no |
| Rhodymeniaceae | no | 8.71 | 3 | 0% | 100% | *Sparlingia pertusa* | 8.97 | no |
| | | | | | | *Rhodymenia sp. 2* | 8.69 | no |
| | | | | | | *Gloiosaccion brownii* | 8.48 | no |
| Schizymeniaceae | no | 9.02 | 1 | - | - | *Schizymenia pacifica* | 9.02 | no |
| Solieriaceae | yes | 9.23 | 2 | 100% | 0% | *Sarcodiotheca gaudichaudii* | 9.32 | yes |
| | | | | | | *Sarcodiotheca furcata* | 9.13 | yes |

**Table 2.C.2. Mean pH* for each of 51 species from Phylum Ochrophyta.** Species data are compiled and averaged by family membership into 18 families for ancestral state reconstruction and stochastic character mapping. Mean species pH* are taken from a meta analysis of 25 pH* studies (Stepien 2015). † indicates data from this study contributed to the species mean. Families in which at least one member has a CCM were designated as having CCMs. Grey shading indicates families and species that are categorized as having CCMs. The cutoff for CCM presence in individual species was pH* > 9.05.

| family | CCM in at least one taxa | mean family pH* | n | % species with CCM | % species without CCM | species | mean species pH* | species CCM |
|---|---|---|---|---|---|---|---|---|
| Alariaceae | yes | 9.23 | 3 | 100% | 0% | *Alaria marginata* † | 9.42 | yes |
| | | | | | | *Alaria esculenta* | 9.33 | yes |
| | | | | | | *Undaria pinnatifida* | 9.09 | yes |
| Chordaceae | yes | 9.20 | 1 | - | - | *Chorda filum* | 9.20 | yes |
| Chordariaceae | yes | 9.68 | 2 | 100% | 0% | *Leathesia difformis* | 10.15 | yes |
| | | | | | | *Leathesia marina* † | 9.21 | yes |
| Desmarestiaceae | no | 8.98 | 1 | - | - | *Desmarestia aculeata* | 8.98 | no |
| Dictyotaceae | yes | 9.00 | 4 | 25% | 75% | *Dictyopteris muelleri* | 9.27 | yes |
| | | | | | | *Dictyota sp. 2* | 8.99 | no |
| | | | | | | *Zonaria angustata* | 8.94 | no |
| | | | | | | *Zonaria turneriana* | 8.82 | no |
| Fucaceae | yes | 9.77 | 7 | 100% | 0% | *Fucus vesiculosus* | 10.03 | yes |
| | | | | | | *Fucus gardneri* † | 9.87 | yes |
| | | | | | | *Fucus spiralis* | 9.84 | yes |
| | | | | | | *Ascophyllum nodosum* | 9.72 | yes |
| | | | | | | *Fucus serratus* | 9.70 | yes |
| | | | | | | *Pelvetia canaliculata* | 9.70 | yes |
| | | | | | | *Pelvetiopsis limitata* † | 9.55 | yes |
| Himanthaliaceae | yes | 9.89 | 1 | - | - | *Himanthalia elongata* | 9.89 | yes |
| Hormosiraceae | yes | 9.77 | 1 | - | - | *Hormosira banksii* | 9.77 | yes |
| Laminariaceae | yes | 9.14 | 6 | 83% | 17% | *Saccharina latissima* | 9.38 | yes |
| | | | | | | *Laminaria digitata* | 9.21 | yes |
| | | | | | | *Macrocystis pyrifera* | 9.14 | yes |
| | | | | | | *Laminaria hyperborea* | 9.10 | yes |
| | | | | | | *Saccharina groendlandica* † | 9.08 | yes |
| | | | | | | *Saccharina sessilis* † | 8.96 | no |
| Lessoniaceae | no | 8.97 | 1 | - | - | *Ecklonia radiata* | 8.97 | no |
| Notheiaceae | yes | 9.85 | 1 | - | - | *Notheia anomala* | 9.85 | yes |
| Ralfsiaceae | yes | 9.48 | 1 | - | - | *Analipus japonicus* † | 9.48 | yes |
| Sargassaceae | yes | 9.27 | 12 | 100% | 0% | *Sargassum muticum* | 9.74 | yes |
| | | | | | | *Halidrys siliquosa* | 9.50 | yes |

| Table 2.C.2 continued. Mean pH* for each of 51 species from Phylum Ochrophyta. | | | | | | | | |
|---|---|---|---|---|---|---|---|---|
| **family** | **CCM in at least one taxa** | **mean family pH*** | **n** | **% species with CCM** | **% species without CCM** | **species** | **mean species pH*** | **species CCM** |
| | | | | | | *Sargassum lacerifolium* | 9.38 | yes |
| | | | | | | *Sargassum henslowianum* | 9.37 | yes |
| | | | | | | *Cystophora retroflexa* | 9.23 | yes |
| | | | | | | *Landsburgia quercifolia* | 9.20 | yes |
| | | | | | | *Carpophyllum flexuosum* | 9.20 | yes |
| | | | | | | *Carpophyllum plumosum* | 9.17 | yes |
| | | | | | | *Carpophyllum maschalocarpum* | 9.15 | yes |
| | | | | | | *Carpoglossum confluens* | 9.14 | yes |
| | | | | | | *Carpophyllum angustifolium* | 9.14 | yes |
| | | | | | | *Sargassum heteromorphum* | 9.08 | yes |
| Scytosiphonaceae | no | 8.94 | 1 | - | - | *Colpomenia sinuosa* | 8.94 | no |
| Seirococcaceae | yes | 9.09 | 3 | 67% | 33% | *Seirococcus axillaris* | 9.19 | yes |
| | | | | | | *Phyllospora comosa* | 9.09 | yes |
| | | | | | | *Marginariella boryana* | 8.99 | no |
| Sporochnaceae | yes | 9.13 | 2 | 50% | 50% | *Carpomitra costata* | 9.35 | yes |
| | | | | | | *Sporochnus sp. 1* | 8.90 | no |
| Stypocaulaceae | yes | 9.24 | 2 | 100% | 0% | *Halopteris sp. 1* | 9.25 | yes |
| | | | | | | *Halopteris paniculata* | 9.23 | yes |
| Xiphophoraceae | yes | 9.39 | 2 | 100% | 0% | *Xiphophora chondrophylla* | 9.45 | yes |
| | | | | | | *Xiphophora gladiata* | 9.34 | yes |

# CHAPTER III

# IMPACT OF GEOGRAPHY, TAXONOMY, AND FUNCTIONAL GROUP ON INORGANIC CARBON USE PATTERNS IN MARINE MACROPHYTES[1]


## ABSTRACT

**1.** Carbon uptake in terrestrial plants functions under near-constant source carbon dioxide ($CO_2$) concentrations and isotopic ratios, but aquatic macrophytes operate in a more complex system where environmental fluxes and biotic interactions undermine assumptions of constant $CO_2$ concentration and $^{13}C/^{12}C$.

**2.** Many marine macrophytes not only passively access $CO_2$ for photosynthesis, but also actively concentrate $CO_2$ and bicarbonate ($HCO_3^-$) using carbon concentration mechanisms (CCMs). These processes change macrophyte carbon fractionation signatures ($^{13}C/^{12}C$) and elevate seawater pH as high as 10.4 in mesocosm pH assays, in which the pH value reached is termed pH*.

**3.** I assembled a global dataset of 2027 marine macrophyte $\delta^{13}C$ and pH assay values for 664 species to assess (i) how macrophyte $\delta^{13}C$ varies with the abiotic parameters sea surface temperature, latitude, and habitat, and the organismal traits of taxonomic and functional group membership, and (ii) how species $\delta^{13}C$ is related to CCM presence or absence, as determined by a pH drift assay.

**4.** Across 613 macrophyte species, collection site distance from the equator was negatively


1 This manuscript previously appeared in *Journal of Ecology*, 2015, volume 103, pages 1372-1383. Included with permission.

related to species $\delta^{13}C$, while collection site variance in sea surface temperature was positively related to species $\delta^{13}C$. Macrophyte tissue $\delta^{13}C$ differed among oceans as well as in intertidal versus subtidal habitats. Species from phylum Rhodophyta had the lowest $\delta^{13}C$, and functional group was related to $\delta^{13}C$, largely due to higher $\delta^{13}C$ in calcifying species.

**5.** Analysis of 141 species with paired pH*-$\delta^{13}C$ data found that these metrics of CCM presence are not independent. As species $\delta^{13}C$ increases so does the probability of species pH* > 9.0, a threshold value of CCM presence in pH assays.

**6.** *Synthesis.* CCMs revealed species patterns in communities at every scale investigated, from local emersion gradients to oceanic and global gradients. Trends in macrophyte $\delta^{13}C$ values indicate that macrophytes rely more on $CO_2$ further from the equator, but have increased use of $HCO_3^-$ at sites with high temperature variance, patterns that may be driven by species turnover rather than intraspecific variation. Patterns in species CCMs will be crucial to understanding how macrophyte communities respond to ocean acidification-induced changes to sea surface temperature and variability.

## INTRODUCTION

While phytoplankton are the primary drivers of carbon cycling in the open ocean (Litchman et al. 2015), marine macrophytes – seaweeds and surfgrasses – play significant roles in coastal carbon cycling, providing the bulk of primary productivity in coastal zones and locally raising seawater pH during peak photosynthesis hours (Wootton et al. 2008). As the oceanic carbonate cycle is increasingly altered by fossil fuel carbon dioxide ($CO_2$, (Orr et al. 2005)), there is growing interest in how macrophytes in coastal systems will continue to interact with carbon. When $CO_2$

dissolves in water, it can bind with a water molecule to form carbonic acid, which can either lose one $H^+$ to form bicarbonate ($HCO_3^-$) or two $H^+$ to form carbonate ($CO_3^{2-}$). At ambient seawater pH of roughly 8.0, $HCO_3^-$ comprises 92% of dissolved inorganic carbon (DIC) in the surface ocean, with carbonate ($CO_3^{2-}$) comprising 7% and $CO_2$ making up the remaining 1%. At seawater pH > 9.0, the DIC equilibrium shifts even further towards $HCO_3^-$, and $CO_2$ concentration approaches zero (Maberly 1990, Raven et al. 2005). Thus, while all macrophytes are able to take up $CO_2$, the majority of them can also access $HCO_3^-$ by employing carbon concentration mechanisms (CCMs), leading to differential fractionation of carbon isotopes in macrophyte tissue (Maberly et al. 1992, Giordano et al. 2005). Indeed, a previous review found that 80% of 100 macrophyte species studied had CCMs (Raven et al. 2002b). DIC can be viewed as a resource among competitors (Connell et al. 2013). There are energetic costs to operating CCMs (Raven et al. 2014), and differential abilities to concentrate carbon may lead to the increased competitiveness of macrophytes without CCMs (Raven et al. 2002b) and shifts in dominance within communities (Low-Décarie et al. 2014) as $CO_2$ availability increases through the process of ocean acidification.

Marine and terrestrial phototrophs alike discriminate between C isotopes during carbon uptake and photosynthesis, but they do so under very different conditions. While atmospheric $CO_2$ $\delta^{13}C$ has decreased over the past 30 years from approximately -7.8‰ (noted as deviations from the $^{13}C/^{12}C$ ratio of the Pee-Dee Belemnite $CaCO_3$ [PDB]) (Ehleringer 1991) to -8.3‰ (Cuntz 2011), atmospheric $CO_2$ $\delta^{13}C$ has a generally low range within a year (± 0.25‰ of mean annual value (Cuntz 2011)). However, in marine systems coastal upwelling, pH and salinity variation, wave action and freshwater estuarine inputs can all influence the local seawater carbon

availability, and dissolved $CO_2$, $HCO_3^-$ and $CO_3^{2-}$ each have a different temperature-dependent $\delta^{13}C$ value (Maberly et al. 1992). Intertidal macroalgae experience the additional complexity of being emerged and exposed to atmospheric $CO_2$ for part of the day, and individuals in tidepools cope with drastic changes in carbon availability and seawater pH (Truchot and Duhamel-Jouve 1980). Due to the slow diffusion of $CO_2$ in water, dissolved inorganic carbon availability in boundary layers surrounding macrophytes may become locally depleted (Hurd 2000, Cornwall et al. 2013) as organisms take up $CO_2$ and increase pH during hours of peak photosynthesis (Wootton et al. 2008). Together, these factors undermine the assumptions of constant isotope signature and availability of source carbon in coastal marine systems as they are generally applied in terrestrial environments.

Marine macrophytes are diverse in their interactions with and influences on the DIC system. Marine macrophytes employ far more diverse CCMs than their terrestrial counterparts, through internal mechanisms within the algal chloroplast, in the surrounding cytosol and plasma membrane, or even outside the organism in the boundary layer (Badger et al. 1998). In addition to passive diffusion of $CO_2$ and $HCO_3^-$, both molecules may be actively transported into the cell through membrane ATPases (Giordano et al. 2005). Seaweeds may secrete substances to acidify parts of their boundary layer, locally shifting the DIC equilibrium to favor the creation of $CO_2$ from $HCO_3^-$. Still many other organisms employ carbonic anhydrases either externally or internally to convert $HCO_3^-$ into $CO_2$ (Moroney et al. 2013). These processes may locally change the total alkalinity of seawater, further shifting the local relative proportions of dissolved $CO_2$, $HCO_3^-$ and $CO_3^{2-}$ (Stepien *et al.*, Chapter 2). Furthermore, calcifying algae, which have a unique relationship with the seawater DIC system, use carbonate to build their calcium carbonate

cellular structure (McConnaughey and Whelan 1997). This diversity of CCMs and access to multiple dissolved inorganic carbon forms can strongly influence the $\delta^{13}C$ of macrophyte tissue.

Naturally occurring stable isotopes of carbon in macrophytes can be used to infer CCM presence. Assuming a seawater $\delta^{13}C$ of 0‰ at 10°C under equilibrium conditions with the atmosphere and carbon isotopic fractionation of -10.72 between $CO_2$ and $HCO_3^-$ (Mook et al. 1974), the $\delta^{13}C$ of seawater $CO_2$ is -10.64‰ and +0.08‰ for $HCO_3^-$ (Maberly et al. 1992). Thus, a tissue $\delta^{13}C > -10$‰ (and close to 0‰) is expected in macrophytes that use only $HCO_3^-$, while species that exclusively take up $CO_2$ would have $\delta^{13}C < -30$ ‰. In reality, the majority of macrophytes use a combination of these two inorganic carbon sources, leading to a $\delta^{13}C$ value falling within these two end members (Raven 1997, Kübler et al. 1999, Raven et al. 2002b). Different forms of the enzyme RUBISCO differ somewhat in their discrimination between carbon isotopes (Raven and Beardall 2014), which may also contribute to 'middle-range' $\delta^{13}C$ values observed among some macrophytes.

More direct methods of inferring CCMs investigate carbon depletion from seawater or inhibit enzymes involved in CCMs. ATPase channels and other ion transport channels can be inhibited and the resulting change in oxygen evolution measured (Moulin et al. 2011), external and internal carbonic anhydrase can be assayed (Wilbur and Anderson 1948, Mercado et al. 1997) or targeted for inhibition (Haglund et al. 1992, Campbell and Fourqurean 2013) and pH drift assays measure the depletion of carbon by macrophytes as the change in seawater pH in an enclosed mesocosm (Maberly 1990). At pH > 9, the concentration of dissolved $CO_2$ is less than 1 µmol/kg seawater (essentially 0% of DIC) so that any further DIC depletion indicates the ability to take up $HCO_3^-$ for use in photosynthesis. I designate the upper boundary of macrophyte-

induced seawater pH change as pH*, reflecting the equilibrium concentration of DIC that a species can access, and analogous to the R* used to describe nutrient depletion (Tilman 1981).

While the presence or absence of and reliance on CCMs in macrophytes with $\delta^{13}C$ values between -30 and -10‰ is more difficult to ascertain, there is a relationship between pH* values and $\delta^{13}C$, in which species lacking CCMs according to a pH assay have corresponding depleted $\delta^{13}C$ values (Maberly et al. 1992). Both metrics measure effects of CCMs, however while a pH drift assay is an immediate measure of current CCM reliance and $HCO_3^-$ use over 24 hours, $\delta^{13}C$ represents a time-integrated measurement of $HCO_3^-$ and $CO_2$ incorporation into macrophyte tissue over the life of the organism. While $HCO_3^-$ use cannot be entirely ruled out at pH* < 9.0, the contribution of bicarbonate to total carbon uptake can be concluded to be low, and species in these ranges largely rely on $CO_2$ as a carbon source for photosynthesis (Maberly et al. 1992).

There is evidence of global and local scale trends in marine macrophyte $\delta^{13}C$. Species in warmer zones have a decreased range of $\delta^{13}C$ values as well as generally higher $\delta^{13}C$ (Raven et al. 2002a, Marconi et al. 2011). This may be because, in contrast to most terrestrial plants, photosynthetic machinery in macrophytes is at nearly the same temperature as the seawater medium (Raven et al. 2002a). Vertical depth trends have also been observed along the coastal emersion gradient from the intertidal to the subtidal, with decreasing $\delta^{13}C$ and pH* values with water depth, likely due to increased light limitation at greater depths (Raven et al. 2002b, Murru and Sandgren 2004).

Organismal traits have also been linked to $\delta^{13}C$ and CCM patterns. Rhodophytes have generally lower $\delta^{13}C$ values than other macroalgal phyla (Raven et al. 2002b). Although marine macrophytes are not as structurally complex as vascular plants, carbon metabolism in seaweeds

is integrated in multicellular structure that in many seaweed groups leads to several angiosperm-like traits (Gómez and Huovinen 2012). Macrophyte morphology has been linked to photosynthetic performance and carbon uptake using functional group categories (Littler and Littler 1980, Steneck and Watling 1982).

In this study, I test the generality and repeatability of local and global scale patterns in $\delta^{13}C$ and pH* values with a dataset of 1753 $\delta^{13}C$ and pH* values from 664 seaweed and surfgrass species. I asked 1) how extrinsic environmental variables influence global macrophyte $\delta^{13}C$ patterns, 2) what intrinsic organismal variables are predictive of species $\delta^{13}C$ values and 3) how species $\delta^{13}C$ is related to CCM presence or absence, as determined by a pH drift assay. I explored the effects of habitat parameters such as ocean basin membership and basin side, sea surface temperature and latitude on species $\delta^{13}C$ values, and investigated how species' functional group membership, taxonomy and physiology correspond to natural $^{13}C$ abundances. I find significant ocean-scale and global-scale environmental patterns in macrophyte inorganic carbon uptake regimes, which are largely the result of turnover in macrophytes species, in addition to trait-based patterns in the relationship between calcification and macrophyte functional group membership and macrophyte $\delta^{13}C$.

## MATERIALS AND METHODS

### Literature search and data compilation

I conducted a literature survey to compile $\delta^{13}C$ and pH drift studies for macroalgae (Chlorophyta, Rhodophyta, Ochrophyta) and surfgrass (Tracheophyta), together termed 'macrophytes.' $\delta^{13}C$ studies conducted prior to 2001 have been well reviewed (Raven et al. 2002b). I searched for

publications between 1960 and 2015 in Google Scholar, based on papers containing at least one of the keywords “pH drift,” “pH drift assay,” “pH compensation,” “carbon isotope,” and “$\delta^{13}C$,” combined with at least one of the keywords “macrophyte,” “seaweed”, “macroalgae,” and “surfgrass.” pH* data from assays run for insufficient time to reach a plateau were excluded, as were composite $\delta^{13}C$ values for tissue samples containing multiple species. Calcifying species $\delta^{13}C$ values were only included if specimens were decalcified prior to isotopic analysis, and specimens for which $\delta^{13}C$ was measured after long-term laboratory manipulations were excluded. The following data were extracted from a final set of 76 papers published between 1964 and 2015: species-level and individual specimen $\delta^{13}C$ and pH* values, geographical coordinates of collection site, date of specimen collection, and collection depth and habitat. $\delta^{13}C$ and pH* values were entered from published tables, or estimated from figures when authors could not be contacted. Data ranged from species means and standard deviations to individual reported values of single specimens. Where collection site coordinates were ambiguous or not indicated (for example, an entire country as a collection locality), latitude and longitude were approximated based on the name and description of the site. Depth data was entered as continuous data (e.g. meters) and habitat was categorized as intertidal, intertidal-subtidal, or subtidal based on the classification in the study. If collection date was not specified, the date was binned as earlier than the date of publication. While most studies were specific to pH* and $\delta^{13}C$ values of macrophytes, many studies included macrophytes as part of a trophic analysis of coastal ecosystems.

**Environmental parameters of collection sites**

Mean monthly sea surface temperature (SST) was compiled for each collection site from the

NOAA SOCAT database (Pfeil et al. 2012, Sabine et al. 2012). Mean annual SST, maximum monthly SST, minimum monthly STT and the range and variance of monthly SST values per site were calculated for the area ± 0.5º latitude and longitude around each collection point. When collection site resolution was only at the scale of an entire country or region, mean monthly SST was downloaded for the minimum area of the collection site as described in the paper. Collection sites were categorized by ocean basin (North Pacific, South Pacific, North Atlantic, South Atlantic, South China, Arctic, Southern, Baltic, Indian) and designated as either from the eastern or western side of a basin. Distance from the equator was noted as the absolute value of latitude. Each collection point was categorized as part of the tropical, temperature or polar zone based on latitude (tropical: -23.5º < site latitude < +23.5º; temperate: -23.5º < site latitude < -66.5º or +23.5º < site latitude < +66.5º; polar: +66.5º < latitude or -65.5º > latitude).

**Organismal traits of macrophyte species in relation to $\delta^{13}C$**

Each species was placed into phylum, class, order, and family using AlgaeBase (Guiry and Guiry 2012). Species and genera names no longer taxonomically accepted were updated to current classifications as detailed in AlgaeBase to more accurately reflect species-level analyses. Species listed at the genus level in publications, e.g. *Ulva sp.*, were assigned unique species IDs based on the collection locality. If unidentified species within a genus came from collection sites separated by greater than 10º longitude and latitude, the species were designated as distinct. For example, *Ulva sp.* from Arbroath, Scotland was designated *Ulva sp. 1* and *Ulva sp.* from Western Australia was designated *Ulva sp. 2*. Each species was assigned to one of seven functional-form groups: the six groups described in (Littler and Littler 1980) as sheet, filamentous, coarsely branched,

leathery, jointed calcareous, or crustose, and a seventh crustose calcifying group. Species were also categorized as calcifying or non-calcifying. Species that could be classified as more than one group or had characteristics of multiple groups were excluded from functional analyses.

**Carbon isotope analysis of species with corresponding pH* data**

For a subset of Northeast Pacific species with published pH* values, but no corresponding $\delta^{13}C$ values, I conducted additional isotope analyses. Tissue samples from 31 intertidal species collected from Shi Shi Beach (48.279 N, -124.683 W) and Slip Point, WA (48.260 N, -124.250 W) in 2013 were dried for 24 hours at 60°C, then ground using a stainless steel ball in a 2010 Geno/Grinder (n = 2 - 12 per species, mode = 4). Calcified species were treated with 100mM HCl for 24 hours followed by three rinses with distilled water to remove calcium carbonate (Marconi *et al.* 2011). Samples were analyzed for $^{13}C/^{12}C$ using a Costech Elemental Analyzer combustion system couple to a Thermo Delta Plus IRMS via a Thermo Conflo IV interface at the University of Chicago Stable Isotope Ratio facility. Cocoa powder was used as an isotopic control, and the reproducibility was within 0.11‰ for $\delta^{13}C$. The $^{13}C$ isotopic enrichment in the algal samples was expressed in the unit notation as deviations from the $^{13}C/^{12}C$ ratio of the Pee-Dee Belemnite $CaCO_3$ (PDB).

**Mean $\delta^{13}C$ and pH* results per species**

Because factors outside of inorganic carbon uptake mechanisms may contribute to macrophyte $\delta^{13}C$ and pH* values, I used mean species values for these two metrics of CCM presence, rather than maximum species values. Mean $\delta^{13}C$ and pH* data were calculated both per species and per

species per site. While dataset $\delta^{13}C$ values ranged from individual specimen values to mean species values, standard deviation of overall $\delta^{13}C$ means for 613 species of seaweed and surfgrass was less than ± 5.5‰, excluding 4 species with $\delta^{13}C$ standard deviation of ± 6-8‰. To investigate whether variation in dataset entry units (individual vs. mean values) influenced final species means, I performed a subsampling routine. For species with more than nine database entries, six entries were randomly sampled and averaged for 1000 iterations. The final mean and standard deviation was then calculated from the 1000 iterations. For 30 species with $n > 9$ in the database, the final standard deviation was less than 1.6‰, indicating that variation in dataset entry units is not strongly influencing species' means.

Unless otherwise noted in primary sources, pH* data was assumed to be on the NSB scale. Due to the difficulty of calibrating for the Total pH scale (pHT) and the 50-year span of the dataset, it is likely that the NBS scale was applied in the majority of papers for which pH scale was not noted. Only one paper indicated that pHT was used of the 76 papers in the final dataset. Therefore, data published on the pHT scale was converted to NBS by the addition of 0.12 pH units.

**Investigating how macrophyte $\delta^{13}C$ varies with environment**

To understand which continuous global environmental parameters are associated with species C isotope values, I investigated the relationship mean $\delta^{13}C$ values per species at a site and site-level SST and latitude. I regressed mean $\delta^{13}C$ per species-site individually against the following environmental parameters using a linear mixed effects model, with collection site as a random effect: distance from equator, mean monthly SST, minimum monthly SST, maximum monthly

SST and range and variance of monthly SST at each site.

To investigate how site ocean basin membership and relative location within a basin was associated with species C isotope values, I first tested for an effect of site ocean basin on species $\delta^{13}C$ per site with an Analysis of Variance (ANOVA). To test for a possible effect of ocean currents and upwelling, I tested for an effect of ocean basin side – west or east – on species $\delta^{13}C$ at a site, using an unpaired Student's t-test.

To investigate how the vertical emersion gradient was associated with C isotope values, I tested for an effect of species habitat (intertidal vs. subtidal) on macrophyte $\delta^{13}C$. Due to the low sample size for intertidal or subtidal habitat classification (299 individual entries for 150 species), species replicates were pooled and averaged across sites. I removed from the larger analysis an additional 33 entries in the dataset coded as intertidal-subtidal as well as 12 species present in both the intertidal and subtidal datasets.

**Investigating macrophyte $\delta^{13}C$ variation with species-level traits**

To understand which organismal traits were associated with mean species $\delta^{13}C$, I performed single factor ANOVAs of macrophyte $\delta^{13}C$ by macrophyte functional group classification and by the species' calcification status (calcifying or non-calcifying). I also tested for an effect of species' phylum membership on $\delta^{13}C$ values with an ANOVA to explore if taxonomy is associated with the natural abundance of macrophyte carbon isotopes.

**Investigating the relationship between $\delta^{13}C$ and pH***

To understand how $\delta^{13}C$ and pH* are related, I created a contingency table for the 142 species in

the dataset that had paired $\delta^{13}C$ and pH* data. Cutoffs were based on the pH* and $\delta^{13}C$ thresholds of pH* < 9.0 and $\delta^{13}C$ < -30‰, each individually indicating CCM absence. To test for an effect of taxonomy, I performed a $\chi^2$ test for the full data table and for each of the phylum tables (Chlorophyta, Ochrophyta, Rhodophyta, Tracheophyta). To test for an overall effect of taxonomy, $\chi^2$ and degrees of freedom were summed across phyla, and from this value the $\chi^2$ and degrees of freedom for the all-species analysis was subtracted.

The pH drift assay is one method to determine whether macrophytes have a carbon concentration mechanism (CCM), but it can be time-intensive and difficult to perform. To investigate how well the more easily-quantified organismal trait of species $\delta^{13}C$ relates to the results of a pH drift assaay, I first assigned CCM presence or absence based on pH* to each species. Species with pH* < 9.0 were designated as lacking a CCM and those with pH* > 9.0 were categorized as having a CCM (Surif and Raven 1989, Maberly et al. 1992). I then used a binomial logistic regression to test for an effect of $\delta^{13}C$ on CCM presence of absence as scored by a pH assay. Average predicted probabilities for CCM presence and absence were then generated for each $\delta^{13}C$ value between -40 and 0‰. I also performed a multinomial logistic regression in which a third CCM category was assigned; species where 8.9 < pH* < 9.1 were designated as ambiguous, as it is possible that the number of replicates or assay run time or temperature could shift these near-threshold results in either direction.

## RESULTS

### Dataset compilation

The final dataset consisted of 2027 entries from 76 papers, with 1707 $\delta^{13}C$ entries and 327 pH*

entries (Appendix 3A). Rhodophyta species made up the majority of the dataset (354 of 664 species: 53%), followed by 27% Ochrophyta, 17% Chlorophyta, and the remaining 3% Tracheophyta (Table 3.1). One hundred forty-two species had both pH* and $\delta^{13}C$ data. Macrophyte pH* and $\delta^{13}C$ values were obtained from specimens collected from 156 sites globally (Figure 3.1). The majority of collection sites were in the temperate zone (142 sites), with only eight sites in the tropics and six in the polar zone, and the vast majority of sites (117, 75%) were from the Northern Hemisphere (Appendix 3A). Seventy-six sites were in the North Atlantic, with the remaining oceanic basins and seas making up the other 80 sites: South Pacific, 20; North Pacific, 17; Mediterranean, 14; Indian, 13; Southern, 7; South China, 6; Arctic, 2; Baltic, 1. Sites ranged in mean annual sea surface temperature from -0.9ºC to 29.1ºC.

**Macrophyte $\delta^{13}C$ variation with the environment**

Collection site mean sea surface temperature (SST), maximum SST, minimum SST and variance of SST were positively related to mean species $\delta^{13}C$ per site (linear mixed model regression, $P$ = 0.008, $P$ = 0.003, $P$ = 0.028 and $P$ = 0.037, respectively) and site distance from the equator was negatively related to mean species $\delta^{13}C$ per site (Figure 3.2, linear mixed model, $P$ = 0.003, coefficient of distance from equator = -0.091 ± 0.029). This distance effect was also found among sites within the temperate zone, excluding the polar zones and the tropics (linear mixed model, $P$ = 0.011). With the exclusion of site SST variance, these variables were also highly correlated (mean SST: max SST = 0.97, mean SST: min SST = 0.97, distance from equator: mean SST = -0.93, distance from equator: max SST = -0.86, site range and var in SST: 0.96). Of these metrics of temperature and latitude, none was significantly better than another.

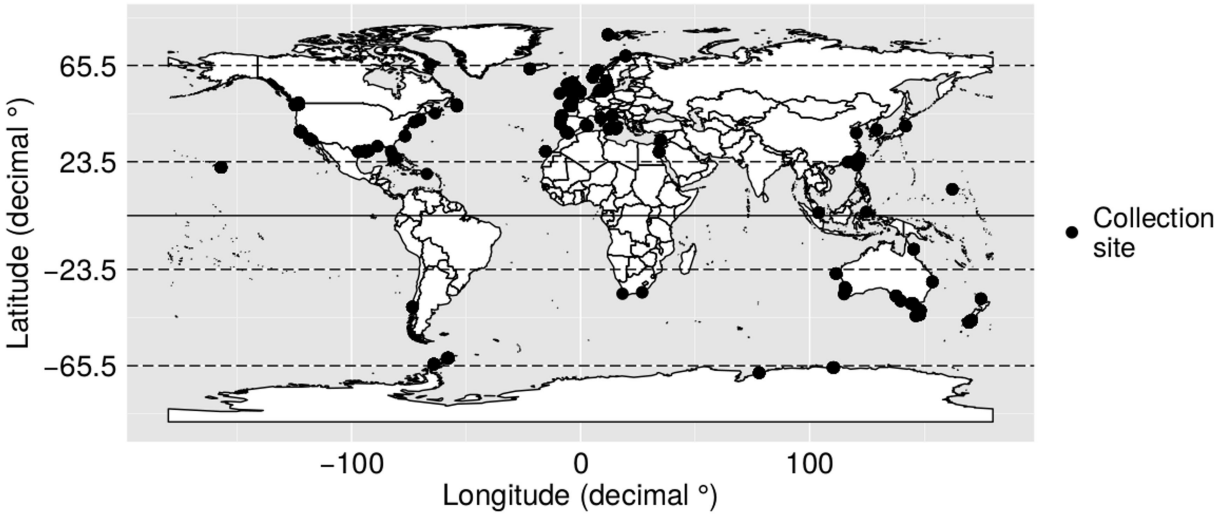


**Figure 3.1.** Source sites for meta analysis. Locations of 135 collection sites for all seaweed and surfgrass values compiled from the literature. Dotted horizontal lines indicate separation between tropical (-23.5º to + 23.5º), temperate (-23.5º to -65.5º and +23.5º to +65.5º) and polar zones (> +65.5º and < -65.5º). Black solid line indicates the equator.

**Table 3.1.** Data composition of meta analysis. Number of species and number of entries extracted from literature and experimental data for each phylum and data type. Numbers in parentheses indicate number of individual entries in the dataset.

| Data type | Chlorophyta | Ochrophyta | Rhodophyta | Tracheophyta | Total |
|---|---|---|---|---|---|
| **Total Species (total entries)** | 116 (344) | 177 (735) | 354 (860) | 17 (87) | 664 (2027) |
| **Species with $\delta^{13}C$ (total entries)** | 113 (305) | 169 (610) | 314 (707) | 17 (84) | 613 (1707) |
| **Species with pH* (total entries)** | 29 (45) | 51 (126) | 110 (153) | 3 (3) | 193 (327) |
| **Species with $\delta^{13}C$ and pH* data (n)** | 26 | 43 | 70 | 2 | 142 |

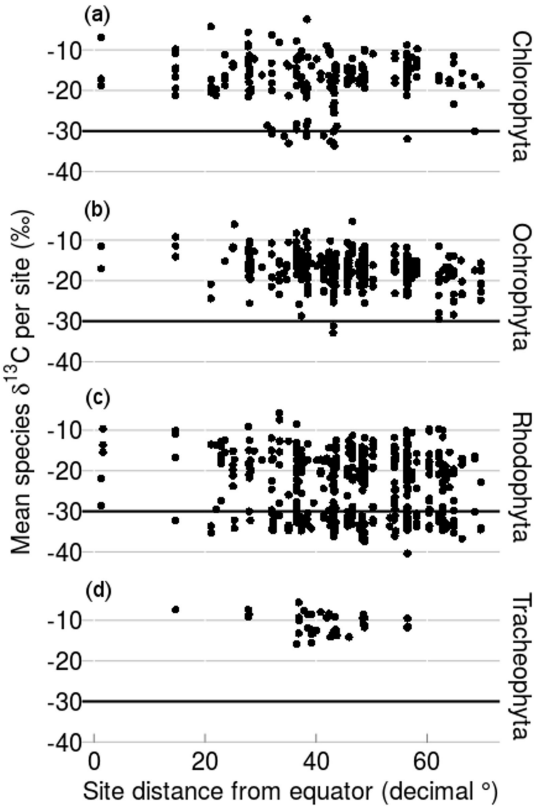


**Figure 3.2.** Site-level macroalgal species $\delta^{13}C$ as a function of site distance from the equator. Tracheophyta was excluded due to low sampling size. Black horizontal line indicates $\delta^{13}C$ = -30‰. Macroalgae with tissue $\delta^{13}C$ below this threshold do not access $HCO_3^-$.

AIC scores for these single factor models were within 2.00 units of each other (Burnham and Anderson 2002): distance from equator, AIC = 8131.45; maximum SST, AIC = 8130.35; mean SST, AIC = 8132.20; site SST variance, AIC = 11294.39, minimum SST, AIC = 11294.54). Climate zone and site SST range were not related to mean species $\delta^{13}C$ per site.

While there was an overall negative relationship between $\delta^{13}C$ per site and distance from equator, there were distinct effects among macrophyte phylum. There was no relationship between distance from equator and Chlorophyta or Tracheophyta $\delta^{13}C$ per site (linear mixed model, $P = 0.641$ and $P = 0.156$, respectively), however Ochrophyta and Rhodophyta $\delta^{13}C$ per

site were strongly negatively related to site distance from equator (linear mixed model, $P < 0.001$, distance coefficient = -0.093 ± 0.022, $P = 0.002$, distance coefficient = -0.125 ± 0.040).

Collection site basin was related to mean species $\delta^{13}C$ per site (ANOVA $F_{7,135} = 4.08$, $P < 0.001$). A linear mixed model of mean $\delta^{13}C$ species per site revealed the following ocean basins were related to $\delta^{13}C$: Arctic (effect $size_{intercept} = -25.02$, $P = 0.000$), Mediterranean (effect size = 8.49, $P = 0.007$), North Atlantic (effect size = 5.70, $P = 0.048$), North Pacific (effect size = 6.82, $P = 0.022$), and South China (effect size = 9.51, $P = 0.012$), and a post-hoc Tukey test found significant pairwise differences between basin macrophyte $\delta^{13}C$ (Table 3.B.1). However, site distance from the equator was also related to site basin (ANOVA, $F_{7,135} = 21.71$, $P < 0.001$), implying that these two variables were linked and covaried. There was no effect of basin side (eastern vs western) on mean species $\delta^{13}C$ per site among basins (unpaired Student's t-test, $t_{1076.53} = -1.52$, $P = 0.128$). However, there was a significant effect of basin side on mean species $\delta^{13}C$ per site within the North Atlantic (unpaired Student's t-test, $t_{155.90} = -2.11$, $P = 0.037$), a basin with enough sites (76) to test for an effect of basin side. Sites from the western North Atlantic had mean macrophyte $\delta^{13}C$ = -18.45 ± 0.58, compared to -19.86 ± 0.33 at eastern sites. Mean SST was also significantly different among eastern and western North Atlantic sites (unpaired Student's t-test, $t_{14.91} = -2.15$, $P = 0.049$). Western basin sites were 16.72 ± 2.22 ºC, compared to cooler eastern ocean sites at 11.88 ± 0.40 ºC.

A total of 150 species could be categorized with a vertical habitat in the dataset from the collection information provided in source papers (91 intertidal and 59 subtidal, 299 individual entries). Those species occurring in both the intertidal and subtidal did not have significantly different $\delta^{13}C$ values between zones (paired Student's t-test, $t_{21.52} = 0.62$, $P = 0.544$) and were

removed from the larger analysis. Mean individual specimen $\delta^{13}C$ was higher in intertidal versus subtidal $\delta^{13}C$ entries (-17.35 ± 0.43‰ S.E. vs. -18.83 ± 0.61‰ S.E., respectively, Student's t-test, $t_{273.06} = 1.98$, $P = 0.049$), but mean species $\delta^{13}C$ was significantly higher in the intertidal than in the subtidal (Student's t-test, $t_{97.69} = -2.45$, $P = 0.016$). Mean intertidal $\delta^{13}C$ was -17.91 ± 0.55‰ S.E., while mean subtidal $\delta^{13}C$ was -20.58 ± 0.94‰ S.E.

**Macrophyte $\delta^{13}C$ variation with species traits**

The distribution of mean species $\delta^{13}C$ values varied by phylum (Figure 3.3, Appendix 3A). Of the seaweed phyla, Ochrophyta had the smallest range of $\delta^{13}C$ values, from -28.70 to -8.76‰. Chlorophyta species ranged from -31.92 to -2.47‰, and Rhodophyta had the largest range of mean seaweed species $\delta^{13}C$ values, from -40.37 to -7.36‰. The angiosperm phylum Tracheophyta, here comprising surfgrasses and eelgrasses, had the smallest overall range, from -14.91 to -7.36‰. Overall, 14% of species surveyed had $\delta^{13}C < -30$‰, indicative of CCM absence. Only 4% of Chlorophyta species had a mean $\delta^{13}C$ indicating CCM absence, compared to 27% of Rhodophytes. All Ochrophyta and Tracheophyta species surveyed had $\delta^{13}C$ indicative of CCM presence. While mean species $\delta^{13}C$ showed a unimodal distribution in Ochrophyta, the Rhodophyta distribution was bimodal, with one peak at approximately -18‰, and another at -33‰ (Figure 3.3). Mean $\delta^{13}C$ for species with CCMs differed by phylum (ANOVA, $F_{3,498} = 32.14$, $P < 0.001$, Figure 3.4). Rhodophyta with CCMs had the lowest $\delta^{13}C$ of -19.13 ± 0.34‰ S.E., and Tracheophyta had the highest mean $\delta^{13}C$ at -10.59 ± 0.73‰ S.E. A post-hoc Tukey test showed significant differences among all phyla ($P < 0.080$), excepting the pairwise Chlorophyta-Ochrophyta comparison ($P = 0.810$). When species lacking CCMs were added the the analysis,

the same patterns emerged (Chlorophyta: -15.67 ± 0.45‰, Ochrophyta: -16.96 ± 0.0.28‰, Rhodophyta: -22.69 ± 0.47‰, ANOVA, $F_{3,528} = 51.41$, $P < 0.001$), and a post-hoc Tukey test showed significant differences among all phyla ($P < 0.020$), excepting the pairwise Chlorophyta-Ochrophyta comparison ($P = 0.810$). Phylum did not have an effect on species $\delta^{13}C$ for species lacking CCMs (ANOVA, $F_{2,108} = 1.89$, $P = 0.156$).

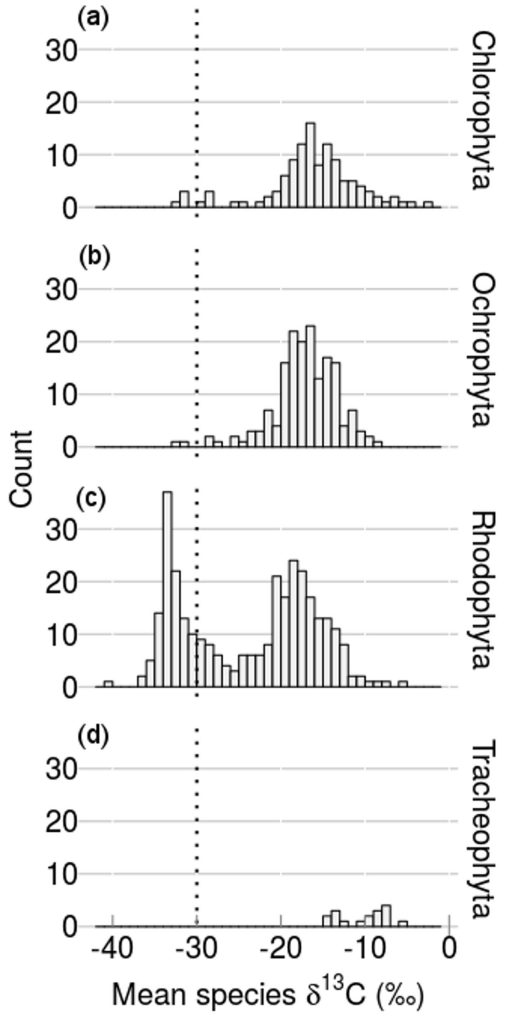


**Figure 3.3.** Histogram of mean species $\delta^{13}C$ by phylum. Each bin is 1‰. Dotted vertical line at -30‰ indicates the threshold below which macrophytes cannot access $HCO_3^-$. Chlorophyta species n = 113; Ochrophyta n = 169; Rhodophyta n = 314; Tracheophyta n = 17. Total species = 664.

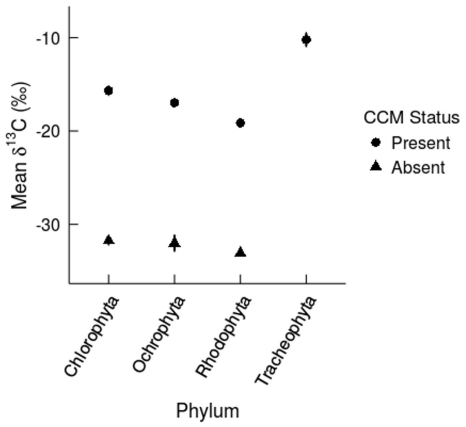


**Figure 3.4.** Mean $\delta^{13}C$ by phylum for species having and lacking a CCM. Error bars indicate standard error. Chlorophyta species n = 113 (109 CCM present, 4 CCM absent); Ochrophyta n = 169 (167 CCM present, 2 CCM absent); Rhodophyta n = 314 (209 CCM present, 105 CCM absent); Tracheophyta n = 17 (all CCM present). Total species = 613.

Of the 613 species $\delta^{13}C$ dataset, 309 species could be classified as belonging to more than one functional group based on morphology and were excluded from subsequent analyses. For the remaining 304 species, mean species $\delta^{13}C$ differed by functional group (ANOVA, $F_{6, 297} = 5.19$, $P < 0.001$, Figure 3.C.1). The filamentous group, with $\delta^{13}C$ = -20.57 ± 0.67‰ S.E., had lower $\delta^{13}C$ than crust calcifiers (-12.67 ± 1.31‰ S.E.), jointed calcareous species (-15.79 ± 1.33‰ S.E.) and thick leathery species (-17.42 ± 0.47‰ S.E.) (Tukey HSD, filamentous-crust calcifier, $P = 0.014$; filamentous-jointed calcareous, $P = 0.007$; filamentous-thick leathery, $P = 0.008$). While non-calcifying species comprised the majority of the $\delta^{13}C$ dataset (569 of 613 species), calcifying species had higher mean species $\delta^{13}C$ (unpaired t-test, $t_{51.84} = 5.06$, $P < 0.001$). Calcifying species had a mean $\delta^{13}C$ of -14.83 ± 1.00‰ S.E., while non-calcifying species had mean $\delta^{13}C$ of -20.11 ± 0.31‰ S.E.

**Organismal predictors of categorical pH assay results: CCM presence or absence**

A $\chi^2$ test of a contingency table of pH* and $\delta^{13}C$ values indicated that these two variables were not independent of each other ($\chi^2 = 64.20$, df = 1, $P < 0.001$ with Yates' continuity correction, Figure 3.5, Table 3.2). Subsequent chi-square analyses of subsets of Rhodophyta and Ochrophyta showed similar dependence of variables (Rhodophyta: $\chi^2 = 41.60$, df = 1, $P < 0.001$; Ochrophyta: $\chi^2 = 19.56$, df = 1, $P < 0.001$, Tables 3.B.2, 3.B.2), but not in the case of Chlorophyta ($\chi^2 = 2.55$, df = 1, $P = 0.111$, Table 3.B.4). Overall, there was a significant effect of taxonomy ($\chi^2$ of overall test subtracted from summed $\chi^2$ of individual phylum-tests = -0.49, df = 2, $P < 0.001$). Habitat also had an effect on pH* continuous values (paired Student's t-test, $t_{20.73} = 3.79$, $P = 0.001$); intertidal species had a mean pH* = 9.81 ± 0.09 S.E. whereas subtidal species have a lower mean value of 9.17 ± 0.15 S.E.

**Table 3.2.** Contingency table of pH* vs $\delta^{13}C$ for all macrophyte species. Mean pH* assay and mean $\delta^{13}C$ values are categorized based on the CCM absence cutoff of pH = 9.0 and $\delta^{13}C$ = -30‰. CCM absence or presence is more difficult to determine in species with tissue $\delta^{13}C$ between -10‰ and -30‰. (Surif & Raven 1989; Maberly 1990; Maberly *et al.* 1992).

| | **$\delta^{13}C$ > -30‰ (CCM + or -)** | **$\delta^{13}C$ < -30‰ (CCM -)** | **Total** |
|---|---|---|---|
| **pH* > 9.0 (CCM +)** | 94 | 2 | 96 |
| **pH* < 9.0 (CCM-)** | 17 | 29 | 46 |
| **Total** | 111 | 31 | 142 |

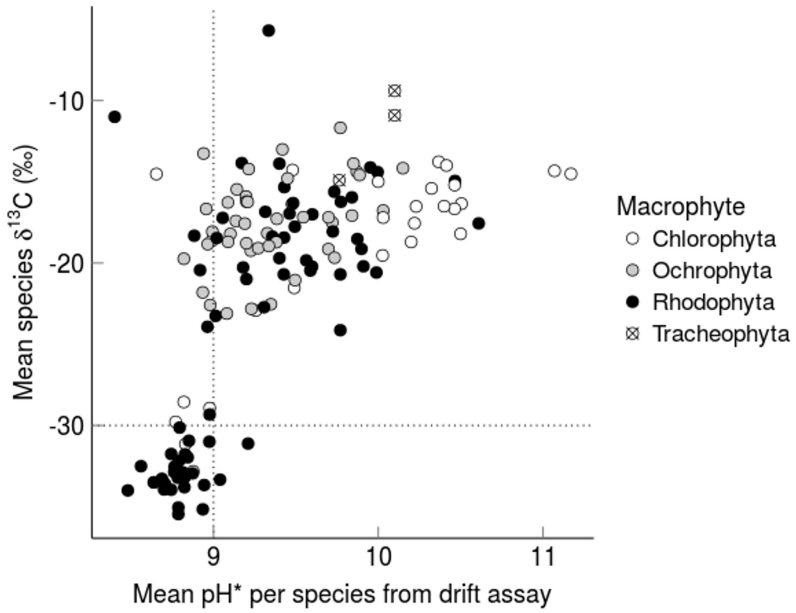


**Figure 3.5.** Mean species $\delta^{13}C$ vs mean pH* from a pH drift assay. Points are colored by seaweed species' phylum (green: Chlorophyta, brown: Ochrophyta, red: Rhodophyta), with surfgrass species in blue. Vertical dotted line indicates pH* = 9.0, above which a seaweed in a pH drift assay is using bicarbonate and designated as having a carbon concentration mechanism. Horizontal dotted line indicates $\delta^{13}C$ = -30‰, below which species are hypothesized not to have a carbon concentration mechanism (Maberly et al. 1992). 865 data points are represented from source literature. n = 109 species

Confirming this association, there was a positive effect of $\delta^{13}C$ on categorical pH assay result (binomial logistic regression and two-tailed z test, z = 6.45, $P < 0.001$). Macrophytes with $\delta^{13}C$ = -30‰ had a 0.17 probability of having pH* > 9.0 in a pH drift assay, while species with $\delta^{13}C$ = -20‰ had a 0.80 probability of having pH* > 9.0 and therefore a classification of CCM presence (Figure 3.6). A multinomial logistic regression in which 8.90 < pH* < 9.10 was categorized as 'ambiguous' – too close to the threshold value to call – confirmed that $\delta^{13}C$ tissue values from -29 to -23‰ were more likely than other $\delta^{13}C$ values to yield an ambiguous pH* (Figure 3.C.2). Species with tissue $\delta^{13}C$ within this range had 0.25-0.31 probability of yielding an ambiguous pH* in a pH drift assay.

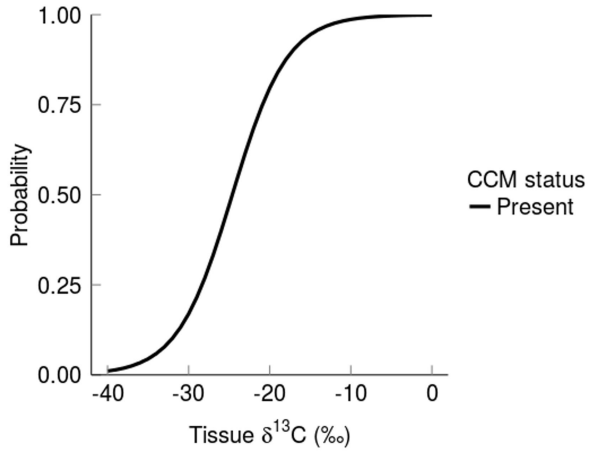


**Figure 3.6.** Predicted probability of categorical pH assay results (CMM presence or absence) based on species $\delta^{13}C$. pH* > 9.00 indicates CCM presence.

## DISCUSSION

### Local, regional and global patterns in macrophyte community $\delta^{13}C$

At the local scale, macrophyte species from subtidal habitats had more depleted $\delta^{13}C$ than species from the intertidal. This is in agreement with other large-scale $\delta^{13}C$ studies (Raven et al. 2002b, Mercado et al. 2009, Hepburn et al. 2011, Marconi et al. 2011, Cornwall et al. 2015). The observed vertical trend in macrophyte $\delta^{13}C$ is also consistent with pH* trends along the emersion gradient, in which intertidal macrophytes have a higher pH* than subtidal species (Murru and Sandgren 2004, Hepburn et al. 2011, Stepien et al. Chapter 2). This strong local vertical gradient in macrophyte $\delta^{13}C$ and pH* values is likely due to light limitation at lower depths that constrains the relatively more costly active carbon uptake using CCMs (Raven et al. 2002b, Murru and Sandgren 2004, Cornwall et al. 2015). In mesocosm experiments, macrophytes grown under low light conditions have lower $\delta^{13}C$ than those grown in high light conditions (Kübler & Raven

1994). Intertidal macrophytes are also exposed to atmospheric $CO_2$, which has a slightly higher $\delta^{13}C$ of -8.3‰ compared to -10.64‰ in seawater (Maberly *et al.* 1992; Cuntz 2011) and may exacerbate patterns of light limitation. In field studies of inter- and subtidal marine macrophyte communities, the proportion of species lacking a CCM in a community increases with increasing depth and can change across seasons for some phyla (Hepburn *et al.* 2011, Cornwall *et al.* 2015), suggesting that CCMs may play a role in structuring marine macrophyte communities.

At the regional scale, there was a significant effect of site ocean basin on macrophyte $\delta^{13}C$. While this trend was likely confounded with basin distance from the equator, some basin pairs that are similar distances from the equator were significantly different from one another (e.g., South Pacific – South China; South Pacific – North Pacific; South Pacific – North Atlantic, Table 3.B.1). Basin side was independent of such confounding concerns, and sites from the eastern North Atlantic had higher species $\delta^{13}C$ than sites from the western North Atlantic, indicating increased macrophyte reliance on $HCO_3^-$ at sites from the western North Atlantic. This trend was as expected based on the higher observed mean temperature of the eastern North Atlantic versus the western side of the basin. These patterns may be due in part to differences in temperature and nutrient availability among and within ocean basins due to global ocean currents (Gruber and Sarmiento 1997). Macrophyte CCMs have demonstrated constrained functioning under limited nutrient regimes, such as decreased phosphorus or nitrogen (Raven and Beardall 2014), as well as under lower temperature regimes (Raven et al. 2002a).

At the global scale, there was a negative relationship between macrophyte $\delta^{13}C$ and collection site distance from the equator (Figure 3.2), in agreement with differing macrophyte $\delta^{13}C$ between eastern vs western North Atlantic sites and studies in which macrophytes in colder

temperature waters have lower $\delta^{13}C$ (Raven et al. 2002a, Mercado et al. 2009). This pattern is in the same direction as the latitudinal gradient in seawater $\delta^{13}C$; biological fractionation by microscopic primary producers leads to depleted $\delta^{13}C$ at high latitudes and high $\delta^{13}C$ at low latitudes (Schmittner et al. 2013). Sea surface $\delta^{13}C$ of DIC ranges approximately 2.2‰ across the oceans (Gruber and Keeling 2001), and is changing due to isotopically lighter fossil fuel carbon (Schmittner et al. 2013). Sea surface temperature, highly correlated with site distance from the equator in this dataset,  may also influence macrophyte $\delta^{13}C$. Contrary to terrestrial phototrophs, photosynthetic machinery in marine macrophytes is at nearly the same temperature as the seawater medium. Physiology may slow at lower temperatures, leading to decreased photosynthetic rates and decreased reliance on active transport of $HCO_3^-$ (Raven et al. 2002a). Additionally, a decrease in seawater temperature from 25ºC to 5ºC shifts the seawater DIC system to favor production of $CO_2$ from $HCO_3^-$, doubling $CO_2$ availability and putting CCM-lacking macrophytes at less of a disadvantage (Raven et al. 2002a).

While seawater $\delta^{13}C$ values and SST contribute to the observed latitudinal gradient, these parameters alone are not sufficient to describe macrophyte $\delta^{13}C$. The regression coefficient for site distance from the equator in a linear mixed model was -0.09 ± 0.03 S.E., indicating the further a macrophyte is from the equator, the more depleted its tissue $\delta^{13}C$ is. For every increase of 1º of latitude from the equator, a site's macrophyte species $\delta^{13}C$ signature decreases by 0.09‰. Macrophytes differing in their distance from the equator by 60º would then be expected to differ in $\delta^{13}C$ signature by 5.4‰, indicating that CCM status of most macrophytes cannot be 'misclassified' due to latitudinal effects alone. Additionally, Chlorophytes did not show a pattern with distance from the equator (Figure 3.2), indicating that not all species are tracking the source

water $\delta^{13}C$; species traits may be responsible in part for the observed trends.

In contrast to other work that found high within-species $\delta^{13}C$ variation by local site depth (Hepburn et al. 2011, Cornwall et al. 2015), within-species $\delta^{13}C$ variation in this study was very low at the global level. Therefore, the observed large-scale negative trend is likely a consequence of differing species composition along the latitudinal gradient – as is the case in the local intertidal to subtidal gradient – rather than within-species variation in $\delta^{13}C$ values. It is possible that undersampling of sites at the extreme ends of distance from equator has contributed to the observed trend. The Northern Hemisphere and specifically the North Atlantic Ocean were over-represented, with 75% of collection sites in the Northern Hemisphere and 49% in the North Atlantic. Tropic and polar sites comprised nearly the same portion of the dataset (roughly 4% each), and there is a clear need for increased sampling in these areas to test the robustness of global macrophyte trends. However, analysis of the latitudinal span within temperate zone sites alone showed a negative relationship between macrophyte $\delta^{13}C$ and distance from equator comparable to that of the entire dataset, suggesting that increased sampling at high latitudes may uphold the pattern.

Interestingly, variance in SST at a site was positively related to macrophyte $\delta^{13}C$; macrophytes experiencing high annual variation in temperatures had $\delta^{13}C$ indicative of increased $HCO_3^-$ reliance. Collection sites with high variance in SST tended to be in bays with freshwater inputs or other areas of potentially unique climate and seawater chemistry, which could contribute to the observed trend. Alternatively, macrophytes may become 'DIC generalists' and rely on both $CO_2$ and $HCO_3^-$ in response to more unpredictable environments (Simpson 1944, MacArthur 1965).

**Macrophyte $\delta^{13}C$ varies with calcifying status and taxonomy**

The mean and range of species $\delta^{13}C$ observed within Chlorophyta, Ochrophyta, and Rhodophyta (Figure 3.3) is largely consistent with other studies (Raven et al. 2002b, Mercado et al. 2009, Marconi et al. 2011, Roleda and Hurd 2012), however the range of Chlorophyta is shifted slightly higher. The low within-species variation in $\delta^{13}C$ values observed in this present study is also concordant with the literature (Appendix 3A, (Mercado et al. 2009)). Only 18% of 613 species surveyed had $\delta^{13}C < -30‰$ and therefore lacked a CCM. This is in agreement with the 20% of species found to lack a CCM in a review of 100 macroalgal species from the Northeast Atlantic (Raven et al. 2002a), indicating that regional-scale patterns may be scalable to the global level.

While there was a significant effect of functional group (Figure 3.C.1), it was largely driven by higher $\delta^{13}C$ in crust calcifiers, jointed calcaerous and thick leathery species compared to filamentous species. From these functional group pairwise results, it is not surprising that calcifying marine macrophytes have significantly higher $\delta^{13}C$ than non-calcifiers. A higher $\delta^{13}C$ in calcifiers may be due in part to the unique relationship between calcifying species and the DIC system. In the proposed 'trans' model of calcification for freshwater and some marine macrophytes with partial calcification, active transport of $Ca^{2+}$ and passive diffusion of $CO_2$ forms $CaCO_3$ and releases H+ in the extracellular matrix (McConnaughey and Whelan 1997), potentially leading to more acidic boundary layers and shifting the DIC equilibrium in the species boundary layer and changing C isotope fractionation patterns. This lower-pH boundary layer would then favor the speciation of $HCO_3^-$, leading to increased uptake of this compound

and higher tissue $\delta^{13}C$. Research on the mechanisms of calcification in marine macrophytes is greatly needed to understand the feedbacks between seawater chemistry and macrophyte fitness (e.g. (McCoy and Kamenos 2015)).

**Concordance of species $\delta^{13}C$ with categorical pH* results**

In agreement with literature findings of increasing pH* with increasing $\delta^{13}C$ (Maberly et al. 1992, Raven et al. 2002b), $\chi^2$ analysis and a subsequent binomial logistic regression found that $\delta^{13}C$ and pH* were not independent of each other. Species with $\delta^{13}C$ = -20‰ have a 0.80 probability of being classified as having CCMs based on a pH assay (Figure 3.6). The slope of the relationship between $\delta^{13}C$ and pH assay outcome was large and positive from -30 to -20‰, indicating that there is rapid increase in the probability of a positive pH assay result (CCM present) in this range of $\delta^{13}C$, from 0.16 to 0.80 probability with a change in macrophyte $\delta^{13}C$ of only 10‰. The difficulty of predicting pH assay outcomes in the $\delta^{13}C$ range of -20 to -25‰, in which CCM presence, absence or ambiguity is equally likely (Figure 3.C.2), may be due to additional effects on $\delta^{13}C$ outside of CCM presence or absence, as illustrated by some of the outliers in paired $\delta^{13}C$-pH* data. While calculations by Maberly *et al.* (1992) indicate that macrophytes with carbon signatures -30‰ < $\delta^{13}C$ < -10‰ may be a result of either $HCO_3^-$ or $CO_2$ usage, the relative reliance on $HCO_3^-$ versus $CO_2$ within this range is unknown. The difficulty of predicting pH assay outcomes in species with $\delta^{13}C$ < -20‰ suggest that $\delta^{13}C$ = -20‰ may serve as a working cutoff for significant reliance on a CCM by macrophytes. Alternatively, species with $\delta^{13}C$ = -24‰ have a greater than 0.50 probability of having a CCM in a pH drift assay – such a threshold may be more appropriate when analyzing CCM presence or absence – a

complex physiological mechanism – as a binary trait.

Use of the NBS pH scale does not appear to have greatly influenced assignment of CCM presence or absence to species. Based on the distribution of pH* and $\delta^{13}C$ (Figure 3.5) and a contingency table of the possible combinations of pH* and $\delta^{13}C$ categories (Table 3.2), only two of 142 species (1%) had pH* greater than 9.0 (CCM presence), but $\delta^{13}C$ signatures indicative of CCM absence. If pH* values were artificially increased due to the difference between the total scale pHT and pHNBS (NBS is 0.12 units higher), I would expect to see more species incorrectly assigned as having a CCM due to a higher pHNBS, but correctly assigned as lacking one based on $\delta^{13}C$.

With regards to the other possible 'mismatched' data category – the relatively large number of paired pH*- $\delta^{13}C$ data that are identified as lacking a CCM according to the pH* drift assay, yet having one according to species' $\delta^{13}C$ – this may indicate problems with and artifacts of the assay design. Higher seawater temperature, lower salinity and too-short duration of the assay can all lower pH* or cause failure of the macrophyte to reach a threshold value. Additionally, some macrophytes may leach substances that can change the total alkalinity of the seawater and hence the pH* (unpublished data C.C. Stepien, C.A. Pfister, J.T. Wootton, Chapter 2). While such artifacts may account for mismatches in CCM assignment between pH* and $\delta^{13}C$ data, in this study only 12% of species analyzed fell in this category.

Though pH assay outcomes and $\delta^{13}C$ values were largely concordant (87% agreement in CCM designation) 17 out of 142 (12%) had paired $\delta^{13}C$-pH* data with conflicting CCM classifications (Table 3.2, Figure 3.5). Those with pH* < 9.0 implying CCM absence, but $\delta^{13}C$ > -30‰, indicated an imprecise association between tissue carbon isotope values and pH drift

assay results for some species. The majority of these species (11) had pH* within 0.1 pH units of the 9.0 cutoff, indicating that the assay may have mis-categorized some species. In three species, pH* was below 9.0, implying CCM absence, and although mean $\delta^{13}C$ was greater than -30‰, species' $\delta^{13}C$ range spanned -30‰. Four species were from the Chlorophyta genus *Caulerpa.* Species from this genus are generally rhizophytes, and as such have a unique relationship with the substrate that may alter $\delta^{13}C$ through nutrient uptake and sediment interactions (Raven *et al.* 2002b). Still other species are slow-growing and may not deplete DIC at a measurable rate over a 24-hour pH drift assay. The differential leakage of $^{12}CO_2$ and $^{13}CO_2$ from the vicinity of photosynthetic machinery into other chloroplast compartments can skew tissue $\delta^{13}C$ (Raven et al. 2002b), and different forms of the Rubisco enzyme may discriminate carbon isotopes slightly different (Raven and Beardall 2014). Additionally, specimen collection site depth and long-term light limitation can influence pH* within species, to the point that in a minority of species it changes the CCM classification from present to absent (Hepburn et al. 2011). pH assays run under differing temperature, light and time regimes with macrophytes of different quality may all influence final pH* as discussed previously. Overall, however, 87% of species with pH* and $\delta^{13}C$ agreed on CCM designation, suggesting that rapid hi-throughput sampling of macrophyte $\delta^{13}C$ may be a more effective way to determine CCM status of a community than more time-intensive pH drift assays.

**Macrophyte carbon uptake in a changing ocean**

Carbon concentration mechanisms revealed species patterns in macrophyte communities at every scale investigated, from local emersion gradients to oceanic and global gradients. Taken together,

these findings indicate that marine macrophytes cannot be treated as simply phototrophic biomass that interacts uniformly with the global carbon cycle. In addition to among-species differences in responses to a changing ocean, ocean acidification and warming may predict opposite effects on seaweed macroecology. As climate change influences species interactions in the ocean (Falkenberg et al. 2013a, 2013b, Kroeker et al. 2013, McCoy and Pfister 2014), we may see a community shift towards species with lower $\delta^{13}C$ as higher concentrations of dissolved $CO_2$ ameliorate local competition between macrophytes with and lacking CCMs. We alternatively may observe increased favoring of species with CCMs and thus higher $\delta^{13}C$ in areas of increased SST (Raven et al. 2002a) along the global latitudinal gradient, and in areas of increasing volatile environments with high variance in SST. Evaluating the relative contributions of increasing SST and increasing seawater DIC in determining seaweed community responses will become increasingly crucial to predicting the ecological effects of climate change. Based on the scale-dependent patterns observed in macrophyte $\delta^{13}C$ from the local intertidal emersion gradient, to oceanic basins, to the global latitudinal gradient, the impacts of ocean acidification will likely differ by scale, and macrophyte species identity, habitat and evolutionary history must be taken into account to fully understand coastal carbon cycling and predict community change.

**ACKNOWLEDGEMENTS**

I thank the National Park Service (Olympic NP, WA, USA) for access to field sites, the Makah Tribal Nation for access to Tatoosh Island and C.A. Pfister, J.T. Wootton, T.D. Price, R. Ree, S.J. McCoy, A.K. Henry, and O.M. Moulton for helpful comments. I also thank the countless researchers who generated and published the data this analysis is based upon. Research was

supported in part by the U.S. National Science Foundation (DGE1144082 to C.C.S., DEB1311286 to C.A. Pfister and C.C.S., OCE0928232 to C.A. Pfister and DEB0919240 to J.T. Wootton) and the U.S. National Institutes of Health (T32 GM007197).

## APPENDIX 3A: MARINE MACROPHYTE $\delta^{13}C$, PH* DATA AND COLLECTION SITES EXTRACTED FROM LITERATURE

Raw datasets for marine macrophyte $\delta^{13}C$ and pH* data (2027 data points from 634 species) and collection sites are currently available at http://onlinelibrary.wiley.com/doi/10.1111/1365-2745.12451/full and will be available on Data Dryad.

## APPENDIX 3B: POST-HOC TEST RESULTS AND CONTINGENCY TABLES OF $\delta^{13}C$ AND PH* VALUES BY PHYLUM

**Table 3.B.1.** Ocean basin post-hoc Tukey results for species $\delta^{13}C$ differences among oceans. * indicates pairwise comparisons that are significantly different from each other at $\alpha = 0.05$.

| Basin | Arctic | Mediterranean | North Atlantic | North Pacific | South China | Southern | South Pacific | Indian |
|---|---|---|---|---|---|---|---|---|
| **Arctic** | - | - | - | - | - | - | - | - |
| **Mediterranean** | 0.001* | - | - | - | - | - | - | - |
| **North Atlantic** | 0.012* | 0.347 | - | - | - | - | - | - |
| **North Pacific** | 0.001* | 1.000 | 0.254 | - | - | - | - | - |
| **South China** | 0.001* | 1.000 | 0.320 | 0.889 | - | - | - | - |
| **Southern** | 0.721 | 0.011* | 0.192 | 0.007* | 0.023* | - | - | - |
| **South Pacific** | 0.750 | < 0.001* | < 0.001* | < 0.001* | 0.003* | 1.00 | - | - |
| **Indian** | 0.284 | 0.135 | 0.879 | 0.148 | 0.126 | 0.986 | 0.760 | - |

**Table 3.B.2.** Contingency table of Rhodophyta species $\delta^{13}C$ and pH* assay values. pH* assay and $\delta^{13}C$ values based on the CCM absence cutoff of pH* = 9.0 and $\delta^{13}C$ = -30‰. CCM absence or presence cannot be determined in species with tissue $\delta^{13}C$ between -10‰ and -30‰.

| | **$\delta^{13}C$ > -30‰ (CCM + or -)** | **$\delta^{13}C$ < -30‰ (CCM -)** | **Total** |
|---|---|---|---|
| **pH* > 9.0 (CCM +)** | 36 | 2 | 38 |
| **pH* < 9.0 (CCM-)** | 5 | 27 | 32 |
| **Total** | 41 | 29 | 70 |

**Table 3.B.3.** Contingency table of Ochrophyta species $\delta^{13}C$ and pH* assay values. pH* assay and $\delta^{13}C$ values based on the CCM absence cutoff of pH* = 9.0 and $\delta^{13}C$ = -30‰. CCM absence or presence cannot be determined in species with tissue $\delta^{13}C$ between -10‰ and -30‰.

| | **$\delta^{13}C$ > -30‰ (CCM + or -)** | **$\delta^{13}C$ < -30‰ (CCM -)** | **Total** |
|---|---|---|---|
| **pH* > 9.0 (CCM +)** | 36 | 0 | 36 |
| **pH* < 9.0 (CCM-)** | 7 | 0 | 7 |
| **Total** | 43 | 0 | 43 |

**Table 3.B.4.** Contingency table of Chlorophyta species $\delta^{13}C$ and pH* assay values. pH* assay and $\delta^{13}C$ values based on the CCM absence cutoff of pH* = 9.0 and $\delta^{13}C$ = -30‰. CCM absence or presence cannot be determined in species with tissue $\delta^{13}C$ between -10‰ and -30‰.

| | **$\delta^{13}C$ > -30‰ (CCM + or -)** | **$\delta^{13}C$ < -30‰ (CCM -)** | **Total** |
|---|---|---|---|
| **pH* > 9.0 (CCM +)** | 19 | 0 | 19 |
| **pH* < 9.0 (CCM-)** | 5 | 2 | 7 |
| **Total** | 24 | 2 | 26 |

## APPENDIX 3C: MEAN $\delta^{13}C$ BY FUNCTIONAL GROUP AND PREDICTING PH*

## RESULTS FROM $\delta^{13}C$

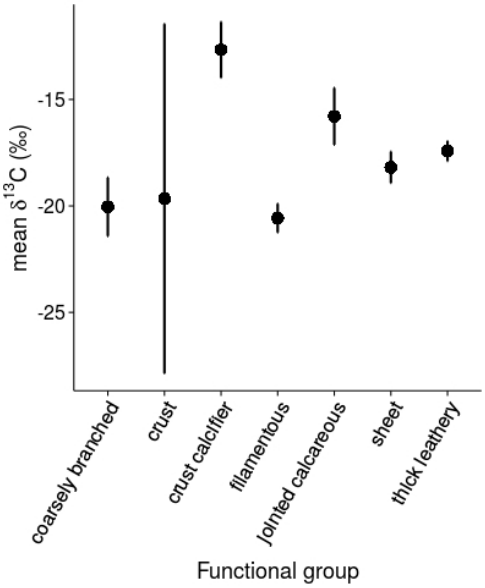


**Figure 3.C.1.** Mean $\delta^{13}C$ by species functional group classification. Functional groups are modified from Littler & Littler (1980). Error bars indicate standard error. Number of species per group varies: coarsely branched: 23; crust: 3; crust calcifier: 7; filamentous: 99; jointed calcareous: 25; sheet: 66; thick leathery: 81. Total species represented = 304.

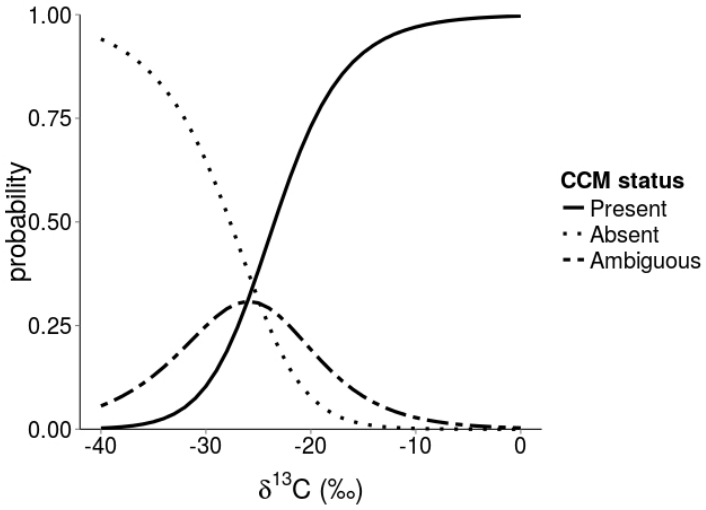


**Figure 3.C.2.** Predicted probabilities of pH* assay results (CCM present, absent or ambiguous) based on species $\delta^{13}C$. A multinomial logistic regression was performed in which CCM presence was categorized as pH* > 9.10, CCM absence where pH* < 8.90, and a third CCM category in which species where 8.90 < pH* < 9.10 were designated as ambiguous. It is possible that the number of replicates or assay run time or temperature could shift these near-threshold results in either direction.

## APPENDIX 3D: REFERENCES FOR ASSEMBLED DATASETS


Andría, J.R., Pérez-Lloréns, J.L. & Vergara, J.J. (1999) Mechanisms of inorganic carbon acquisition in *Gracilaria gaditana* nom. prov. (Rhodophyta). *Planta*, **208**, 564–573.

Axelsson, L. & Uusitalo, J. (1988) Carbon acquisition strategies for marine macroalgae. *Marine Biology*, **97**, 295–300.

Baeta, A., Valiela, I., Rossi, F., Pinto, R., Richard, P., Niquil, N. & Marques, J.C. (2009) Eutrophication and trophic structure in response to the presence of the eelgrass *Zostera noltii*. *Marine Biology*, **156**, 2107–2120.

Beardall, J. & Roberts, S. (1999) Inorganic carbon acquisition by two Antarctic macroalgae, *Porphyra endiviifolium* (Rhodophyta: Bangiales) and *Palmaria decipiens* (Rhodophyta: Palmariales). *Polar Biology*, **21**, 310–315.

Black Jr, C.C. & Bender, M.M. (1976) $\delta^{13}C$ values in marine organisms from the Great Barrier Reef. *Australian Journal of Plant Physiology*, **3**, 25-32.

Bode, A., Alvarez-Ossorio, M.T. & Varela, M. (2006) Phytoplankton and macrophyte contributions to littoral food webs in the Galician upwelling estimated from stable isotopes. *Marine Ecology Progress Series*, **318**, 89–102.

Carvalho, M.C. de & Eyre, B.D. (2011) Carbon stable isotope discrimination during respiration in three seaweed species. *Marine Ecology Progress Series*, **437**, 41-49.

Carvalho, M.C. de, Hayashizaki, K.-I. & Ogawa, H. (2009) Carbon stable isotope discrimination: a possible growth index for the kelp *Undaria pinnatifida*. *Marine Ecology Progress Series*, **381**, 71–82.

Carvalho, M.C. de, Hayashizaki, K.-I. & Ogawa, H. (2010) Effect of pH on the carbon stable isotope fractionation in photosynthesis by the kelp *Undaria pinnatifida*. *Coastal Marine Science*, **34**, 135-139.

Corbisier, T.N., Petti, M.A., Skowronski, R.S. & Brito, T.A. (2004) Trophic relationships in the nearshore zone of Martel Inlet (King George Island, Antarctica): $\delta^{13}C$ stable-isotope analysis. *Polar Biology*, **27**, 75–82.

Cornwall, C.E., Hepburn, C.D., Pritchard, D., Currie, K.I., McGraw, C.M., Hunter, K.A. & Hurd, C.L. (2012) Carbon-use strategies in macroalgae: differential responses to lowered pH and implications for ocean acidification. *Journal of Phycology*, **48**, 137–144.

Cornwall, C.E., Revill, A.T. & Hurd, C.L. (2015) High prevalence of diffusive uptake of $CO_2$ by macroalgae in a temperate subtidal ecosystem. *Photosynthesis Research*, **124**, 181-190.

Dethier, M.N., Sosik, E., Galloway, A.W., Duggins, D.O. & Simenstad, C.A. (2013) Addressing assumptions: variation in stable isotopes and fatty acids of marine macrophytes can confound conclusions of food web studies. *Marine Ecology Progress Series*, **478**, 1–14.

Deudero, S., Blanco, A., Box, A., Mateu-Vicens, G., Cabanellas-Reboredo, M. & Sureda, A. (2010) Interaction between the invasive macroalga *Lophocladia lallemandii* and the bryozoan *Reteporella grimaldii* at seagrass meadows: density and physiological responses. *Biological Invasions*, **12**, 41–52.

Dromgoole, F.I. (1978) The effects of oxygen on dark respiration and apparent photosynthesis of marine macro-algae. *Aquatic Botany*, **4**, 281–297.

Dunton, K.H. (2001) $\delta^{15}N$ and $\delta^{13}C$ Measurements of Antarctic peninsula fauna: trophic relationships and assimilation of benthic seaweeds. *American Zoologist*, **41**, 99–112.

Fenton, G.E. & Ritz, D.A. (1988) Changes in carbon and hydrogen stable isotope ratios of macroalgae and seagrass during decomposition. *Estuarine, Coastal and Shelf Science*, **26**, 429–436.

Fenton, G.E. & Ritz, D.A. (1989) Spatial variability of $^{13}C$:$^{12}C$ and D:H in *Ecklonia radiata* (C. Ag.) J. Agardh (Laminariales). *Estuarine, Coastal and Shelf Science*, **28**, 95–101.

Filgueira, R. & Castro, B.G. (2011) Study of the trophic web of San Simón Bay (Ría de Vigo) by using stable isotopes. *Continental Shelf Research*, **31**, 476–487.

Fischer, G. & Wiencke, C. (1992) Stable carbon isotope composition, depth distribution and fate of macroalgae from the Antarctic Peninsula region. *Polar Biology*, **12**, 341–348.

Fredriksen, S. (2003) Food web studies in a Norwegian kelp forest based on stable isotope ($\delta^{13}C$ and $\delta^{15}N$) analysis. *Marine Ecology Progress Series*, **260**, 71–81.

Gillies, C.L., Stark, J.S., Johnstone, G.J. & Smith, S.D. (2012a) Carbon flow and trophic structure of an Antarctic coastal benthic community as determined by $\delta^{13}C$ and $\delta^{15}N$. *Estuarine, Coastal and Shelf Science*, **97**, 44–57.

Gillies, C.L., Stark, J.S., Johnstone, G.J. & Smith, S.D. (2013) Establishing a food web model for coastal Antarctic benthic communities: a case study from the Vestfold Hills. *Marine Ecology Progress Series*, **478**, 27–41.

Gillies, C.L., Stark, J.S. & Smith, S.D. (2012b) small-scale spatial variation of $\delta^{13}C$ and $\delta^{15}N$ isotopes in Antarctic carbon sources and consumers. *Polar Biology*, **35**, 813–827.

Golléty, C., Riera, P. & Davoult, D. (2010) Complexity of the food web structure of the

*Ascophyllum nodosum* zone evidenced by a $\delta^{13}C$ and $\delta^{15}N$ study. *Journal of Sea Research*, **64**, 304–312.

Hepburn, C.D., Pritchard, D.W., Cornwall, C.E., McLeod, R.J., Beardall, J., Raven, J.A. & Hurd, C.L. (2011) Diversity of carbon use strategies in a kelp forest community: implications for a high $CO_2$ ocean. *Global Change Biology*, **17**, 2488–2497.

Hill, J.M. & McQuaid, C.D. (2009) Variability in the fractionation of stable isotopes during degradation of two intertidal red algae. *Estuarine, Coastal and Shelf Science*, **82**, 397–405.

Holmer, M., Duarte, C., Boschker, H. & Barrón, C. (2004) Carbon cycling and bacterial carbon sources in pristine and impacted Mediterranean seagrass sediments. *Aquatic Microbial Ecology*, **36**, 227–237.

Israel, A. & Beer, S. (1992) Photosynthetic carbon acquisition in the red alga *Gracilaria conferta*. *Marine Biology*, **112**, 697–700.

Jaschinski, S., Brepohl, D.C. & Sommer, U. (2008) Carbon sources and trophic structure in an eelgrass (*Zostera marina* L.) bed based on stable isotope and fatty acid analyses. *Marine Ecology Progress Series*, **358**, 103–114.

Johnston, A.M. & Raven, J.A. (1986) The utilization of bicarbonate ions by the macroalga *Ascophyllum nodosum* (L.) Le Jolis. *Plant, Cell & Environment*, **9**, 175–184.

Jolliffe, E.A. & Tregunna, E.B. (1970) Studies on $HCO_3^-$ ion uptake during photosynthesis in benthic marine algae. *Phycologia*, **9**, 293–303.

Kang, C.-K., Choy, E.J., Son, Y., Lee, J.-Y., Kim, J.K., Kim, Y. & Lee, K.-S. (2008) Food web structure of a restored macroalgal bed in the eastern Korean peninsula determined by C and N stable isotope analyses. *Marine Biology*, **153**, 1181–1198.

Kevekordes, K., Holland, D., HÄubner, N., Jenkins, S., Koss, R., Roberts, S., Raven, J.A., Scrimgeour, C.M., Shelly, K., Stojkovic, S. & Beardall, J. (2006) Inorganic carbon acquisition by eight species of *Caulerpa* (Caulerpaceae, Chlorophyta). *Phycologia*, **45**, 442–449.

Korb, R. (2003) Lack of dietary specialization in adult *Aplysia californica*: evidence from stable carbon isotope composition. *Journal of the Marine Biological Association of the UK*, **83**, 501–505.

Laurand, S. & Riera, P. (2006) Trophic ecology of the supralittoral rocky shore (Roscoff, France): A dual stable isotope ($\delta^{13}C$, $\delta^{15}N$) and experimental approach. *Journal of Sea Research*, **56**, 27–36.

Leclerc, J.-C., Riera, P., Leroux, C., Lévêque, L., Laurans, M., Schaal, G. & Davoult, D. (2013) Trophic significance of kelps in kelp communities in Brittany (France) inferred from isotopic comparisons. *Marine Biology*, **160**, 3249–3258.

Lepoint, G., Nyssen, F., Gobert, S., Dauby, P. & Bouquegneau, J.-M. (2000) Relative impact of a seagrass bed and its adjacent epilithic algal community in consumer diets. *Marine Biology*, **136**, 513–518.

Maberly, S.C. (1990) Exogenous sources of inorganic carbon for photosynthesis by marine macroalgae. *Journal of Phycology*, **26**, 439–449.

Maberly, S.C., Raven, J.A. & Johnston, A.M. (1992) Discrimination between $^{12}C$ and $^{13}C$ by marine plants. *Oecologia*, **91**, 481–492.

Marconi, M., Giordano, M. & Raven, J.A. (2011) Impact of taxonomy, geography, and depth on $\delta^{13}C$ and $\delta^{15}N$ variation in a large collection of macroalgae. *Journal of Phycology*, **47**, 1023–1035.

McMeans, B.C., Rooney, N., Arts, M.T. & Fisk, A.T. (2013) Food web structure of a coastal Arctic marine ecosystem and implications for stability. *Marine Ecology Progress Series*, **482**, 17–28.

Mercado, J.M., de los Santos, C.B., Lucas Pérez-Lloréns, J. & Vergara, J.J. (2009) Carbon isotopic fractionation in macroalgae from Cádiz Bay (Southern Spain): Comparison with other bio-geographic regions. *Estuarine, Coastal and Shelf Science*, **85**, 449–458.

Moncreiff, C.A. & Sullivan, M.J. (2001) Trophic importance of epiphytic algae in subtropical seagrass beds: evidence from multiple stable isotope analyses. *Marine Ecology Progress Series*, **215**, 93–106.

Murru, M. & Sandgren, C.D. (2004) Habitat matters for inorganic carbon acquisition in 38 species of red macroalgae (Rhodophyta) from Puget Sound, Washington, USA. *Journal of Phycology*, **40**, 837–845.

Nilsen, M., Pedersen, T., Nilssen, E.M. & Fredriksen, S. (2008) Trophic studies in a high-latitude fjord ecosystem-a comparison of stable isotope analyses ($\delta^{13}C$ and $\delta^{15}N$) and trophic-level estimates from a mass-balance model. *Canadian Journal of Fisheries and Aquatic Sciences*, **65**, 2791–2806.

Ouisse, V., Riera, P., Migné, A., Leroux, C. & Davoult, D. (2012) Food web analysis in intertidal *Zostera marina* and *Zostera noltii* communities in winter and summer. *Marine Biology*, **159**, 165–175.

Parker, P.L. (1964) The biogeochemistry of the isotopes of carbon in a marine bay. *Geochimica et Cosmochimica Acta*, **28**, 1155-1164.

Pinnegar, J.K., Polunin, N.V.C. (2000) Contributions of stable-isotope data to elucidateing food webs of Mediterranean rocky littoral fishes. *Oecologia*, **122**. 399-409.

Raven, J.A. (1991) Implications of inorganic carbon utilization: ecology, evolution, and geochemistry. *Canadian Journal of Botany*, **69**, 908–924.

Raven, J.A., Beardall, J., Johnston, A.M., Kübler, J.E. & Geoghegan, I. (1995) Inorganic carbon acquisition by *Hormosira banksii* (Phaeophyta: Fucales) and its epiphyte *Notheia anomala* (Phaeophyta: Fucales). *Phycologia*, **34**, 267–277.

Raven, J.A., Beardall, J., Johnston, A.M., Kübler, J.E. & McInroy, S.G. (1996) Inorganic carbon acquisition by *Xiphophora chondrophylla* (Phaeophyta, Fucales). *Phycologia*, **35**, 83–89.

Raven, J.A. & Johnston, A.M. (1991) Photosynthetic inorganic carbon assimilation by *Prasiola stipitata* (Prasiolales, Chlorophyta) under emersed and submersed conditions: relationship to the taxonomy of *Prasiola*. *British Phycological Journal*, **26**, 247–257.

Raven, J.A., Johnston, A.M., Kübler, J.E., Korb, R., McInroy, S.G., Handley, L.L., Scrimgeour, C.M., Walker, D.I., Beardall, J., Vanderklift, M. & others. (2002) Mechanistic interpretation of carbon isotope discrimination by marine macroalgae and seagrasses. *Functional Plant Biology*, **29**, 355–378.

Raven, J.A., Johnston, A.M., Newman, J.R. & Scrimgeour, C.M. (1994) Inorganic carbon acquisition by aquatic photolithoatrophs of the Dighty Burn, Angus, UK: uses and limitations of natural abundance measurements of carbon isotopes. *New Phytologist*, **127**, 271–286.

Raven, J.A. & Osmond, C.B. (1992) Inorganic C acquisition processes and their ecological significance in inter-and sub-tidal macroalgae of North Carolina. *Functional Ecology*, **6**, 41–47.

Riera, P., Escaravage, C. & Leroux, C. (2009) Trophic ecology of the rocky shore community associated with the *Ascophyllum nodosum* zone (Roscoff, France): A $\delta^{13}C$ vs $\delta^{15}N$ investigation. *Estuarine, Coastal and Shelf Science*, **81**, 143–148.

Rigolet, C., Thiébaut, E. & Dubois, S.F. (2014) Food web structures of subtidal benthic muddy habitats: evidence of microphytobenthos contribution supported by an engineer species. *Marine Ecology Progress Series*, **500**, 25-41.

Rosenfelder, N. & Vetter, W. (2012) Stable carbon isotope composition ($\delta^{13}C$ values) of the halogenated monoterpene MHC-1 as found in fish and seaweed from different marine

regions. *Journal of Environmental Monitoring*, **14**, 845-851.

Rossi, F., Baeta, A. & Marques, J.C. (2015) Stable isotopes reveal habitat-related diet shifts in facultative deposit-feeders. *Journal of Sea Research*, **95**, 172–179.

Runcie, J.W., Gurgel, C.F.D. & Mcdermid, K.J. (2008) *In situ* photosynthetic rates of tropical marine macroalgae at their lower depth limit. *European Journal of Phycology*, **43**, 377–388.

Sand-Jensen, K. & Gordon, D.M. (1984) Differential ability of marine and freshwater macrophytes to utilize $HCO_3^-$ and $CO_2$. *Marine Biology*, **80**, 247–253.

Schaal, G., Riera, P. & Leroux, C. (2009) Trophic significance of the kelp *Laminaria digitata* (Lamour.) for the associated food web: a between-sites comparison. *Estuarine, Coastal and Shelf Science*, **85**, 565–572.

Schaal, G., Riera, P. & Leroux, C. (2010) Trophic ecology in a Northern Brittany (Batz Island, France) kelp (*Laminaria digitata*) forest, as investigated through stable isotopes and chemical assays. *Journal of Sea Research*, **63**, 24–35.

Smith, B.N. & Epstein, S. (1971) Two categories of $^{13}C/^{12}C$ ratios for higher plants. *Plant Physiology*, **47**, 380-384.

Steinarsdóttir, M.B., Ingólfsson, A. & Ólafsson, E. (2009) Trophic relationships on a fucoid shore in south-western Iceland as revealed by stable isotope analyses, laboratory experiments, field observations and gut analyses. *Journal of Sea Research*, **61**, 206–215.

Surif, M.B. & Raven, J.A. (1989) Exogenous inorganic carbon sources for photosynthesis in seawater by members of the Fucales and the Laminariales (Phaeophyta): ecological and taxonomic implications. *Oecologia*, **78**, 97–105.

Surif, M.B. & Raven, J.A. (1990) Photosynthetic gas exchange under emersed conditions in eulittoral and normally submersed members of the Fucales and the Laminariales: interpretation in relation to C isotope ratio and N and water use efficiency. *Oecologia*, **82**, 68–80.

Thomas, E.A. & Tregunna, E.B. (1968) Bicarbonate ion assimilation in photosynthesis by *Sargassum muticum*. *Canadian Journal of Botany*, **46**, 411–415.

Tregunna, E.B. & Thomas, E.A. (1968) Measurement of inorganic carbon and photosynthesis in seawater by $pCO_2$ and pH analysis. *Canadian Journal of Botany*, **46**, 481–485.

Vizzini, S. & Mazzola, A. (2006) Sources and transfer of organic matter in food webs of a Mediterranean coastal environment: evidence for spatial variability. *Estuarine, Coastal*

*and Shelf Science*, **66**, 459–467.

Wang, W.-L. & Yeh, H.-W. (2003) $\delta^{13}C$ values of marine macroalgae from Taiwan. *Botanical Bulletin of Academia Sinica*, **44**, 107-112.

Wozniak, A.S., Roman, C.T., Wainright, S.C., McKinney, R.A., James-Pirri, M.J. (2006). Monitoring food web changes in tide-restored salt marshes: a carbon stable isotope approach. *Estuaries and Coasts*. **29**, 568-578.

Zhang, X., Hu, H. & Tan, T. (2006) Photosynthetic inorganic carbon utilization of gametophytes and sporophytes of *Undaria pinnatifida* (Phaeophyceae). *Phycologia*, **45**, 642–647.

Zou, D. (2014) The effects of severe carbon limitation on the green seaweed, *Ulva conglobata* (Chlorophyta). *Journal of Applied Phycology*, **26**, 2417–2424.

Zou, D., Gao, K. & Chen, W. (2011) Photosynthetic carbon acquisition in *Sargassum henslowianum* (Fucales, Phaeophyta), with special reference to the comparison between the vegetative and reproductive tissues. *Photosynthesis Research*, **107**, 159–168.

Zou, D., Xia, J. & Yang, Y. (2004) Photosynthetic use of exogenous inorganic carbon in the agarophyte *Gracilaria lemaneiformis* (Rhodophyta). *Aquaculture*, **237**, 421–431.

# CHAPTER IV

# PHYLOGENETIC, RICHNESS AND ABUNDANCE RESPONSES TO DISTURBANCE IN ROCKY INTERTIDAL MACROALGAL ASSEMBLAGES


## ABSTRACT

While phylogenetic pattern in communities can be difficult to interpret, patterns of phylogenetic clustering and overdispersion are apparent in nature. I investigated phylogenetic assemblage structure in a Northeast Pacific macroalgal assemblage to understand the role of evolutionary history in Rhodophyta assemblage responses to a pulse abiotic disturbance and press biotic disturbances, mediated by a steep local environmental gradient. While assemblages generally recovered species richness within 1-2 years and showed no effect of treatment on cumulative richness, total macrophyte, animal and bare space abundance took longer to converge to control conditions. In contrast to the low and high zones, species-specific percent cover in the middle intertidal zone lagged behind total macrophyte abundance in convergence to control conditions. The mid zone also had the highest phylogenetic species variance, and thus the most dissimilar communities, contrary to expectations of strong environmental filtering along the intertidal emersion gradient.


## INTRODUCTION

Communities often comprise a non-random sample of regional species pools, whether in phenotypic or phylogenetic terms (Weiher and Keddy 1995, Kraft et al. 2007), and result from

many environmental and ecological processes acting differentially on species. With increasing acknowledgment that community diversity influences ecosystem function and stability (Harmon et al. 2009, Hector 2011, Cadotte et al. 2012), a major focus of community ecology has been to determine the relative contributions of environmental and organismal variables to species interactions and community assembly. Environmental filtering has been proposed as a mechanism of species sorting (Silvertown 2004), and may be evident in the phylogenetic signature of communities. Environmental filtering, where the physiological demands of a habitat limit colonization and establishment of species to a subset of adapted lineages, yields a phylogenetically clustered pattern (Weiher and Keddy 1995, Webb et al. 2002). In contrast, since related species are likely to need similar resources, competitive exclusion may prevent close relatives from co-occurring, resulting in a pattern where community members are phylogenetically overdispersed.

While phylogenetic community structure is a powerful tool to evaluate the generation and maintenance of diversity, ecological mechanisms of community assembly cannot be inferred from patterns of phylogenetic structure alone. Clustering or overdispersion of phenotypes can complicate phylogenetic community patterns (Cavender-Bares et al. 2006, Losos 2008). Additionally, environmental stresses and competition can occur simultaneously, leading to the expectation that both clustering and overdispersion may occur. Despite challenges in interpreting processes from phylogenetic community structure, communities often trend towards overdispersion in both phylogenetic studies (Kraft and Ackerly 2011) and early taxonomic ratio studies (Simberloff 1970). Investigating phylogenetic patterns is useful in identifying

community-level trends (Losos 2011), and more broadly aids our understanding of how coexistence may control macroevolution, and how macroevolution may control local coexistence (Gerhold et al. 2015).

Many studies have integrated phylogenetic and phenotypic community metrics into evaluations of community assembly (Cavender-Bares et al. 2004, Kembel and Hubbell 2006, Graham and Fine 2008, Kraft and Ackerly 2011). However, few studies take into account additional dynamic ecological processes such as herbivory, disturbance or colonization, or fine-scale environmental patterns such as temperature gradients or habitat heterogeneity (Verdú and Pausas 2007, Helmus et al. 2010, Cadotte and Strauss 2011).

Though it has long been known that disturbance contributes to species diversity (Connell 1978, Huston 1979), we are beginning to understand that its effects can be seen in the evolutionary history of communities. Disturbance has been demonstrated to be a driver of phylogenetic clustering, as in woody plant communities (Cavender-Bares and Reich 2012, Norden et al. 2012) and in zooplankton communities (Helmus et al. 2010). Fire disturbance has led to phylogenetic clustering (Verdú and Pausas 2007), and studies of forest succession have found that early-successional species are closely related, but late successional species are more distantly related (Norden et al. 2012). In successional patterns or community recovery to pulsed disturbances, extinction, colonization and environmental modification could each lead to phylogenetic clustering or dispersion (Li et al. 2015); both extinction of closely related species or colonization of distantly related species can lead to overdispersion. In a 44 year study of succession, species

colonization, not competitive exclusion, drove community overdispersion over long-term succession; colonization of distant relatives rather than extinction of close relatives drove phylogenetic patterns (Li et al. 2015). While some studies have made use of variation in disturbances as unique treatments (Cavender-Bares and Reich 2012, Forrestel et al. 2015), many studies lump a diversity of disturbance types and frequencies or rely on chronosequences (Yessoufou et al. 2013).

Herbivory is an important form of biotic disturbance that strongly structures communities. Excluding large herbivores in savanna environments resulted in impoverished species diversity and restructured communities, but phylogenetic structure depended largely on initial community conditions; where communities were initially largely overdispersed, excluding large herbivores led to more clustering. Where communities were initially more clustered, exclusion of herbivores shifted community structure towards overdispersion (Yessoufou et al. 2013). White-tailed deer in forest ecosystems have been described as a biotic filter and generally reduce phylogenetic diversity (Begley-Miller et al. 2014). It is unclear how differential herbivory pressure may impact phylogenetic diversity in successional processes.

The Northeast Pacific rocky intertidal is characterized by both physical disturbances (Dayton 1971, Paine and Levin 1981) and strong herbivore effects (Lubchenco 1983, Paine 1984). Physical and biological stress varies across small spatial scales, resulting in discrete habitat zonation of macroalgae and variable grazer and physical disturbance pressures over meters in vertical extent. Physical environmental stressors include: temperature (Helmuth and Hofmann

2001); substrate texture (Brawley and Johnson 1991), wave disturbance (Paine and Levin 1981); and light and nutrient availability (Stephenson and Stephenson 1972). At a small scale (< 1 $m^2$) phylogenetically disparate taxa compete directly for resources, and interaction strengths for these organisms are quantifiable (Wootton 1997, Wootton and Emmerson 2005, Wood et al. 2010). These species are differentially successful in their responses to disturbance, grazers and tide height stresses, potentially leading to distinct suites of adaptive traits and different patterns of phylogenetic structure in the low, mid and high zones.

While ecological communities subjected to severe or constant disturbance are often low in diversity (Connell 1978, Chase 2007), the red, green and brown macroalgae (Rhodophyta, Chlorophyta, Phaeophyta) of the rocky intertidal community are remarkably diverse. In the Northeast Pacific, tens of species, with a diversity of morphology, phylogenetic history, competitive abilities and resistance to herbivores co-occur over scales less than a square meter (Lubchenco and Gaines 1981, Paine 1984). Macroalgae compete strongly for shared limiting resources in extreme environments; high phylogenetic distance, high environmental stress and high biotic stress (competition and herbivory) allow for testing of the correlations of each of these factors in community assembly. Successional dynamics, competitive interactions, and species membership are influenced by grazers in rocky shores areas globally (Menge 1976, Lubchenco 1983, Paine 1984, Duggins and Dethier 1985, McCoy and Pfister 2014). Macroalgae may be under increased pressure from herbivory in the mid and low zones, as grazers are more abundant in these zones (Bustamante et al. 1995, Bracken et al. 2011).

In sum, there is a strong gradient over a scale of only meters over which species are differentially successful in their responses to disturbance, grazers and tide height stresses, potentially leading to distinct suites of adaptive traits and different patterns of phylogenetic structure in the low, mid and high zones. To understand phylogenetic patterns in species colonization and extirpation, I examined whether closely related species sort similarly across a 4-year community response to disturbance along the intertidal gradient. I used three axes of variation to investigate the role of species traits and evolutionary history on rocky intertidal algal communities: 1) a distinct temperature, wave and light stress gradient; 2) pulsed habitat-generating disturbances; and 3) grazer disturbance. I hypothesized 1) If community phylogenetic structure is increasingly clustered along the emersion gradient from the low zone to the high zone, environmental filtering may contribute to community structure. I predicted that communities would be more phylogenetically clustered at higher tidal heights, where environmental stressors such as temperature, desiccation and UV exposure are more intense. In recovering communities following a pulsed habitat-clearing disturbance, I hypothesized 2) that early recruiting species would be more phylogenetically similar, but that later recruiting species would lead to phylogenetic dispersion and eventually converge to control community levels of structure. If grazers were reduced following disturbances, I hypothesized that 3) absence of grazers would prevent communities from converging to control phylogenetic community structure, leading to a longterm phylogenetically clustered community that is lower in phylogenetic diversity than control macroalgal assemblages. To understand how phylogenetic community structure differed from other community diversity metrics, I compared phylogenetic metrics to species richness, beta diversity and multi-dimensional evaluations of biodiversity. Because patterns of trait

evolution may influence species co-occurrence patterns and therefore phylogenetic community structure, I investigated the evolutionary history of habitat occupation in the red macroalgae.

## MATERIALS AND METHODS

### Experimental design

To investigate evidence for phylogenetic conservatism along an environmental gradient and in disturbance niches, I examined whether closely related species sort similarly across a 4-year community response to disturbance along a well-established intertidal emersion gradient. To study how macroalgal assemblages colonize free habitat after a pulse disturbance, disturbance treatments with ambient grazers were compared to control communities. To investigate whether herbivores affected phylogenetic community structure, disturbance treatments with reduced grazers were compared to disturbance treatments with ambient grazers.

To investigate the effects of emersion, grazers and disturbance on macroalgal assemblages, 0.25 $m^2$ areas were delineated along the environmental gradient of the intertidal zone in the low, mid and high zones. These established plots were monitored over four years on an eastern-facing rocky bench on Tatoosh Island, WA (48.39°N, 124.74°W) over an area of approximately 40 by 10 m spanning two rocky benches (Fig 4.1) in the low, mid and high intertidal zones. For the purposes of this study, the low zone was characterized by kelp dominance (Phaeophyta), mid zone plots were established in the area just below the lower edge of the mussel bed, and high zone plots were established just above the upper edge of the mussel band, among a mixed community of barnacles and seaweed (Plate 4.1). Relative plot height was measured from the

center of the plot using a laser level. To calculate tide height at each plot, height data were then grounded to a marker of known height based on six observations each of low and high tide using a tide gauge. I used these spatial coordinates of plots to further ask if differences between plots within each zone were related to pairwise distances among them.

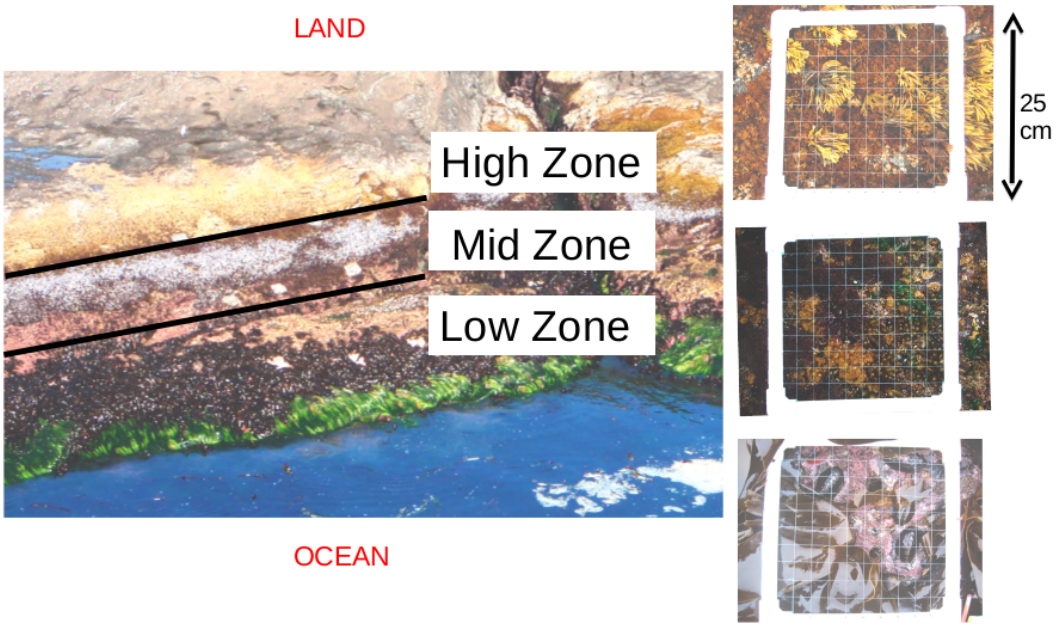


**Plate 4.1.** Basic characteristics of the rocky intertidal. Image of field experiment site and intertidal zone description. Black lines separate zones from each other. Insets on right depict from top to bottom, high, mid and low zone quadrats with vegetation and invertebrates characteristic of each zone.


**Figure 4.1.** Map of experimental plots on Tatoosh Island, WA. Tan polygons are rocky benches, and approximate the shape of the landscape when the tide is low.

Within each zone, two disturbance treatments were applied alongside a community control in a blocked pattern. To investigate the effects of a pulse disturbance on subsequent algal colonization and community structure, the disturbed plots were scraped with a wire brush to remove all biomass, along with a 0.10 m buffer zone around each plot, and then sterilized with KOH to create free habitat. To investigate how herbivory might mediate algal colonization of free habitat, a second disturbance treatment was established as above, in which grazer abundance was reduced (Plate 4.2). Mobile herbivorous invertebrates were manually removed from plots during each census period, and a 5 cm wide copper sheet was installed surrounding the plot to act as a deterrent to invertebrates entering the area (Johnson 1992).

Plots were marked in the upper left and bottom right corners with stainless steel hardware and flagged with colored zip ties for later location. Seventy-two community plots were established from 2011 to 2012. In 2011, 18 plots were installed each in the low, mid and high

zones (n = 6 per treatment). In 2012, three additional replicates per treatment were established in

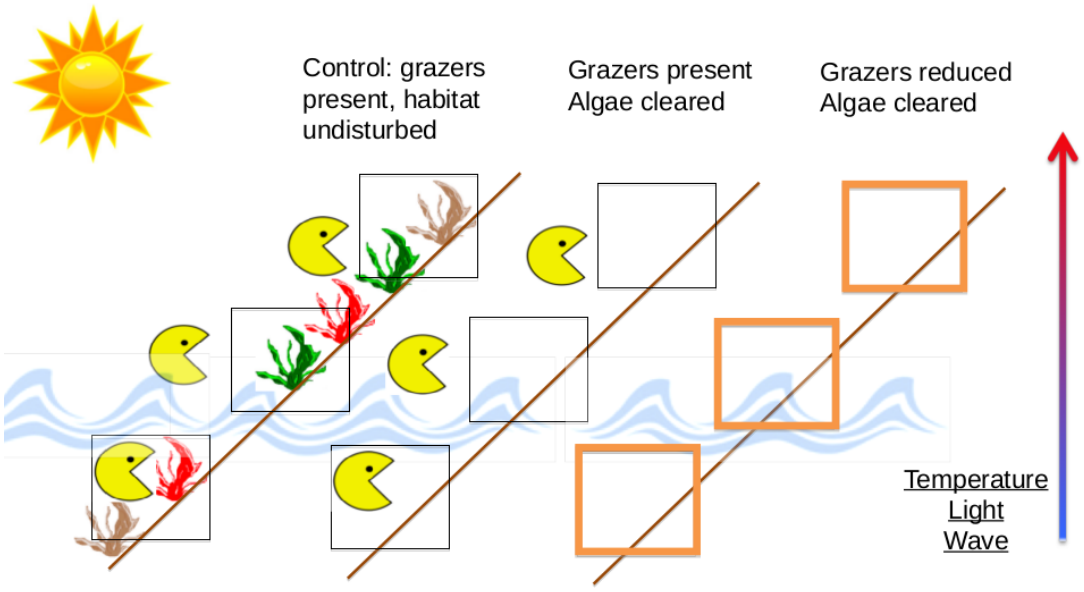


a)

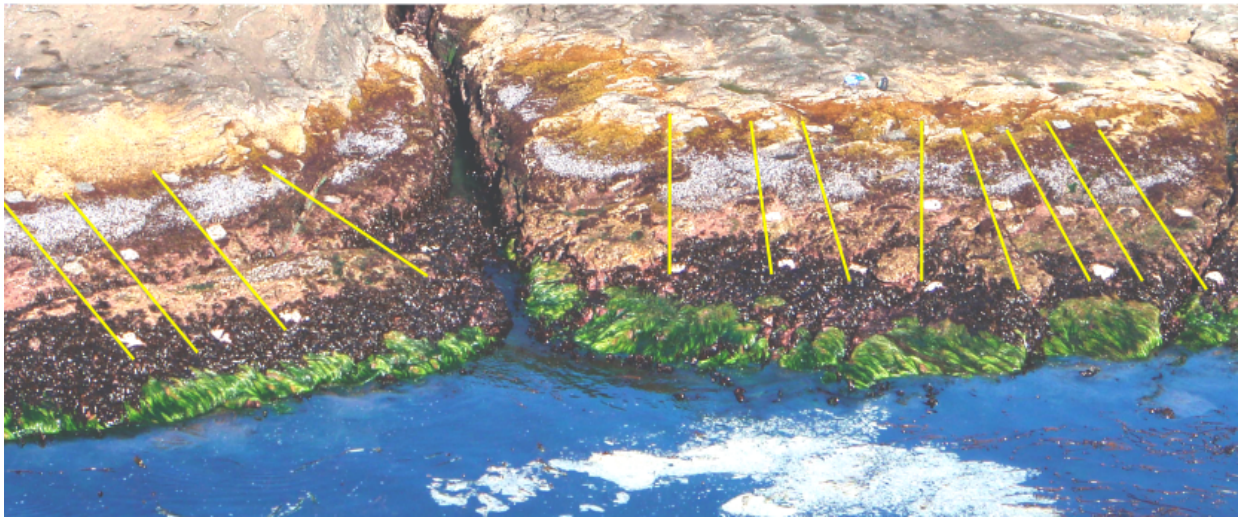

b)

**Plate 4.2.** Schematic of experimental design with three separate treatments. a) schematic. b) transects of treatments outlined in yellow in the field.

the low and mid zone, for a total of nine replicates in the low and mid zone for each treatment, and six replicates per treatment in the high zone. Tide heights ranged from 58 cm to 301 cm above the average of all low tide heights (mean low low water). Community plots in the low intertidal (58 to 101cm in tide height), were at a distinct height from those in the mid zone (135-191 cm), and high zone (250-301 cm).

**Quantifying algal diversity and abundances in treatment plots**

Community plots were censused 3 times in 2011 monthly in June, July and August, 4 times in 2012 monthly from May to August, and twice thereafter in 2013 and 2014 in April/May and August. For each plot, all macroalgal species were recorded, a photo of the plot was taken with a 100-cell 25 x 25 cm quadrat overlaid, and percent cover for each species and for bare rock (free habitat) was estimated. I assessed mobile and sessile invertebrates in the percent cover estimates, recorded the number of individuals and measured each individual for length. Grazing invertebrates found in a community marked for the grazer reduction treatment were removed and placed at an adjacent bench 40 m from experimental plots. When plots could not be assessed in the field due to logistical and time constraints, rare species were logged and percent covers were estimated from photos later. This method was comparable to the in-field method based on dual field and photo assessments of the same community. Where there were species in plots that could not be identified, an individual of the unidentified species was searched for outside the plot and sampled for later DNA barcoding. If no other individuals of the species were present outside the community plots, a minimal tissue sample was removed from within the plot (1-2 $cm^2$), taking care not to destroy the individual. All invertebrate and macroalgal species were searched

for in each plot, and if a species was not found a zero was entered for the species.

**Regional species pool assessments**

To understand what proportion of regional species pool diversity is represented in local macroalgal plots, I assembled a regional macroalgal species pool for the region around Tatoosh Island, WA. I searched AlgaeBase (Guiry and Guiry 2012) for species from all classes of algae containing at least one marine macroalgal species that had a distribution recorded in Oregon, Washington, or British Columbia. Florideophyceae, Ulvophyceae, Phaeophyceae, Bangiophyceae, Trebouxiophyceae, and Compsopogonophyceae were found within this range. Charophyceae, Pelagophyceae, and Klebsormidiophyceae did not have any members with a noted distribution from Oregon through British Columbia. Names that were synonyms or not taxonomically accepted were then replaced with the currently accepted names as indicated by AlgaeBase. Species were then cross-checked against a comprehensive Northeast Pacific regional key (Gabrielson et al. 2012) covering from Cape Spencer, Alaska south to Oregon to determine if species' ranges or dispersal capabilities might overlap with Tatoosh Island, Washington, or if species were strictly subtidal. Species in the regional key that were not present in AlgaeBase were added to the taxa list. Species present in the AlgaeBase distribution but absent in the keys were removed, as many of the unique AlgaeBase records were based on local keys that were from the 70s to the 90s, comparable to but older than the most updated key of the same region (Gabrielson et al. 2012). Based on data in the keys, microalgae and epiphytic, endophytic and epizoic algae were excluded from the regional species pool. Filamentous algae not readily identified in the field were also excluded. If algae were reported as having 'rare' occurrences in

WA, they were included in the dataset. Because of Tatoosh Island's proximity to southern British Columbia and the general southward currents in this part of the Northeast Pacific Ocean, species recorded in southern BC were included in the dataset. However, records of species endemic to southern Oregon were unlikely to disperse northward to Tatoosh Island and were excluded from the dataset. Species were also excluded temporally – those that were present in winter but not in Spring or Summer were excluded (e.g., some members of the *Pyriopia* genus in family Bangiaceae). Varieties, subspecies and forma were excluded from the final regional species pool, as well as species not identified to the species levels (e.g. “species 1”).

**Environmental data collection**

To create a map of plot locations and understand how abiotic stressors varied among plots with similar tide heights, pairwise distances were calculated between experimental plots (Appendix 4A). To characterize the abiotic emersion gradient macroalgal assemblages inhabit, desiccation, tide height and wave action were measured for each experimental plot (Appendix 4B).

**Species ecological trait data collection from the field experiment**

The evolutionary history of habitat membership may influence species co-occurrence patterns and therefore phylogenetic community structure. Species were first classified by the number of zones they inhabited: one, two or three. To test the directionality of treatment effects on the number of zones a species occupied, pairwise comparisons of species zone counts were performed across treatments and species were categorized as having gained or lost zones in one treatment relative to another treatment. To describe which red macroalgal species are intertidal

generalists versus restricted to a single zone, I categorized each species based on its presence in 1 versus multiple intertidal zones.

To understand if a species was rare within a treatment I determined how many replicates each species occupied in a treatment. To understand how long a species occupied a plot, I summed the cumulative presence of a species per plot (how many census intervals was the species present) and got the mean and maximum presence per treatment per zone. While this metric does not take into account the length of time a species occupies a plot before it disappears (turnover), it does serve as a metric for how often the species can be found in the community and if a species was unique to an experimental treatment.

**Statistical analysis of census data**

To assess the efficacy of the grazer reduction treatments, grazer sizes and log-transformed grazer counts were compared between between disturbance treatments with ambient versus reduced grazers using an unpaired t-test. To determine how communities changed over time among treatments and zones, summary community statistics were performed for each plot, including species richness (alpha diversity), the degree of similarity in species richness between plots (beta diversity), cumulative richness and seaweed, free habitat and animal abundance. Beta diversity was calculated by Whittaker's definition: the ratio of total number of species in a collection of sites (gamma diversity) and the average richness per one site, minus 1 (Whittaker 1960). Gamma diversity was calculated for each zone across all treatments, then beta diversity was calculated by dividing gamma diversity for a zone by the mean alpha diversity per plot for

each treatment. T-tests were then applied between control and disturbance ambient grazer treatments, and between disturbance ambient versus reduced grazer treatments, to determine when species richness and the other metrics were no longer significantly different among treatments, and community composition had thus converged.

All species in community plots were categorized and summed into seaweeds, animals (sessile and mobile species) and free habitat (bare rock, dead seaweed or mussels) and was normalized to 100% for comparisons. Because animal abundance varied among plots, we normalized algal cover to the available cover (bare habitat + seaweed cover) for subsequent analyses. Abundance data were arcsine square-root transformed, and then an ANOVA was applied to see if there was an effect of treatment on plant, animal or free habitat abundance.

Non-metric multidimensional scaling (NMDS) was performed on macroalgal communities using species presence and percent cover to understand how communities change through time and among zones and treatments. A Bray-Curtis distance matrix was applied, and environmental fit of data was performed with 9999 permutations using the package vegan (Oksanen et al. 2015). Environmental and treatment data was input into the matrix for each community plot at a given census interval: desiccation rates, tide height, wave action, zone membership, treatment, total seaweed, animal and bare space at a given interval, and days since establishment.

**Constructing a phylogeny of red algal species**

Because the vast majority of macroalgal species in the community were red algal species we built a community phylogeny of all recorded red macroalgae using a combination of previously published DNA sequence data on GenBank and newly sequenced DNA based on my field tissue collections. Previously published DNA sequences were retrieved from the GenBank Dec 2015 release on February 2, 2016 using an automated Python script. Data were downloaded for a combination of mitochondrial, chloroplast and nuclear markers at both the genus and species level (Appendix 4C, Table 4.C.1). Targeted DNA sequencing of 18 species was then performed to fill in gaps in the 7-gene dataset (Appendix 4C, Table 4.C.2).

Tissue was collected from the field, stored, and the DNA extracted according to McDevit and Saunders (2009), with the protocol modified for a spin column procedure. Five genes with relatively high sequence coverage on GenBank were targeted for sequencing: the mitochondrial gene COI, ribosomal genes LSU and SSU, and chloroplast genes rbcL and psaA, with published sequences used for the other two genes, the chloroplast gene psbA and ribosomal gene ITS. Primers and PCR conditions were used in the order described in Saunders and Moore (2013). Amplified regions were sequenced at the UChicago Comprehensive Cancer Center DNA Sequencing and Genotyping Facility on an Applied Biosystems 3730XL sequencer. DNA chromatograms were viewed and processed in SeqTrace (Stucky 2012). Cytochrome oxidase I (COI) sequences were then BLASTed against the Barcode of Life Database (BOLD) and GenBank nucleotide databases using the BOLD Identification Request system (Ratnasingham and Hebert 2007) and the GenBank BLAST system to confirm field identifications. Sequences

were aligned by gene in Clustal (Larkin et al. 2007) using automated multiple alignment, and edited manually in Mesquite (Maddison and Maddison 2011). A substitution model was then selected using ModelTest (Posada and Crandall 1998) under default settings. In cases where tissue could not be extracted or DNA regions did not amplify, and the species was a monotypic genus within the community dataset, published sequences from a close relative were used.

Phylogenetic analysis was performed using the seven genes on BEAST (Drummond et al. 2012), with unlinked substitution models and clock models for each partition. *Porphyra umbilicalis* was constrained as an outgroup to the rest of the taxa, based on its basal membership to Bangiaeceae and the rest of the taxa in Florideophyceae in the published literature (Verbruggen et al. 2010). Substitution models we selected based on ModelTest results for each gene alignment (Appendix 4C, Table 4.C.1). An uncorrelated lognormal relaxed clock was chosen for each partition, with the rate fixed at 1.0. A speciation birth-death process was selected as a tree prior (Gernhard 2008). Lognormal prior distributions were chosen for substitution rates. MCMC analyses were run until all ESS values were greater than 200, approximately 50 million generations. Trees were sampled every 5000 generations to generate a sample 10,000 of trees. Consensus trees were created for each gene in TreeAnnotator (Rambaut and Drummond 2014) using a burn-in of 25%, median heights for node heights and targeting a tree with maximum clade credibility.

After single gene trees were analyzed and compared to each other, we generated a multigene tree using all 7 genes. A partitioned concatenated analysis was performed using the seven genes on BEAST with the same settings for single gene trees, except that genes were linked by tree

topology and branch lengths. MCMC analyses were run until all ESS values were greater than 200, approximately 100 million generations. Trees were sampled every 10000 iterations to generate a sample 10,000 of trees; the seven-gene consensus tree was built in TreeAnnotator as previously described for single gene trees.

**Phylogenetic community diversity of plots**

For presence-absence analyses I used the richness-independent metric Phylogenetic Species Variability (PSV) (Helmus et al. 2007). For abundance-weighted analyses I employed Phylogenetic Species Evenness (PSE) (Helmus et al. 2007). PSV and PSE were calculated for each treatment and zone, by experiment year. T-tests were applied to pairwise treatment comparisons within each zone and year to investigate when algal assemblages from different treatments converged. I also tested for an effect of zone on phylogenetic community structure using an ANOVA.

**Exploring the evolutionary history of habitat membership**

Phylogenetic constraints on the evolutionary history of habitat membership may influence species co-occurrence patterns and therefore phylogenetic community structure. Habitat membership determined from field experiments was mapped onto the consensus tree to understand how changes in trait states under differing treatments might change the evolutionary history of the tree. I performed ancestral state reconstruction and stochastic character mapping (Huelsenbeck et al. 2003) on ecological traits using the R packages “ape” (Paradis et al. 2014) and “phytools” (Revell 2012). A single-rate transition matrix was applied that constrained

transitions to sequential numbers of zones. For example, a species expanding its range from one zone to three zones would have to undergo two transitions: expanding from one to two zones, and then expanding from two to three zones. To test if treatments had a unidirectional effect on species ranges – whether, for example, there was phylogenetic signal in species that increased their range in disturbance treatments versus controls – I tested for significant phylogenetic signal in species range shifts in the control versus disturbance with grazers treatments, and in the disturbance ambient versus reduced grazer treatments.

## RESULTS

### Physical parameters and tide height

There was a significant positive relationship between plot distances and differences in tide height in the low zone (linear regression, $F_{1,349} = 38.5$, $R^2 = 0.10$, $p < 0.001$), indicating that closer plots are more similar in tide height than more distant plots in this zone. However, there was no effect of plot proximity on tide heights in the mid or high zone; adjacent community plots were no more similar in tide height than distant plots within the mid and high zones.

Intertidal zone was logically a strong determinant of Denstone™ dissolution, indicating exposure to moving water increased lower in the intertidal (Appendix 4B, Figure 4.B.3, ANOVA $F_{2,69} = 271.1$, $p < 0.001$). A post-hoc Tukey analysis found that all zones were significantly different from each other (low-mid $p = 0.026$; mid-high $p < 0.001$; low-high $p < 0.001$). There was also a relationship between plot location and Denstone™ dissolution rate within the low and mid zones, where the further south a plot was located along the bench, the less mass remained (linear

regression, low zone $F_{1,25} = 32.6$, $R^2 = 0.57$, $p < 0.001$; mid zone $F_{1,25} = 43.4$, $R^2 = 0.63$, $p < 0.001$, Figure 4.B.4.). This pattern was in line with expectations given that waves first break over the south end of the rocky bench where plots were arrayed, and subsequently lose energy from friction with the bottom as they move to the north.

Desiccation effects, as indicated by agar water loss, significantly differed by zone (ANOVA $F_{2,69} = 12.32$, $p < 0.001$, Appendix 3B), with the high zone experiencing the most desiccation. While there was no relationship between algal cover and desiccation rate within zones (ANOVA by zone, all $p > 0.05$), there was a relationship between increasing algal cover and decreasing desiccation among all zones (linear regression, $F_{1,69} = 11.5$, $R^2 = 0.14$, $p = 0.001$).

**Grazers reduction treatment affected grazer counts by zone**

Control treatment macroalgal plots showed differing grazer counts by intertidal height (Fig 4.2), where chiton counts decreased in abundance with tidal height (ANOVA, $F_{2,92} = 43.01$, $p < 0.001$, Tukey's HSD, all pairwise comparisons $p < 0.03$). Snails showed the opposite pattern and increased with tidal height (ANOVA $F_{2,68} = 57.96$, $p < 0.001$, Tukey HSD, low-high $p < 0.001$, mid-high $p < 0.001$). Limpet abundance did not differ across intertidal zones ($F_{2,68} = 0.46$, $p = 0.631$).

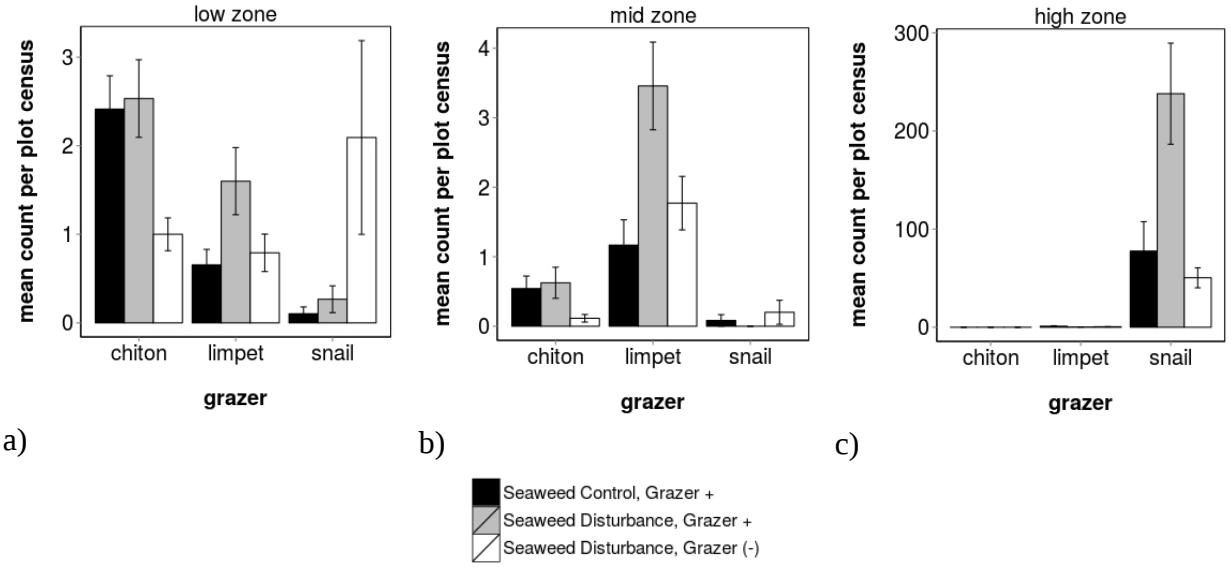


**Figure 4.2.** Herbivore counts in the low, mid and high zone. Mean animal counts +/- standard error for 3 animal groups in each treatment in the a) low, b) mid and c) high zones for the 2012 census season, when grazer reduction treatment was most consistent. Note different y axis scale for each panel. Chitons are generally *Katharina tunicata*, limpets are members of the *Lottia* genus, and snails are members of the *Littorina* genus.

Within each intertidal zone grazer removal treatments usually, but not always, kept grazers at lower abundance. Chiton numbers were kept lower in low and mid zones, limpets were reduced in low zone, and snails were reduced in the high zone (Figure 4.2, Table 4.1). These treatment effects are likely conservative estimates, because they only reflect densities just before grazer removals were maintained. Densities in grazer removal treatments were necessarily much lower after treatments were periodically maintained through manual removal, and would remain lower than plots without grazer manipulation for some (undetermined) period of time following this activity. Chiton size decreased in the mid zone, and snail size actually increased in high zone grazer reductions, despite being lower in number. Decreasing chiton size is consistent with a selection bias, where larger chitons are more easily found and therefore removed more effectively. However, increasing snail size may indicate density competition.

**Table 4.1.** Herbivore count and size changes by treatment. Unpaired t-test results of herbivore counts and size changes in grazer reduction disturbance treatments relative to ambient grazer disturbance treatments. "–" indicates that no individuals of that herbivore type were found. Arrows indicate the directionality of counts of size in grazer reduction treatments compared to ambient grazer disturbance treatments, with percents the size of the change. For example, "↓ 30%" indicates that a grazer count or size decreased in grazer reduction treatments relative to ambient grazer treatments by 30%. These data are depicted in Figure 4.2.

| Grazer variable | Low Zone | Mid Zone | High Zone |
|---|---|---|---|
| Chiton count | ↓ **60%** **$t_{67}$ = 3.01, p = 0.003** | ↓ **83%** **$t_{34}$ = 2.08, p = 0.045** | – |
| Chiton size | $t_{82}$ = 0.07, p = 0.946 | ↓ **64%** **$t_{6}$ = -5.49, p = 0.001** | – |
| Limpet count | ↓ **50%** **$t_{60}$ = 2.15, p = 0.036** | $t_{50}$ = 1.46, p = 0.152 | $t_{51}$ = 0.88, p = 0.384 |
| Limpet size | $t_{77}$ = -1.48, p = 0.142 | $t_{133}$ = -1.05, p = 0.295 | $t_{6}$ = -0.16, p = 0.875 |
| Snail count | $t_{71}$ = -1.80, p = 0.076 | $t_{34}$ = -1.42, p = 0.166 | ↓ **79%** **$t_{46}$ = -2.73, p = 0.009** |
| Snail size | $t_{11}$ = 0.57, p = 0.583 | – | ↑ **2%** **$t_{1900}$ = -3.30, p = 0.001** |

**Experimental algal species pool reflects the regional pool**

AlgaeBase searching revealed 610 unique macrophyte species with records in Oregon, Washington or British Columbia (Appendix 3D). After cross-checking with the regional key (Gabrielson et al. 2012) for additional species, synonymous taxa, and species unique to AlgaeBase but not listed in the more specific Keys, 606 species remained. Then using species life histories and more specific geographic ranges, 259 species were removed. First, 56 species whose ranges did not overlap with northern Washington were removed. Of the species with potential range overlaps with northern Washington based on species records, 52 species that were only ever observed subtidally were removed. Of the remaining 498 intertidal species within

geographic range, 153 epibionts or parasites were removed, resulting in 345 taxa. Eighty-six of these 339 species were filamentous and thus less likely to be field-identified, due to many of the key characteristics being only visible under microscope. Seventy-one of these filamentous species were removed from the regional species pool based on their difficulty to field-identify, leaving a final species pool of 274 intertidal epilithic macroalgal and surfgrass species with range and habitat overlaps with Tatoosh Island, WA. AlgaeBase taxonomy was used to categorize species by Class membership.

The 53 macroalgal species found in experimental plots over 4 years represented 19% of the regional intertidal species pool. The proportions of species by Class in our experimental plots largely mirrored that of the regional species pool, with the exception of greater representation of Florideophyceae and a lower fraction of Phaeophyceae in experimental plots (Table 4.2).

**Table 4.2.** Comparison of regional versus experimental species pools by class membership. Number of species and percent of total pool are shown. Monocotyledonae is the only angiosperm class present and includes surfgrass species, while all other classes are macroalgae.

| Class | Regional pool (% total) | Experimental plots (% total) | Difference between local and regional |
|---|---|---|---|
| Florideophyceae | 152 (55%) | 35 (66%) | +11% |
| Phaeophyceae | 66 (24%) | 10 (19%) | -5% |
| Ulvophyceae | 33 (12%) | 6 (11%) | -1% |
| Bangiophyceae | 13 (5%) | 1 (2%) | -3% |
| Monocotyledonae | 6 (2%) | 1 (2%) | 0% |
| Trebouxiophyceae | 4 (1%) | 0 (0%) | -1% |
| Total taxa | 274 | 53 | |

**Macrophyte, animal and bare space abundance**

Species richness in controls decreased with increasing tide height (Figure 4.3). All zones showed treatment-specific effects on free habitat, animal and macrophyte percent cover in the first two years (Table 4.E.1). In the first year, disturbance treatments consistently had lower plant abundance, lower animal abundance and greater free space than controls. In the second year, all three zones had higher seaweed abundance and lower animal abundance in grazer reduction disturbance treatments compared to ambient grazer disturbance plots. In the third year, there was no longer a treatment effect in the mid zone on macrophyte (ANOVA, $F_{2,33} = 0.66$ $p = 0.523$), animal ($F_{2,33} = 0.41$ $p = 0.669$) or habitat abundance ($F_{2,33} = 0.29$ $p = 0.754$). The low and high zones, however, showed treatment specific effects on abundance categories until they converged in the fourth year (Table 4.E.1).

**Species richness is largely independent of treatments after the first year**

All three zones had significantly lower species richness per plot in disturbance treatments with grazers versus control plots in year 1 (Figure 4.3, Student's t test, low zone $t_{24} = 6.85$, $p < 0.001$, mid zone $t_{25} = 6.84$, $p < 0.001$, high zone $t_{18} = 8.41$, $p < 0.001$). After year 1 only the low zone showed significant differences in species richness by treatment, in year 3 ($t_{32} = 2.94$, $p = 0.006$). There was generally no effect of grazers on species richness in disturbance plots (Figure 4.3b) with the exception of the second year in the mid zone, in which the grazer reduction treatment had fewer species than plots with grazers present ($t_{54} = 2.95$, $p = 0.005$).

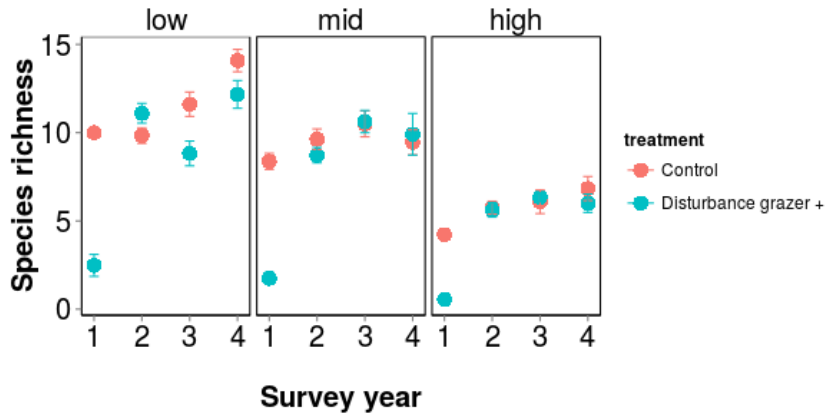


a)

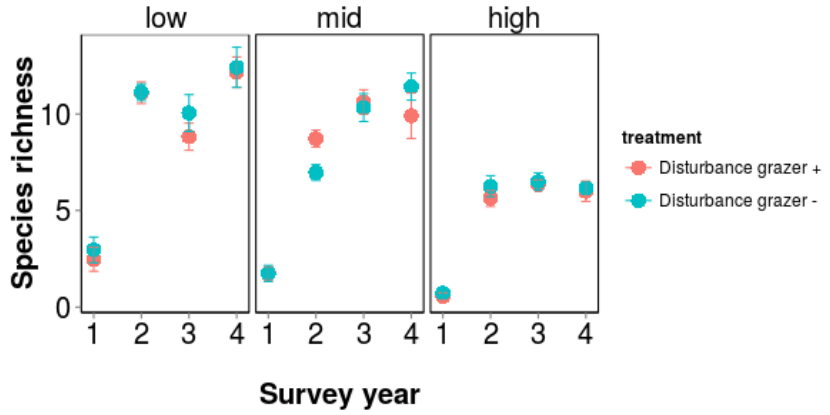


b)

**Figure 4.3.** Comparisons of mean species richness per plot by treatment and zone. a) Control vs disturbance treatments with ambient grazers. b) Disturbance treatments with ambient versus reduced grazers. Error bars indicate standard errors. Mid zone year 1 points are overlapping in panel b).

**Cumulative per-plot richness differs by zone**

There was an effect of zone on cumulative plot richness (ANOVA, $F_{2,21} = 22.81$, $p < 0.001$), with lower cumulative richness in the high zone compared to the mid and low zones (Figure 4.4, Tukey HSD, low-high $p < 0.001$, mid-high $p < 0.001$, mid-low $p = 0.260$). The same trend was observed in disturbance treatments with grazers present (ANOVA, $F_{2,21} = 10.96$, $p < 0.001$, Tukey HSD, low-high $p < 0.001$; mid-high $p = 0.006$, mid-low $p = 0.448$). In reduced grazer disturbance

treatments, the mid zone was no longer distinguishable from the high zone in cumulative richness and the low zone became distinct (ANOVA, $F_{2,21} = 12.34$, $p < 0.001$; Tukey HSD, low-high $p < 0.001$, mid-high $p = 0.105$, mid-low $p = 0.016$). Within a zone, there was no effect of treatment on cumulative richness (ANOVA, low zone $F_{2,24} = 1.24$, $p = 0.309$; mid zone $F_{2,24} = 0.42$, $p = 0.664$; high zone $F_{2,15} = 0.95$, $p = 0.408$).


**Figure 4.4**. Mean cumulative richness per plot in control, disturbance with ambient grazers and disturbance with reduced grazers treatments. Cumulative richness is all species that were ever seen in each plot over the 4-year experiment. Error bars indicate standard error.

**Beta diversity differs by treatment and year within zones**

Although plot species richness was largely unaffected by treatment after the first year, beta diversity showed more variation. In two out of three zones, disturbance treatment plots were more dissimilar in species composition than control plots by the end of the experiment (Figure 4.5). Beta diversity was calculated by Whittaker's definition: the ratio of total number of species in a collection of sites and the average richness per one site, minus 1 (Whittaker 1960). Beta diversity was calculated by dividing gamma diversity for a zone by the mean alpha diversity per plot for each treatment. The higher the beta diversity, the more dissimilar plots are. Disturbance

treatments were very high in beta diversity in the census interval after installation in year 1, indicating that that replicates within these treatments were more dissimilar from each other than in control plots in species composition and shared fewer species (Figure 4.5a). Disturbance treatments in the low zone had a higher beta diversity than control treatments in years 3 and 4 (Figure 4.5b). Low beta diversity in year 4 control plots in the low and high zone indicate that control plots were more similar in species composition in these zones than corresponding disturbance treatments.

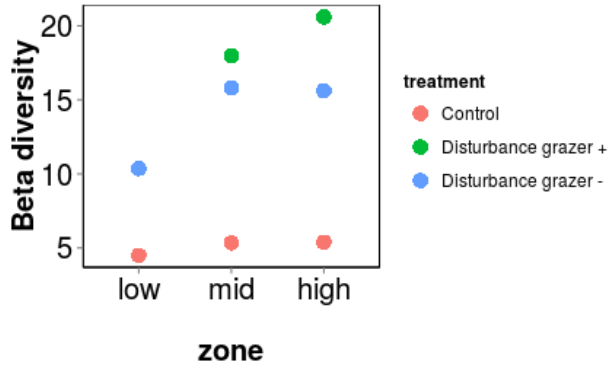


a)

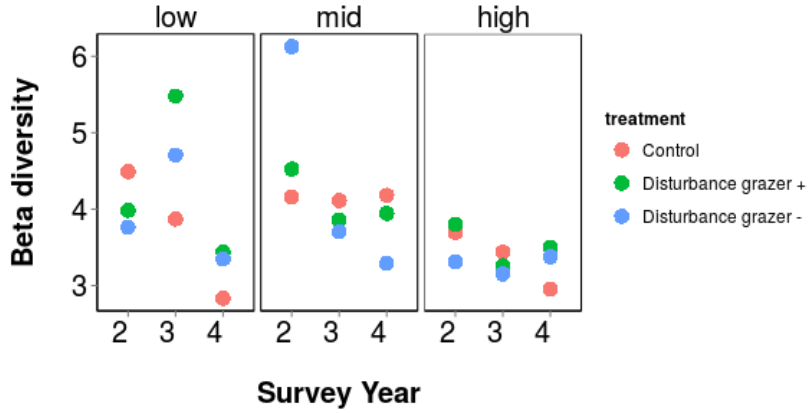


b)

**Figure 4.5.** Beta diversity for each treatment within a zone. a) Year 1, with extremely high beta diversity due to early recovery and b) years 2 through 4. The disturbance grazer + point overlapped with disturbance grazer - in the low zone of year 1 in a).

**Frequency of species occurrence within a zone and treatment**

To understand how common or rare species were within a zone and treatment, and whether species differences among treatments were driven largely by a single appearance of a species or a consistent presence common to many replicates, I first determined how many replicates each species occupied in each zone and treatment. In the low zone, species present in disturbance treatments were most commonly found in 2 to 4 replicates, while species in control treatments were most commonly found in all replicates. In the mid zone however, species were most commonly found in 2 to 4 replicates for all treatments. In contrast to low zone controls, single-replicate occurrences of species were the most common pattern in high zone controls.

Within a zone, the majority of species that were rare within a single treatment – that occurred in only one replicate of a treatment – could also be found in other treatments. Of 13 species that were rare within treatments in the low zone – i.e., species that were found in only 1 replicate per treatment – only 3 (23%) were actually unique to one treatment (Table 4.F.1). For example, within the low zone *Mazzaella flaccida* was found in only 1 replicate control treatment, but it was also found in more than one replicate in the disturbance treatments. In contrast, within the low zone *Osmundea spectabilis* was found in only one replicate of a disturbance treatment without grazers, and was not found in either of the other treatments. Of 21 instances in which a species occurs in 1 replicate within a treatment in the mid zone, 6 (29%) are also unique to a single treatment. In the high zone, there are 14 cases of a species occurring in 1 replicate within a treatment, but only 4 (29%) of these species are truly unique across the high zone.

While being rare within a treatment did not guarantee that a species would be unique to that treatment (Table 4.F.1), the vast majority of species that were unique to a single treatment in the mid and high zone did indeed occur in only 1 replicate (Table 4.F.2). To understand which species were unique to treatments, species lists were compared between control and disturbance treatments with ambient grazers, and between disturbance treatments with ambient vs reduced grazers. Of 18 unique species identified in pairwise comparisons in the low zone, 4 (22%) were found in only 1 replicate within a treatment. In the mid zone however, 11 of 12 species (92%) that were unique to a treatment only occurred in a single plot replicate. Of 8 species in the high zone that were unique to a single treatment, 6 (75%) were found in only one replicate. These patterns indicate that treatment differences within the mid and high zone may be driven by rare species more than in the low zone.

Of the 6 uniquely occurring brown algal species in the low zone reduced grazer disturbance plot (Table 4.F.1), *Melanosiphon sp.* and *Pelvetiopsis limitata* were limited to only 1 of 9 replicates. *Fucus gardneri* occurred in 2 replicates, *Egregia menziesii* in 3 replicates, *Alaria marginata* in 4 replicates and *Analipus japonicus* in 6 of 9 replicates.

**Macroalgal treatments converge on control assemblages at different rates among zones in ordination analyses**

Non-metric multidimensional scaling analyses of plot algal richness and abundance yielded treatment effects that differed from analyses of macrophyte, animal and habitat abundance alone. Disturbance treatments took different lengths of time to converge on to control plot

characteristics depending on the zone (Table 4.3) based on non-metric multidimensional scaling analysis. In the low zone, disturbance treatments were indistinguishable from controls only in the third year of the study, while mid zone plots did not converge on control community assemblages until the fourth year of the study (Figure 4.6). There was little effect of treatment in the high zone; even in the first year of the study right after treatments were established, communities appeared to be indistinguishable by treatment, though for part of season 2 and season 3 there was an effect of treatment. Overall, the different diversity metrics used to investigate changes in macroalgal assemblages over time showed different patterns in the amount of time to convergence (Figure 4.7).

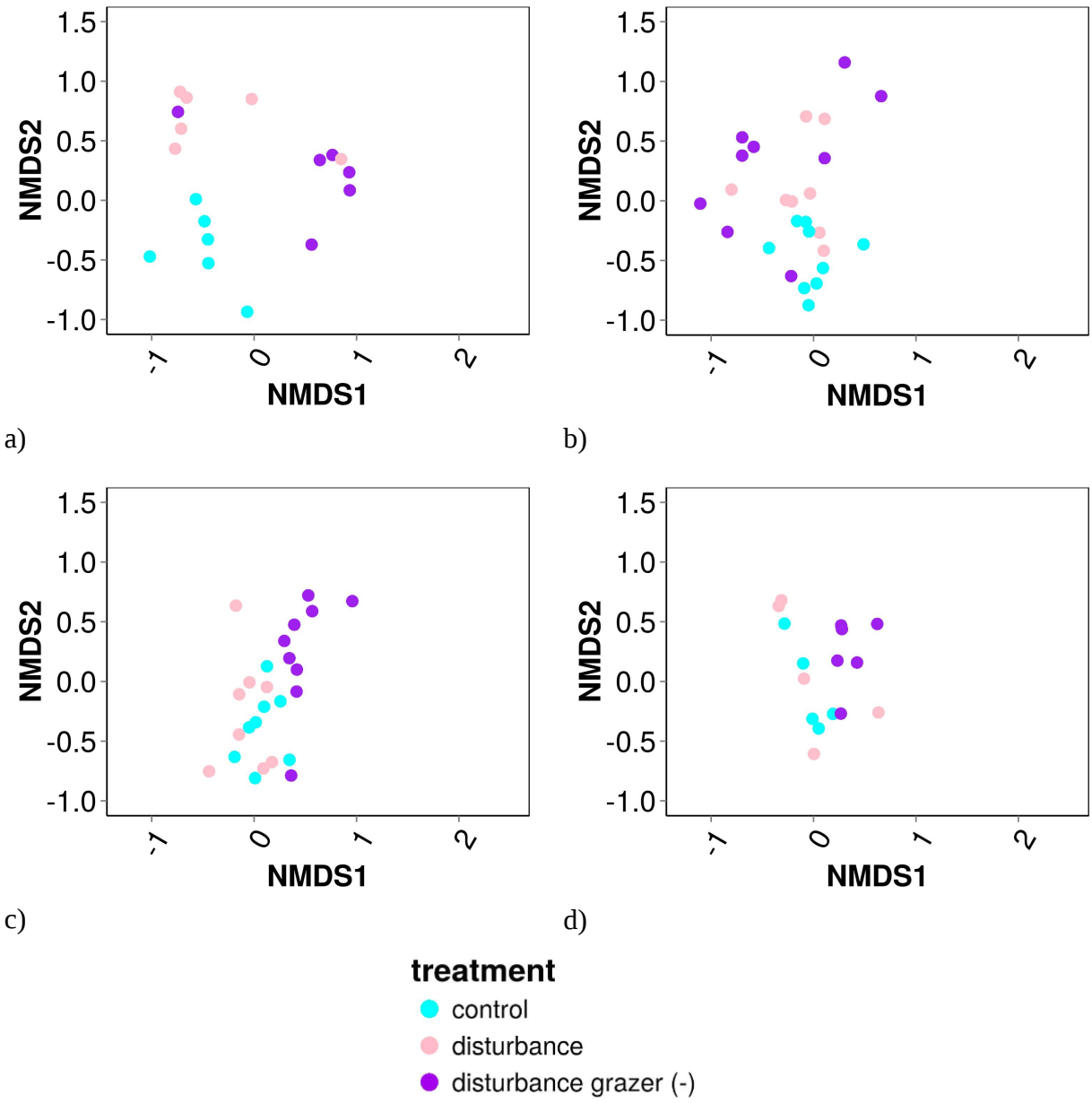


**Figure 4.6.** NMDS tracking seaweed communities by treatment over four years in the mid zone. a) year one, two months after installation; b) year two; c) year three, and d) year four.

| **Table 4.3.** Results of fitting treatment categories to a Bray-Curtis NMDS. p values indicate whether treatment had a significant effect on algal assemblages within a zone and year. | | | |
|---|---|---|---|
| Census time point | Low zone | Mid zone | High zone |
| Early season 1 | **p < 0.001** | **p = 0.036** | p = 0.089 |
| Late season 1 | **p < 0.001** | **p < 0.001** | p = 0.651 |
| Early season 2 | **p = 0.043** | **p < 0.001** | **p = 0.044** |
| Late season 2 | **p = 0.003** | **p < 0.001** | p = 0.357 |
| Early season 3 | p = 0.092 | **p = 0.019** | **p = 0.017** |
| Late season 3 | p = 0.582 | **p < 0.001** | p = 0.237 |
| Early season 4 | p = 0.090 | p = 0.065 | p = 0.884 |
| Late season 4 | **p = 0.036** | p = 0.089 | p = 0.283 |

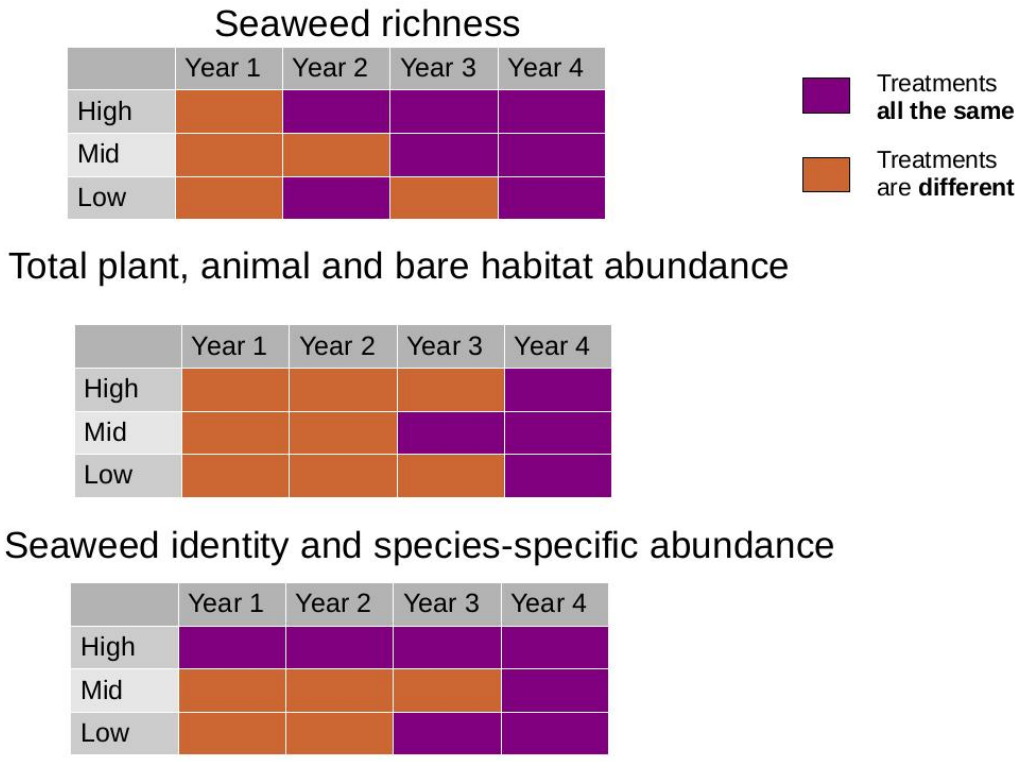


Figure 4.7. Side-by-side comparison of differing diversity metrics.

**Phylogenetic community structure indicates an effect of grazers in disturbance communities**

Phylogenetic species variability in controls in the low zone differed significantly from disturbance treatments with ambient grazers only in year 1 ($t_4 = 5.91$, $p = 0.003$, Figure 4.8a). In the mid zone, only 1 plot had more than 2 red algal species during the first year of succession so phylogenetic species richness could not be statistically compared across treatments. However, the second through fourth year showed no significant differences in PSV between control and disturbance grazer + treatments (year 2, $t_{40} = 0.20$, $p = 0.846$; year 3, $t_{27} = -0.52$, $p = 0.607$; year 4, $t_{20} = 0.04$, $p = 0.970$). The high zone also had no disturbance grazer + plots with greater than 1 red algal species in it so could not have a PSV metric the first year. However, in year 2 disturbance grazer ambient treatments had significantly higher PSV than control treatments ($t_{36} = -0.37$, $p < 0.001$), indicating that species were on average more distantly related in disturbance grazer + plots than control treatments in the high zone during year 2.

When PSV was compared between disturbance treatments with ambient versus reduced grazers, there was a significant effect of grazers on PSV. In the low zone, grazer reduction treatments were significantly more closely related than ambient grazer disturbance treatments in the first year ($t_8 = -2.99$, $p = 0.017$). In the mid zone, grazer reduction treatments were less closely related than ambient grazer plots ($t_{20} = 2.60$, $p = 0.017$) in year 3. There was no effect of grazers in high zone disturbance plots. Reduction of grazers led to lower PSV and more closely related macroalgal assemblages in the low and mid zone compared to disturbance assemblages with ambient grazers.

In the low zone, PSV in grazer reduction treatments was significantly different from PSV in control treatments every year after the first year (year 1 $t_6 = -0.67$, $p = 0.526$ , year 2, $t_{53} = -2.11$, $p = 0.039$; year 3, $t_{29} = 3.12$, $p = 0.004$; year 4, $t_{15} = 2.24$, $p = 0.041$). The mid zone however only saw this trend in year 3 ($t_6 = -0.67$, $p = 0.526$), and the high zone only in year 2 ($t_6 = -0.67$, $p = 0.526$).

Phylogenetic species evenness is the PSV metric with species relative abundance incorporated. After the first year during which disturbance treatments were installed, disturbance grazer + plots were largely similar to control plots in PSE for all zones, with the exception of year 2 in the high zone ($t_{32} = -7.81$, $p < 0.001$, Figure 4.8b). An effect of grazers on disturbance macroalgal assemblages was only found in year 4 in the low zone, where grazer reduction led to more closely related assemblages ($t_{32} = -7.81$, $p < 0.001$), and in the second year in the high zone ($t_{35} = 3.87$, $p < 0.001$). Grazer reduction plots in the low zone never fully recovered the PSE observed in control and disturbance plots with grazers.

There was an effect of zone on both PSV (mixed effects ANOVA, $F_{2,208} = 51.13$, $p < 0.001$) and PSE (mixed effects ANOVA, $F_{2,208} = 34.81$, $p < 0.001$). In years 1 through 3 the mid zone was more distantly related in red algal assemblage makeup than the low and high zones (Tukey HSD, low-mid $p < 0.001$, mid-high $p < 0.001$, low-high $p = 0.999$). However, in the final year of the study none of the zones were significantly different in PSV.

For the first two years of the study, assemblages had the lowest PSE and thus were the most closely related in the high zone, followed by the low zone, and then the mid zone (Tukey HSD all $p < 0.001$). This effect was no longer present in the 4$^{th}$ year of the study.

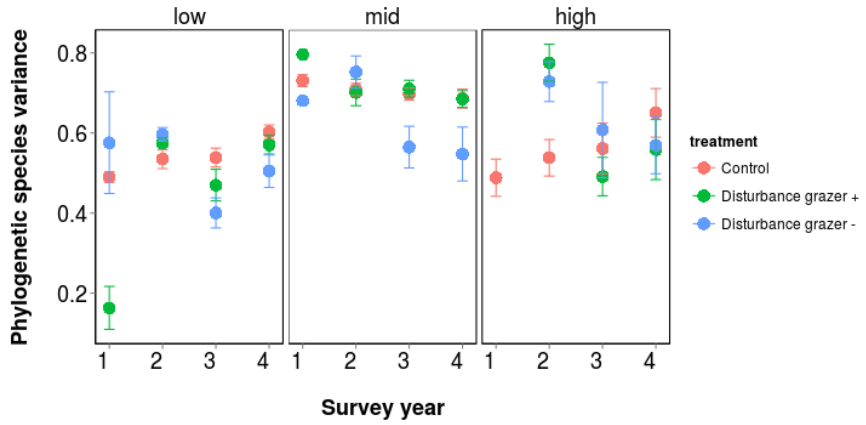


a)

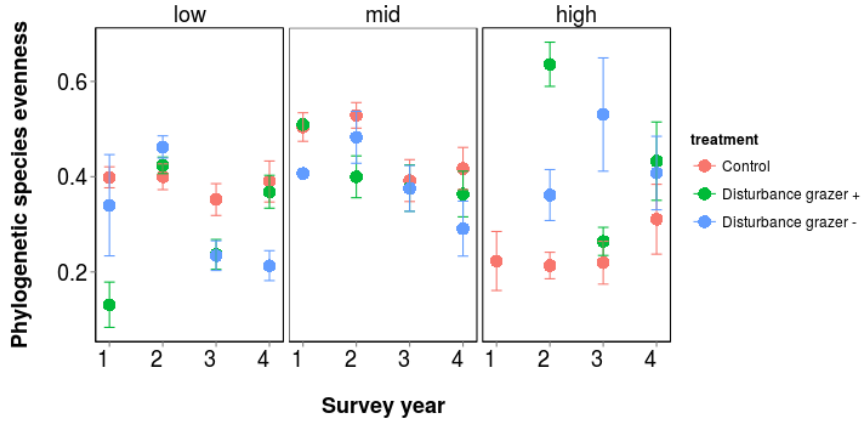


b)

**Figure 4.8.** Phylogenetic species variance and evenness, by treatment, zone and year for red macroalgae. a) Phylogenetic species variance and b) phylogenetic species evenness. Disturbance treatment values are missing in panel b) high zone because no plots in the high zone had greater than 1 red algal species in the first year. Phylogenetic species variance quantifies how phylogenetic relatedness decreases the variance of a hypothetical unselected or neutral trait shared by all species in a community. The expected value of PSV is one when all species in a sample are unrelated (i.e., a star phylogeny) and approaches zero as species become more related. Phylogenetic species evenness is PSV with relative species abundances incorporated. PSE = 1 only if all species abundances are equal and the species phylogeny is a star.

**Habitat membership is labile**

There was no phylogenetic signal in the number of zones a species inhabited, nor was there signal in the pattern of species' range expansions or contractions under different treatments (Figure 4.8). Pagel's $\lambda$ for the discrete trait of number of zones inhabited by species in the control treatment was significantly less than 1 ($\lambda = 6.65 \times 10^{-5}$, $p < 0.001$) and was comparable to $\lambda = 0$ ($p = 1.000$), i.e., a star phylogeny, indicating that the number of zones a species inhabits is largely independently derived. Results were the same for disturbance treatments with ambient grazers ($\lambda = 6.65 \times 10^{-5}$, p[$\lambda$ equals 1] < 0.001, p[$\lambda$ not different from 0] = 1.000) and in disturbance treatments with reduced grazers ($\lambda = 0.47$, p[$\lambda$ equals 1] < 0.001, p[$\lambda$ not different from 0] = 0.474). There was no phylogenetic signal in species range shifts in the control versus disturbance treatments with grazers present ($\lambda = 6.65 \times 10^{-5}$ [actual value], p[$\lambda$ equals 1] < 0.001, p[$\lambda$ not different from 0] = 1.000), nor the disturbance grazers present versus disturbance reduced grazer treatments ($\lambda = 6.65 \times 10^{-5}$ [actual value], p[$\lambda$ equals 1] < 0.001, p[$\lambda$ not different from 0] = 1.000). The results were the same when species were classified as belonging to either a single zone (single-zone species were exclusively found in the low zone) or multiple zones by treatment.

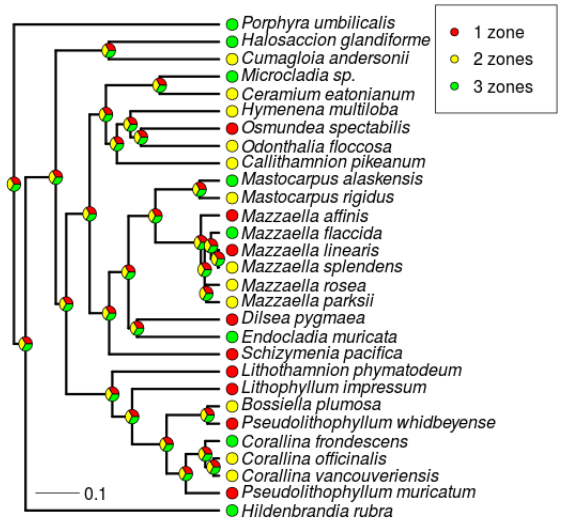


a)

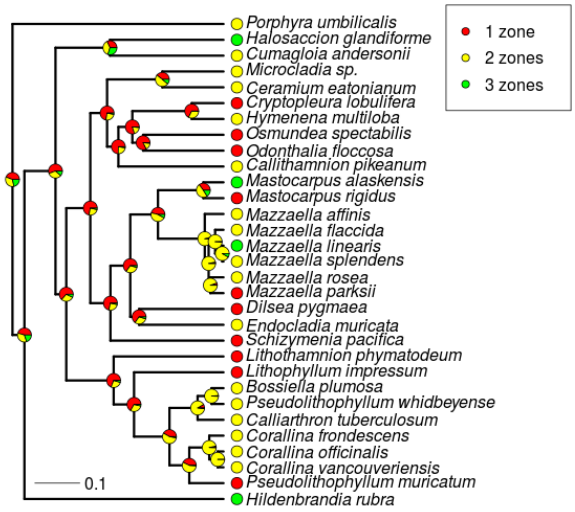


c)

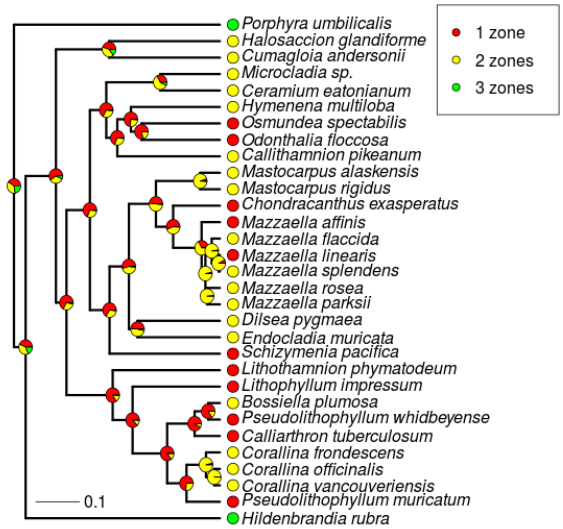


b)

**Figure 4.8.** Ancestral trait reconstruction of the number of zones a species inhabits for each treatment. a) control treatments, b) disturbance treatments and c) disturbance treatments with reduced grazers. Internal nodes represent likelihood of each trait state for the hypothetical ancestor.

## DISCUSSION

The diversity metrics evaluated in the field experiment did not all yield the same results. There was a negative relationship between species richness per plot and tidal height that was also

reflected in cumulative richness per plot. However the low and mid zone showed similar per plot cumulative richness but distinct species richness, potentially indicating higher turnover in the less species-rich mid zone to accumulate similar numbers of species over time as the low zone. Additionally, similar species richness among treatments indicates that disturbance and herbivores do not affect the number of species a 0.25 $m^2$ area can support. While disturbance and grazers had no effect on species richness and very little effect on cumulative richness, these factors did affect species identity in the plot, indicating some turnover. For example, 6 brown algal species were only observed in the low zone grazer reduction plots, despite no treatment effect on cumulative richness or species richness values.

Cumulative richness was not different among treatments within a zone, but treatments were different among zones. Low and mid zone controls and disturbance plots with grazers had higher per plot cumulative richness. This reflects findings from pulse disturbance studies in the literature, where rarely- and occasionally-flooded plots had similar cumulative tree species richness in tropical forests, but frequently flooded plots had lower cumulative richness (Giehl and Jarenkow 2015). However, the mid zone resembled the high zone in low cumulative richness in disturbance treatments when grazers were reduced. This indicates that grazer reduction with disturbance decreased mid zone cumulative richness to look less like the mid zone and more like the high intertidal zone in the overall number of species that occurred in a plot over the four-year experiment.

Based on species richness per plot, plots generally converged on control treatments within 1 year

in all zones, but treatment differences in percent cover remained well after the first year. Grazer reduction led to higher seaweed abundance compared to grazer ambient treatments in the first and second years in all zones, but no differences in species richness (with the exception of lowered species richness in the mid zone). Indeed, low and high zone disturbance treatments didn't converge to control percent cover values until the 4$^{th}$ year.

By richness and abundance metrics, disturbance treatments converged to control values within the span of the four-year study in all zones. However, treatment affected phylogenetic species variance in the low zone in years three and four, such that disturbance plots with reduced grazers had significantly lower PSV and more closely related assemblages. This effect was not observed in year two. While grazers may not be necessary for diverse macroalgae to recruit into a plot, grazers in the low zone may be necessary for diverse algal assemblages to persist in this zone.

Non-metric multidimensional scaling analyses found few treatment effects in the high zone, and the longest time to recovery in the mid zone. This metric takes into account richness and abundance, here recorded as percent cover. These species-specific abundance data indicate that although total macroalgal cover analyses showed that macroalgal cover was lower in high zone disturbance plots compared to control plots until year 4 of the study, the relative proportions of species-specific percent cover were not significantly different by treatment. In the mid intertidal zone, NMDS results indicated that treatments did not converge on control assemblage richness and percent cover until the 4$^{th}$ year. However, total animal, macrophyte and free habitat percent cover converged to control proportions by year three. This was the opposite trend of the high

zone: in the mid intertidal, species-specific abundances were different from control abundances, despite no differences in total macrophyte percent cover. In the low intertidal, total macrophyte percent cover lagged behind species-specific percent cover in converging to control plot proportions. The mid zone therefore showed a unique pattern, in which species-specific percent cover recovery lagged behind total percent cover.

Despite differences in the rate and path of recovery among zones and treatments, convergence of most treatments to control assemblage conditions within four years corresponds to recovery times recorded in the literature. An 18-year survey of sessile species in middle intertidal 60 x 60 cm plots on Tatoosh Island found that most plots underwent one to two disturbance/succession cycles within that time period (Wootton and Forester 2013). Another study in the same region found that assemblages converged to pre-disturbance conditions in 17-39 months (Paine 1984).

Increases in assemblage relatedness during succession supported findings in the literature of more phylogenetically clustered communities early in succession and that become more even through time (Li et al. 2015). However, the effect of grazers on phylogenetic species variance and evenness was more varied. Reducing grazers decreased phylogenetic diversity in the low zone in year 1 and in the mid zone in year 3 compared to disturbance plots with ambient grazers. Thus, the presence or absence of grazers did not cause significant effects in assemblages recovering from a pulse disturbance. However, reducing grazers did lead to significantly lower PSV in the low zone every year after the first year compared to controls. Thus while disturbance treatments were not significantly different from each other, disturbance with grazer reduction

treatments were significantly lower in PSV than control plots, leading to increased assemblage relatedness in plots with reduced grazers. In the low intertidal zone, the presence of grazers may increase phylogenetic diversity.

Contrary to predictions that phylogenetic species variance would decrease with increasing tide height, the mid intertidal zone had the highest phylogenetic species variance and evenness, meaning that mid zone macroalgal assemblages were the least closely related when compared with the other two zones. I predicted a positive relationship between tide height and relatedness, because potentially constraining environmental conditions higher in the intertidal would filter out all but a few closely-related, stress-resistant taxa. The mid zone was not significantly different from low zone in desiccation pressure (Figure 3.B.1), but it did experience significantly more wave action.

This pattern of intermediate species richness, but maximum phylogenetic diversity, is rare in the literature. The opposite pattern has been observed: maximum species richness of Himalayan songbirds in mid-elevations – potentially due to patterns in resources – but intermediate phylogenetic species variability (Price et al. 2014). Several studies have found maximum species richness and maximum phylogenetic diversity in mid-elevations. Ant diversity along an elevational gradient showed phylogenetic diversity and species richness peaked in middle elevations (Smith et al. 2014). Middle-range epiphytic fern assemblages have also shown more phylogetically dispersed communities than in low or high ranges (Kluge and Kessler 2011), with corresponding highest richness in the middle of the range. High richness and high phylogenetic

diversity in a mid-range has been hypothesized to be a result of selection for species that are more distinct and may be able to take advantage of more niches (Kluge and Kessler 2011). Other studies have found the pattern expected in this study: a negative relationship between phylogenetic diversity and elevation, with intermediate richness or no strong richness pattern (Graham and Fine 2008, Hoiss et al. 2012), or a tight correlation between richness and phylogenetic diversity (Machac et al. 2011).

While the finding that assemblages recovering from disturbance were initially more phylogenetically clustered and become less clustered over time is not surprising, it's unclear what caused the declines and subsequent recoveries in PSV and PSE. Colonization of more distant relatives or extinction of close relatives could both drive the observed phylogenetic patterns (Li et al. 2015). Because species richness was generally not affected by treatment and recovered to control levels by the second year of the experiment, rates of colonization and extirpation may be similar. The next step is to identify species that are entering and leaving plots at each time point, to understand colonization and extinction patterns in close and distant relatives. Additionally, expanding this analysis to include brown and green algae would assess if similar patterns are found in these Phyla, and whether overall community patterns change.

**ACKNOWLEDGEMENTS**

I thank the Makah Tribal Nation for access to Tatoosh Island and C.A. Pfister, J.T. Wootton, T.D. Price, R. Ree, and the Pfister-Wootton lab for helpful comments. Research was supported in part by the U.S. National Science Foundation (DGE1144082 to C.C.S., DEB1311286 to C.A. Pfister

and C.C.S., OCE0928232 to C.A. Pfister and DEB0919240 to J.T. Wootton) and the U.S. National Institutes of Health (T32 GM007197).

## APPENDIX 4A: DISTANCES BETWEEN EXPERIMENTAL PLOTS

### Calculating pairwise distances between community plots

To assess if there was an effect of distance on community similarity, I generated a matrix of pairwise distances between plots using a combination of GPS data, measured pairwise distances and calculated distances to minimize measurement error. While GPS horizontal error for latitude and longitude is generally low (mode ≈ 1 m) according to GPS Standard Positioning Service quarterly analyses of the Federal Aviation Association (NSTB/WAAS T&E Team 2014), stations in San Juan, WA and Seattle, WA near my field experiment site, had a 95% horizontal GPS error accuracy was within 3.29 and 2.19 m, respectively. An analysis of the error rate of our own handheld GPS found that GPS-derived distances differed from field-based meter stick measurements by 0.52 to 1.78 m (26-89% error) at a 2 m distance. Because most experimental plots were generally between 0.10 and 10.00 m of each other, I could not rely upon GPS alone to precisely denote the location of nearby plots, and thus supplemented GPS data with field-based distance measurements in a relative coordinate system.

Of the 2556 unique pairwise distances between all 72 plots in the experiment, we measured 179 pairwise plot distances to the nearest cm (7% of the total pairwise distances) using a tape measure and calculated the rest. Due to height differences and landscape heterogeneity among plots in the intertidal zone from the low to the high zone, we held tape measures at a constant height above the center of each plot to minimize the effects of height differences on the pairwise distances. An average of five distances were recorded from each plot, ranging from three to 12 measurements per plot.

To establish anchor points for the coordinate system and obtain long-range measurements between non-adjacent, distant plots, I measured the GPS coordinates of three plots in the far corners of the field installation. We recorded GPS coordinates for plot 1, the north-eastern-most plot in the experiment, in the low intertidal (48.391483º, -124.738500º); plot 55, the north-western-most plot in the study, in the high intertidal zone (48.391800º, -124.738450º); and plot 70 , the 3rd most south-western plot, in the high zone (48.391816º, -124.738516º). Plot 70 was approximately 30 m away from plots 1 and 55, a distance that would have a comparatively lower error rate for GPS coordinates. Because our handheld GPS exhibited high error rates at small distances and the majority of community plots were within 5 m of each other, I converted GPS coordinates for these three plots to a relative coordinate system to solve for unknown coordinates and pairwise distances in the map of 72 experimental community plots.

To generate a set of coordinates for the 69 remaining plots, I performed a general purpose optimization in R using the optim function in the 'stats' package, with the goal of minimizing the squared sum of errors between known field-measured pairwise plot distances and pairwise distances from the proposed coordinates solution. Unknown coordinates were randomly seeded values within the bounds of the 3 anchored plots and then varied according to the BFGS method, a variable metric algorithm (Shanno 1970). After varying the coordinate values, an updated pairwise distance matrix was calculated and compared to field-measured distances using the sum of squared errors (SSQ). The optimization was run for 10 million generations, or until the SSQ converged on a minimum value. As each optimization run converged on a minimum total SSQ,

plot pairwise distances with the highest individual squared errors were identified as candidates for varying coordinates in the subsequent run (Table 4.A.1), and plots with low SSQs were anchored. The next run then proceeded beginning with the best-fit coordinates of the last run, and the updated anchored and varying plots.

**Best-fit model of pairwise distances**

Initial optimization with randomly seeded coordinates bound by the three anchored plot points yielded a large SSQ = 718843 $cm^2$ (Table 4.A.1). The elevation gradient among community plots in the intertidal may have contributed to high initial error. For example, when the coordinate solution from the first optimization run was mapped and inspected visually for accuracy, plots 1 and 2 appeared out of place compared to field-sketched maps and photos. The field measured distance between plot 1 in the low zone and plot 55 in the high zone was 950 cm, however the GPS-derived distance was 520 cm, which may not have reflected the change in elevation between the plots and yielded large errors in plots adjacent to plot 1. Thus, while plot 1 was used as a third anchor to initially orient the coordinate system, subsequent runs allowed this plot and nearby plots to vary, while anchoring the rest (Runs 2-4, Table 4.A.1). Once this area of the map was resolved, a new region of plots on the southern rocky bench of the field installation were identified as having the highest squared errors. Community plots on the southern rocky bench also had high variation in elevation; these plot coordinates were varied in a subsequent run, while plots on the northern rocky bench were anchored, to arrive at a final coordinate solution with a low SSQ of 23696 $cm^2$ (Run 5, Table 4.A.1).

Ninety-four percent of pairwise distances in this coordinate solution had SSQ < 500 $cm^2$, and 85% had SSQ < 250 $cm^2$ indicating that the optimized coordinate system did a fairly good job approximating true field-measure distances, and could be subsequently used to approximate the remaining 2377 pairwise distances not measured in the field. Raw errors summed to 1470 cm over the 179 field-measured pairwise distances. Distance measurements averaged an error of 8 +/- 1 cm, corresponding to a mean error rate of 6 +/- 1% (absolute value of field-based minus calculated distances, divided by field-based distance). In the case of differences between field-measured and calculated pairwise distances, 92% of calculated distances were within 20 cm of the actual distance, 84% within 15 cm of the actual distance, and 68% within 10 cm. One hundred fifty-three of 179 pairwise distances (85%) had an error rate less than 10%, while 74% of pairwise distances had an error rate less than 5%, and 60% had an error rate less than 2.5% (**Figure 4.A.1**).


a) b)

**Figure 4.A.1.** Fit of plot distance estimates. a) Histogram of residual differences (absolute value of field-measured distance minus calculated distance) between 179 plot pairwise distances. Calculated plot pairwise distances are from an optimized relative coordinate matrix. b) Histogram of % error rate between 179 field-measured plot pairwise distances and calculated plot pairwise distance from a optimized relative coordinate matrix. Metric is the absolute difference between field and 'found' distances, divided by field distances.

## APPENDIX 4B: ABIOTIC PARAMETERS OF THE EMERSION GRADIENT

### Measuring differences in environmental desiccation pressure among community plots

While macrophytes vary in their desiccation rates, variation in environmental desiccation pressure among nearby communities is less well documented. To measure the cumulative effects of wind and heat on the environmental desiccation pressure among macroalgal communities, I evaluated the environmental effects each community plot was subjected to over part of a summer low tide using gel agarose cubes. Agarose, a polysaccharide polymer extracted from red macroalgae, is a good approximation of seaweeds and when mixed and heated with water forms a firm gel that slowly dries out under arid conditions. This technique has been previously applied to assess environmental affects among intertidal sites (citation). I made a 1% agarose gel, and cut the gel into 2 x 2 x 1 cm cubes, averaging 4 ± 0.02 g standard error. I weighed each agar cube prior to deployment, then stored cubes individually in airtight vials until deployment. Ten control cubes were stored in airtight vials for the duration of the study to account for any mass lost during storage and subsequently calibrate later analyses of field deployed cubes. All cubes were made and initially weighed on July 15$^{th}$ 2012.

Cubes were deployed during morning low tide on August 3, 2012 – a sunny, dry day – to investigate desiccation at the higher end of the range of environmental conditions. To prevent substrate differences from confounding the effects of pure desiccation from wind and sun, I placed cubes on a 0.4" thick plywood circle as a substrate barrier (1.5" in diameter) on top of any macroalgal biomass present in the plot. Cubes were placed on the substrate barrier in the center

of each community plot for 3 hours during low tide. Cubes were then recovered and immediately returned to their airtight vials (which were closed during deployment to maintain conditions within the vial), and reweighed on August 4$^{th}$ along with control cubes.

Desiccation rates were calculated as mass lost per hour, and were normalized as percent mass lost over the 3 hour trial. Variation in desiccation rates were then investigated among zones and within zones. To test for an effect of zone on desiccation rates, an ANOVA was applied. A linear regression was applied to plot coordinate data to understand if there was a spatial effect of plot placement from the north to south of the bench. Also, community pairwise differences in desiccation were plotted again community pairwise distances within a zone to test if closer communities shared more similar desiccation environments.

**Environmental desiccation pressure varies among zones**

Cubes were deployed an average of 182 +/- 0.3 SE minutes, or nearly exactly 3 hours, from 7:07 am to 10:50 am. Time of deployment was between 7:07 and 7:50 am to deploy the 72 agar cubes and between 10:13 and 10:50 am to pick them up. Despite all cubes being deployed for the same amount of time, the percent wet mass lost was significantly different by zone (ANOVA $F_{2,69}$ = 12.32, $p < 0.001$, Figure 4.B.1). Low zone agar cubes lost an average of 13.9 +/- 1.9%, mid zone cubes lost 19.1 +/- 2.1 %, and high zone cubes lost a mean of 29.9 +/- 2.6%. Within zones, there was no effect of treatment on desiccation rate ($F_{2,24}$ = 0.783, $p = 0.469$) in the low zone, nor was there an effect of position along the horizontal north to south transect of the rocky bench that the plots were installed along (linear regression $F_{1,25}$ = 1.32, $R_2$ = 0.05, $p = 0.262$) or an effect of plot

algal cover (linear regression, $F_{1,25} = 0.83$, $R_2 = 0.03$, $p = 0.370$). Mid zone results mirrored those of the low zone, as well as the high zone, with the exception of an effect of increasing desiccation rates from north to south along the northern rocky bench the experiment was installed on (linear regression, $F_{1,10} = 8.21$, $R^2 = 0.45$, $p = 0.017$). Overall, there was no difference in desiccation pressure between plot treatments. While there was no relationship between algal cover and desiccation rate within zones, there was a relationship between increasing algal cover and decreasing desiccation among all zones (linear regression, $F_{1,69} = 11.5$, $R^2 = 0.14$, $p = 0.001$). Desiccation increased with increasing nonalgal cover (sessile invertebrates, $F_{1,69} = 9.6$, $R^2 = 0.12$, $p = 0.003$) and increasing bare rock ($F_{1,69} = 5.6$, $R^2 = 0.08$, $p = 0.021$), but algal cover showed the strongest relationship (Figure 3.B.2). In the low and mid zones, there was a small but significant effect of plot pairwise distance on plot pairwise desiccation differences (linear regression $F_{1,349} = 4.5$, $R^2 = 0.01$, $p = 0.035$; $F_{1,349} = 5.7$, $R^2 = 0.02$, $p = 0.017$ respectively), however this was not significant in the high zone. Community plots near each other within the low and mid zones tended to have more similar desiccation rates.

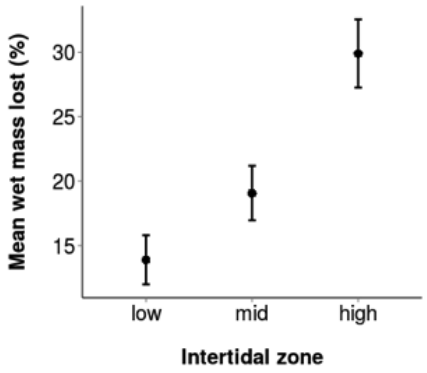


**Figure 4.B.1.** Mean percent wet mass lost per community plot in the low, mid and high zones. Error bars indicate standard error.

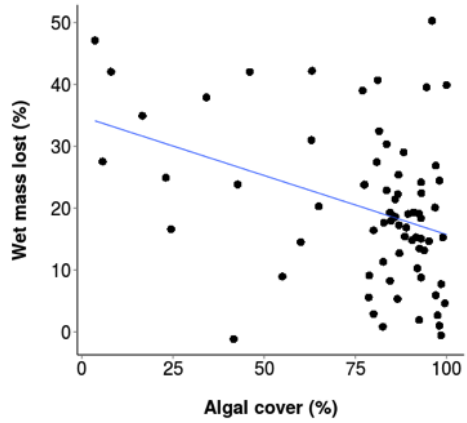


**Figure 4.B.2.** Desiccation as a function of algal cover. Wet mass lost is depicted versus corresponding algal percent cover for each agar cube, where each point is an agar cube deployed at a different experimental plot.

**Measuring differences in wave action among zones and community plots**

To determine the relative intensity of wave action among tidal zones and among plots within tidal zones, the relative dissolution rates of Denstone™, a commercially available gypsum (calcium sulfate) powder for dental work, were studied at each plot. The dissolution of gypsum or gypsum-based plaster of Paris plaster blocks (historically called 'clod cards' has been previously used to determine differences in 'water motion' (Muus 1968, Doty 1971). While calibrating in-field dissolution rates to control lab dissolution conditions has some challenges (Porter *et al.* 2000) because calibration conditions rarely mimic field conditions, this technique can be used to indicate and compare boundary layer thickness and mass-transfer rates in a fluctuating flow-dominated environment. Denstone™ cylinders were cast in a film cannister with a 3” stainless steel screw through the center. After the Denstone™ cured for 2 days at room temperature, cylinders were dried in a drying oven at 60 degrees C and massed every 6-8 hours

to the nearest 0.1 g until masses stabilized to within 0.3 g, approximately 24 hours. The rocky intertidal could be characterized as a fluctuation-dominated flow environment (the ratio of steady flow speed to fluctuation intensity is smaller than 1), in which flow is constantly changing direction due to crashing and receding waves (Terray *et al.* 1996), as opposed to flow environments with more steady flow relative to fluctuation intensity. In areas with higher wave action and more frequent inundation by water, the Denstone™ will dissolve more quickly.

Denstone™ cylinders were installed in the middle of the left border immediately outside each of the 72 community plots. Cylinders were deployed for 4 days during a low tide series from May 29 to June 1, 2014. Mean significant wave height during this time was 1.30 +/- 0.04 m, with a maximum significant wave height of 2.07 m (6.79 ft), and 30% of time periods exhibiting significant wave height greater than 1.5 m. Significant wave height is calculated as the average of the highest one-third of all wave heights during a 20 minute sampling period. After Denstone™ cylinders were recovered, they were dried in a drying oven at 60 degrees until masses stabilized to within 0.3 g as in the initial pre-deployment protocol.

**Wave action varied along a north-south gradient due to the path of water breaking**

Dissolution rates were significantly different among zones (Figure 4.B.3, ANOVA $F_{2,69} = 271.1$, $p < 0.001$). A post-hoc Tukey analysis found that all zones were significantly different from each other (low-mid $p = 0.026$; mid-high $p < 0.001$; low-high $p < 0.001$). There was also a relationship between plot location and Denstone™ dissolution rate within the low and mid zones, where the further south a plot was located along the bench, the less mass remained (linear

regression, low zone $F_{1,25} = 32.6$, $R^2 = 0.57$, $p < 0.001$; mid zone $F_{1,25} = 43.4$, $R^2 = 0.63$, $p < 0.001$, Figure 4.B.4.). Dissolution rates were more similar among plots that were closer together in the low and mid zones (linear regression low zone $F_{1,349} = 84.9$, $R^2 = 0.20$, $p < 0.001$; mid zone $F_{1,349} = 141$, $R^2 = 0.29$, $p < 0.001$). While this same trend was observed in the high zone ($F_{1,151} = 8.5$, $R^2 = 0.05$, $p = 0.004$), the fit was poor.

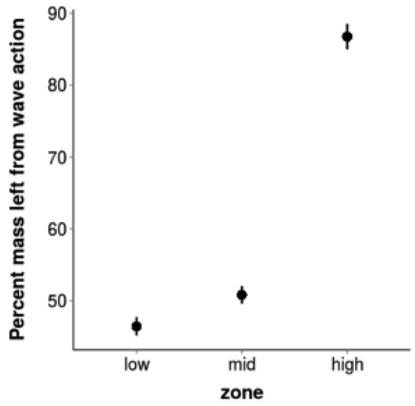


**Figure 4.B.3.** Mean percent mass remaining of Denstone™ per zone. Error bars indicate standard error.

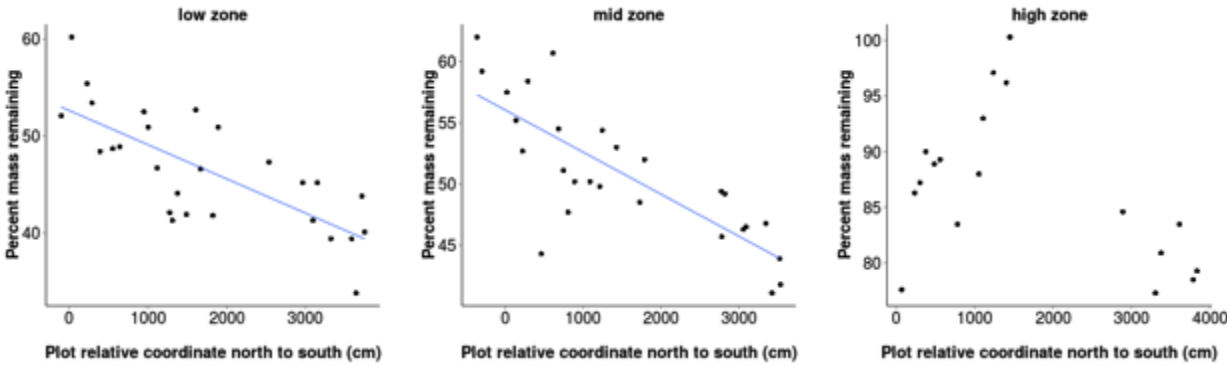


a) b) c)

**Figure 4.B.4.** Dissolution effect by plot location on rocky bench. Percent Denstone™ remaining after 4-day deployment as a function of community plot location along a north-south transect in the a) low, b) mid and c) high zones. The low and mid zone show more Denstone™ dissolution (less % mass remaining) the further south along the rocky bench and the closer to the point where waves break on the bench.

## APPENDIX 4C: DNA SEQUENCE SOURCES FOR RED ALGAL PHYLOGENY

**Table 4.C.1.** Seven genes, their length and corresponding type and best-fit evolution substitution model based on ModelTest analysis of single-gene alignments.

| Gene | Length (bp) | Marker type | Substitution Model |
|---|---|---|---|
| COI | ~664 | Mitochondria | GTR + I + G |
| rbcL | ~1350 | Chloroplast | GTR + G |
| psaA | ~1600 | Chloroplast | GTR + G |
| psbA | ~950 | Chloroplast | GTR |
| LSU | ~2700 | Ribosomal | GTR + I + G |
| ITS | ~650-1100 | Ribosomal | TN93 + G |
| SSU | ~1800 | Ribosomal | GTR + I + G |

**Table 4.C.2.** Accession numbers for red macroalgal species identified in and surrounding community plots. A indicates taxa for which at least one of the 7 sequences belongs to another species of the considered genus. B indicates sequences belonging to another species of the considered genus. The corresponding genus is indicated below the accession number. Bolded sequence numbers indicate sequences isolated for this study. Sequences in COI column indicate the barcoding sequence used and subsequent matches to sequences in GenBank or BOLD. Total number of species for each gene is listed as a percent at the end of each gene column.

| taxa | rbcL | COI | LSU | SSU | ITS | psaA | psbA |
|---|---|---|---|---|---|---|---|
| *Bossiella plumosa* | KT782044.1 | JQ615591.1<br>**CS036_COI** | **CS036_LSU** | **CS036_SSU** | KJ592030.1 | **CS036_psaA** | KJ637861.1 |
| *Calliarthron tuberculosum* | HQ322299.1 | KM254938.1<br>**CS039_COI** | **CS039_LSU** | U60944.1 | - | **CS039_psaA** | JQ422198.1 |
| *Callithamnion pikeanum* | FJ415864.1 | KM254846.1 | DQ022795.1 | AF488380.1 | - | EU195027.1 | EU195042.1 |
| *Ceramium eatonianum*[a] | FJ795531.1[b]<br>*C. pacificum* | KM254791.1<br>**CS045_COI** | **CS045_LSU** | **CS045_SSU** | AF543798.1[b]<br>*C. siliquosum* | DQ787605.1[b]<br>*C. secundatum* | DQ787644.1[b]<br>*C. secundatum* |
| *Chiharaea silvae* | **CS034_rbcL** | HQ544268.1<br>**CS034_COI** | **CS034_LSU** | **CS034_SSU** | KC157875.1 | **CS034_psaA** | JQ677021.1 |
| *Chondracanthus exasperatus*[a] | AF146194.2 | GQ398091.1 | GQ338089.1 | L34046.1[b]<br>*C. lophii* | DQ869132.1 | DQ787628.1[b]<br>*C. intermedius* | DQ787662.1[b]<br>*C. intermedius* |
| *Corallina frondescens* | KT782102.1 | JQ615675.1 | JQ615930.1 | - | JQ615876.1 | - | JQ422227.1 |
| *Corallina officinalis* | JN701476.1 | JQ615730.1 | JQ615932.1 | FM180103.1 | JQ615882.1 | KM369094.1 | KJ637655.1 |
| *Corallina vancouveriensis* | HQ322334.1 | JQ615808.1<br>**CS035_COI** | JQ615943.1 | **CS035_SSU** | JQ615901.1 | - | KJ637656.1 |
| *Cryptopleura lobulifera* | AF254176.1 | - | AF259421.1 | - | - | - | - |
| *Cryptopleura ruprechtiana* | AF254179.1 | KM254996.1<br>**CS007_COI** | AF259423.1 | **CS007_SSU** | - | **CS007_psaA** | - |
| *Cumagloia andersonii* | JX878365.1 | KC251462.1 | AF419137.1 | DQ343669.1 | - | KT886291.1 | KT886228.1 |
| *Dilsea pygmaea*[a] | JN403068.1 | AY970616.1 | JN403056.1 | U33126.1[b]<br>*D. californica* | AF317095.1[b]<br>*D. californica* | - | - |
| *Endocladia muricata* | KF026496.1 | KF026475.1 | KF026504.1 | U33127.1 | - | - | - |
| *Grateloupia sp.*[a] | **CS003_rbcL** | KJ648550.1<br>**CS003_COI** | **CS003_LSU** | U33132.1 | AF412013.1 | DQ787630.1[b]<br>*G. divaricata* | DQ787664.1[b]<br>*G. divaricata* |
| *Halosaccion glandiforme* | KT886265.1 | KT886173.1 | AF528052.1 | L26193.1 | - | KT886304.1 | KT886246.1 |
| *Hildenbrandia rubra* | DQ787557.1 | GQ497309.1 | AF419136.1 | AF108409.1 | AY028843.1 | DQ787593.1 | DQ787633.1 |
| *Hymenena multiloba* | **CS002_rbcL** | KM254737.1<br>**CS002_COI** | **CS002_LSU** | **CS002_SSU** | - | **CS002_psaA** | - |
| *Lithophyllum impressum*[a] | HQ322335.1 | KM254959.1[b]<br>*L. sp1* | KM977986.1[b]<br>*L. racemus* | AB576007.1[b]<br>*L. insipidum* | - | KM369117.1[b]<br>*L. pustulatum* | KJ418415.1[b]<br>*L. sp.* |
| *Lithothamnion phymatodeum*[a] | KP142766.1[b]<br>*L. glaciale* | KC861502.1[b]<br>*L. corallinoides* | JQ615946.1[b]<br>*L. glaciale* | JQ896261.1[b]<br>*L. corallinoides* | - | - | JQ422235.1[b]<br>*L. glaciale* |
| *Mastocarpus alaskensis* | HQ437877.1 | KM254487.1<br>**CS032_COI** | **CS032_LSU** | **CS032_SSU** | HQ437783.1 | - | - |
| *Mastocarpus jardinii* | U04031.1 | GQ380156.1<br>**CS049_COI** | GQ338093.1 | - | DQ872497.1 | **CS049_psaA** | - |
| *Mastocarpus papillatus* | U04028.1 | GQ380322.1<br>**CS004_COI** | GQ338097.1 | - | EU186037.1 | **CS004_psaA** | - |
| *Mastocarpus rigidus* | HQ437898.1 | - | - | - | HQ437850.1 | - | - |

| | | | | | | | |
|---|---|---|---|---|---|---|---|
| *Mazzaella affinis* | KF839926.1 | AY970576.1 | KF839942.1 | - | AF401064.2 | - | - |

**Table 3.C.2 continued.** Accession numbers for red macroalgal species identified in and surrounding community plots.

| **taxa** | **rbcL** | **COI** | **LSU** | **SSU** | **ITS** | **psaA** | **psbA** |
|---|---|---|---|---|---|---|---|
| *Mazzaella flaccida* | KF839911.1 | AY970574.1 | KF839928.1 | - | EU090972.1 | - | - |
| *Mazzaella linearis* | KF839922.1 | AY970584.1 | - | - | EU090961.1 | - | - |
| *Mazzaella oregona* | KF839906.1 | AY970603.1 **CS033_COI** | KF839935.1 | **CS033_SSU** | AF398530.2 | **CS033_psaA** | - |
| *Mazzaella parksii* | KF839917.1 | AY970601.1 | KF839930.1 | - | AY225231.1 | - | - |
| *Mazzaella rosea* | KF839916.1 | AY970600.1 **CS023_COI** | KF839933.1 | **CS023_SSU** | AY225232.1 | **CS023_psaA** | - |
| *Mazzaella splendens* | KF839908.1 | AY970611.1 **CS001_COI** | KF839940.1 | **CS001_SSU** | AF401067.2 | - | - |
| *Microcladia sp.*[a] | GQ252479.1 | KM254307.1[b] *M. coulteri* **CS046_COI** | DQ238799.1[b] *M. borealis* | **CS046_SSU** | - | DQ787608.1[b] *M. borealis* | DQ787647.1 |
| *Neorhodomela larix*[a] | GQ252554.1 | KM254241.1 | KC795863.1[b] N. munita | AY617140.1 | - | - | - |
| *Odonthalia floccosa*[a] | GQ252492.1 | KM254674.1 **CS051_COI** | JX572172.1[b] *O. dentata* | AY617141.1 | - | - | - |
| *Osmundea spectabilis*[a] | GQ252562.1 | KM254866.1 | KJ961424.1[b] *O. pinnatifida* | GU223795.1[b] *O. pinnatifida* | AF082341.1[b] *O. pinnatifida* | - | - |
| *Palmaria palmata* | U28421.1 | KT886175.1 | KC494650.1 | FR744765.1 | AY029385.1 | DQ787599.1 | U28165.1 |
| *Polysiphonia hendryi*[a] | KJ957815.1[b] *P. morrowii* | KM254503.1 **CS018_COI** | **CS018_LSU** | **CS018_SSU** | KM894087.1[b] *P. akkeshiensis* | DQ787625.1[b] *P stricta* | DQ787659.1[b] *P. stricta* |
| *Porphyra umbilicalis*[a] | JN787113.1 | JN028587.1 | JN029245.1[b] *P. miniata* | DQ535255.1[b] *P. purpurea* | AY322146.1 | DQ308442.1[b] *P leucosticta* | DQ787632.1[b] *P. sp.* |
| *Pseudolithophyllum muricatum* | KJ591680.1 | HQ544676.1 | JQ615948.1 | - | - | - | JQ422243.1 |
| *Pseudolithophyllum whidbeynse* | - | KJ591950.1 | - | - | - | - | - |
| *Schizymenia pacifica* | AY294393.1 | KM254490.1 **CS009_COI** | AF419129.1 | U33136.1[b] *S. dubyi* | KP725184.1 | KM359991.1 | KM360014.1 |
| *Weeksia coccineaa* | KM360031.1 | EU189324.1 | EF033611.1[b] *W. reticulata* | - | AF317120.1 | KM359984.1 | KM360007.1 |
| **Total coverage** | 98% | 95% | 93% | 71% | 66% | 56% | 51% |

## APPENDIX 4D: GEOGRAPHIC SOURCES FOR REGIONAL SPECIES POOL

**Table 4.D.1.** Regional pool source data by state from AlgaeBase. Results are categorized by Class, and final regional pool composition is based on the regional key by Gabrielson *et al.* (2012). Each cell is the number of species returned per class. * indicates a minority of species in the class are macroscopic. Total unique taxa is pooled from AlgaeBase data across regions, excluding forma, subspecies and varieties. Final regional pool indicates pool after cross-checking AlgaeBase with regional key by Gabrielson *et al.* (2012), adding species present in the Keys but absent in AlgaeBase, and excluding taxa outside the intertidal, taxa outside the geographic range, and microscopic taxa or taxa with unique (non-epilithic) life histories.

| Class | Oregon, USA | Washington, USA | British Columbia, CA | Total unique taxa | Final regional species pool |
|---|---|---|---|---|---|
| Florideophyceae | 259 | 323 | 359 | 345 | 152 |
| Phaeophyceae | 95 | 101 | 103 | 125 | 66 |
| Ulvophyceae | 66 | 77 | 88 | 92 | 33 |
| Bangiophyceae | 23 | 39 | 47 | 33 | 13 |
| Compsopogonophyceae | 7 | 9 | 7 | 8 | 0 |
| Trebouxiophyceae | 1 | 1 | 1 | 1 | 4 |
| Total taxa | 451 | 550 | 605 | 604 | 268 |

## APPENDIX 4E: ANOVA of plant, animal and free habitat abundance

**Table 4.E.1.** ANOVA results and post-hoc Tukey HSD p values from pairwise tests for a treatment effect on free habitat, animal abundance and macrophyte abundance. Second and third column show paired Tukey comparison if applicable.

| | | | **Low** | **Mid** | **High** |
|---|---|---|---|---|---|
| **Year 1** | **Free habitat** | | $F_{2,50} = 11.78$ **p < 0.001** | $F_{2,51} = 14.37$ **p < 0.001** | $F_{2,51} = 1148$ **p < 0.001** |
| | Control | Disturbance gr + | **0.005** | **< 0.001** | **< 0.001** |
| | Control | Disturbance gr - | **< 0.001** | **< 0.001** | **< 0.001** |
| | Disturbance gr - | Disturbance gr + | 0.332 | 0.996 | 0.412 |
| | **Animal abundance** | | $F_{2,50} = 8.58$ **p < 0.001** | $F_{2,51} = 28.14$ **p < 0.001** | $F_{2,51} = 23.32$ **p < 0.001** |
| | Control | Disturbance gr + | **0.002** | **< 0.001** | **< 0.001** |
| | Control | Disturbance gr - | **0.002** | **< 0.001** | **< 0.001** |
| | Disturbance gr - | Disturbance gr + | 1 | 0.981 | 1 |
| | **Macrophyte abundance** | | $F_{2,50} = 8.82$ **p < 0.001** | $F_{2,51} = 8.71$ **p < 0.001** | $F_{2,51} = 341.8$ **p < 0.001** |
| | Control | Disturbance gr + | **0.024** | **0.002** | **< 0.001** |
| | Control | Disturbance gr - | **< 0.001** | **0.002** | **< 0.001** |
| | Disturbance gr - | Disturbance gr + | 0.323 | 0.996 | 0.681 |
| | | | | | |
| | | | **Low** | **Mid** | **High** |
| **Year 2** | **Free habitat** | | $F_{2,69} = 6.47$ **p = 0.003** | $F_{2,68} = 8.10$ **p < 0.001** | $F_{2,68} = 42.53$ **p < 0.001** |
| | Control | Disturbance gr + | **0.002** | **< 0.001** | **< 0.001** |
| | Control | Disturbance gr - | 0.52 | 0.063 | **< 0.001** |
| | Disturbance gr - | Disturbance gr + | 0.047 | 0.2 | 0.562 |
| | **Animal abundance** | | $F_{2,69} = 4.72$ **p = 0.012** | $F_{2,68} = 15.31$ **p < 0.001** | $F_{2,68} = 17.19$ **p < 0.001** |
| | Control | Disturbance gr + | 0.986 | **0.02** | **< 0.001** |
| | Control | Disturbance gr - | **0.032** | **< 0.001** | 0.228 |
| | Disturbance gr - | Disturbance gr + | **0.021** | **0.023** | **< 0.001** |
| | **Macrophyte abundance** | | $F_{2,69} = 7.60$ **p < 0.001** | $F_{2,68} = 4.80$ **p = 0.011** | $F_{2,68} = 43.38$ **p < 0.001** |
| | Control | Disturbance gr + | **0.005** | 0.992 | **< 0.001** |
| | Control | Disturbance gr - | 0.983 | **0.021** | **< 0.001** |
| | Disturbance gr - | Disturbance gr + | **0.003** | **0.03** | **0.005** |
| | | | | | |
| | | | **Low** | **Mid** | **High** |
| **Year 3** | **Free habitat** | | $F_{2,34} = 0.47$ p = 0.63 | $F_{2,33} = 0.66$ p = 0.523 | $F_{2,33} = 3.82$ **p = 0.032** |
| | Control | Disturbance gr + | n/a | n/a | 0.617 |
| | Control | Disturbance gr - | n/a | n/a | **0.027** |

| | | | | | |
|---|---|---|---|---|---|
| | Disturbance gr - | Disturbance gr + | n/a | n/a | 0.192 |
| | **Animal abundance** | | $F_{2,34}$ = 5.93<br>**p = 0.006** | $F_{2,33}$ = 0.41<br>p = 0.669 | $F_{2,33}$ = 7.35<br>**p = 0.002** |
| | Control | Disturbance gr + | 0.959 | n/a | **0.005** |
| | Control | Disturbance gr - | **0.022** | n/a | 0.988 |
| | Disturbance gr - | Disturbance gr + | **0.011** | n/a | **0.007** |
| **Table 4.E.1 continued.** ANOVA results and post-hoc Tukey HSD p values from pairwise tests for a treatment effect on free habitat, animal abundance and macrophyte abundance. | | | | | |
| | | | **Low** | **Mid** | **High** |
| | **Macrophyte abundance** | | $F_{2,34}$ = 4.33<br>**p = 0.021** | $F_{2,33}$ = 0.285<br>p = 0.754 | $F_{2,33}$ = 4.17<br>**p = 0.024** |
| | Control | Disturbance gr + | 0.902 | n/a | **0.019** |
| | Control | Disturbance gr - | 0.072 | n/a | 0.251 |
| | Disturbance gr - | Disturbance gr + | **0.027** | n/a | 0.428 |
| | | | | | |
| | | | **Low** | **Mid** | **High** |
| **Year 4** | **Free habitat** | | $F_{2,33}$ = 0.56<br>p = 0.578 | $F_{2,31}$ = 0.25<br>p = 0.784 | $F_{2,33}$ = 3.34<br>**p = 0.048** |
| | Control | Disturbance gr + | n/a | n/a | 0.919 |
| | Control | Disturbance gr - | n/a | n/a | 0.124 |
| | Disturbance gr - | Disturbance gr + | n/a | n/a | 0.055 |
| | **Animal abundance** | | $F_{2,33}$ = 0.68<br>p = 0.514 | $F_{2,31}$ = 0.83<br>p = 0.446 | $F_{2,33}$ = 1.20<br>p = 0.314 |
| | Control | Disturbance gr + | n/a | n/a | n/a |
| | Control | Disturbance gr - | n/a | n/a | n/a |
| | Disturbance gr - | Disturbance gr + | n/a | n/a | n/a |
| | **Macrophyte abundance** | | $F_{2,33}$ = 0.11<br>p = 0.898 | $F_{2,31}$ = 0.544<br>p = 0.586 | $F_{2,33}$ =0.89<br>p = 0.421 |
| | Control | Disturbance gr + | n/a | n/a | n/a |
| | Control | Disturbance gr - | n/a | n/a | n/a |
| | Disturbance gr - | Disturbance gr + | n/a | n/a | n/a |

## APPENDIX 4F: FREQUENCY OF SPECIES OCCURRENCES AMONG REPLICATES, TREATMENTS AND ZONES

**Table 4.F.1.** Species occurring in only one plot replicate within a treatment (indicating rarity). * indicates that the species occurs only in that treatment within a zone. Subscript R, P and C indicate Phylum membership in Rhodophyta, Phaeophyta or Chlorophtyta.

| | Treatment | | |
|---|---|---|---|
| Zone | Control grazers present | Disturbance grazers present | Disturbance grazers reduced |
| Low | Rhodophyta:<br>*Corallina cretacea,*<br>*Endocladia muricata,*<br>*Mastocarpus alaskensis,*<br>*Mazzaella flaccida* | Chlorophyta:<br>*Cladophora columbiana*<br><br>Phaeophyta:<br>*Leathesia difformis*<br><br>Rhodophyta:<br>*Cyptopleura lobulifera**<br>*Mazzaella rosea* | Chlorophyta:<br>*Codium setchellii*<br><br>Phaeophyta:<br>*Melanosiphon sp.**<br>*Pelvetiopsis limitata*<br><br>Rhodophyta:<br>*Calliarthron tuberculosum*<br>*Osmundea spectabilis** |
| Mid | Phaeophyta:<br>*Ralfsia fungiformis*<br><br>Rhodophyta:<br>*Cumagloia andersonii,*<br>*Mazzaella parksii,*<br>*Mazzaella splendens,*<br>*Odonthalia floccosa** | Chlorophyta:<br>*Codium setchellii*<br><br>Phaeophyta:<br>*Alaria mariginata*<br>*Saccharina groendlandica**<br><br>Rhodophyta:<br>*Calliarthron tuberculosum**<br>*Corallina cretacea**<br>*Corallina officinalis*<br>*Hymenena multiloba*<br>*Mazzaella splendens*<br>*Pseudolithophyllum whidbeyense** | Phaeophyta:<br>*Corallina officinalis*<br>*Dilsea pygmaea*<br>*Hymenena multiloba*<br>*Plocamiun cartilagineum*<br><br>Rhodophyta<br>*Melansiphon sp.**<br>*Ralfsia fungiformis*<br>*Saccharina sessilis* |
| High | Phaeophyta:<br>*Melanosiphon sp.**<br><br>Rhodophyta:<br>*Corallina frondescens**<br>*Cumagloia andersonii*<br>*Halosaccion glandiformis*<br>*Mazzaella affinis*<br>*Mazzaella flaccida*<br>*Microcladia borealis**<br>*Porphyra sp.* | Chlorophyta:<br>*Acrosiphonia coalita*<br><br>Rhodophyta:<br>*Cumagloia andersonii*<br>*Halosaccion glandiformis*<br>*Mazzaella affinis*<br>*Mazzaella flaccida* | Phaeophyta:<br>*Analipus japonicus** |

**Table 4.F.2.** Pairwise comparisons of unique species in control vs disturbance treatments with grazers present, and disturbance treatments with and without grazers. The first two columns look for an effect of disturbance, while the second two columns compare the presence of grazers. * indicates species occurred in only 1 replicate within the treatment and thus was comparatively rare in the treatment. Subscript R, P and C indicate Phylum membership in Rhodophyta, Phaeophyta or Chlorophtyta.

| | Disturbance effect | | Grazer effect | |
|---|---|---|---|---|
| Zone | Control grazers present | Disturbance grazers present | Disturbance grazers present | Disturbance grazers reduced |
| Low | Rhodophyta:<br>*Endocladia muricata*<br>*Mazzaella flaccida*<br>*Porphyra sp.* | Chlorophyta:<br>*Cladophora columbiana**<br>*Codium setchellii*<br><br>Phaeophyta:<br>*Ralfisa fungiformis*<br><br>Rhodophyta:<br>*Calliarthron tuberculosum*<br>*Cryptopleura lobulifera**<br>*Mazzaella linearis* | Rhodophyta:<br>*Corallina cretacea*<br>*Cryptopleura lobulifera**<br>*Mastocarpus alaskensis*<br>*Mazzaella linearis* | Phaeophyta:<br>*Analipus japonicus*<br>*Alaria marginata*<br>*Egregia menziesii*<br>*Fucus gardneri*<br>*Melanosiphon sp.**<br>*Pelvetiopsis limitata**<br><br>Rhodophyta:<br>*Chondracanthus exasperatus*<br>*Porphyra sp.* |
| Mid | Phaeophyta:<br>*Saccharina sessilis*<br><br>Rhodophyta:<br>*Mazzaella parksii**<br>*Odonthalia floccosa** | Phaeophyta:<br>*Saccharina groendlandica**<br><br>Rhodophyta:<br>*Calliarthron tuberculosum**<br>*Corallina cretacea**<br>*Mazzaella affinis*<br>*Pseudolithophyllum whidbeyense** | Chlorophyta:<br>*Codium setchelli**<br><br>Phaeophyta:<br>*Alaria marginata**<br>*Saccharina groendlandica**<br><br>Rhodophyta:<br>*Calliarthron tuberculosum**<br>*Corallina cretacea**<br>*Mazzaella affinis*<br>*Pseudolithophyllum whidbeyense** | Phaeophyta:<br>*Melanosiphon sp.**<br>*Saccharina sessilis**<br><br>Rhodophyta:<br>*Dilsea pygmaea**<br>*Mazzaella parksii* |
| High | Phaeophyta:<br>*Melanosiphon sp.**<br><br>Rhodophyta:<br>*Corallina frondescens**<br>*Mastocarpus rigidus*<br>*Microcladia borealis** | Chlorophyta:<br>*Acrosiphonia coalita**<br><br>Rhodophyta:<br>*Mazzaella linearis* | Rhodophyta:<br>*Halosaccion glandiforme**<br>*Mazzaella linearis* | Phaeophyta:<br>*Analipus japonicus**<br><br>Rhodophyta:<br>*Mastocarpus rigidus* |

## LITERATURE CITED


Adey, W. H., and J. M. Vassar. 1975. Colonization, succession and growth rates of tropical crustose coralline algae (Rhodophyta, Cryptonemiales)*. *Phycologia* 14:55–69.

Agrawal, A. A., D. D. Ackerly, F. Adler, A. E. Arnold, C. Cáceres, D. F. Doak, E. Post, P. J. Hudson, J. Maron, K. A. Mooney, M. Power, D. Schemske, J. Stachowicz, Sharon Strauss, M. G. Turner, and E. Werner. 2007. Filling key gaps in population and community ecology. *Frontiers in Ecology and the Environment* 5:145–152.

Aliscioni, S., H. L. Bell, G. Besnard, P.-A. Christin, J. T. Columbus, M. R. Duvall, E. J. Edwards, L. Giussani, K. Hasenstab-Lehman, K. W. Hilu, T. R. Hodkinson, A. L. Ingram, E. A. Kellogg, S. Mashayekhi, O. Morrone, C. P. Osborne, N. Salamin, H. Schaefer, E. Spriggs, S. A. Smith, and F. Zuloaga. 2012. New grass phylogeny resolves deep evolutionary relationships and discovers $C_4$ origins. *New Phytologist* 193:304–312.

Alstyne, K. L. V., T. A. Nelson, and R. L. Ridgway. 2015. Environmental chemistry and chemical ecology of “green tide” seaweed blooms. *Integrative and Comparative Biology* :icv035.

Andersson, A. J., K. L. Yeakel, N. R. Bates, and S. J. de Putron. 2014. Partial offsets in ocean acidification from changing coral reef biogeochemistry. *Nature Climate Change* 4:56–61.

Anthony, K. R. N., J. A. Kleypas, and J.-P. Gattuso. 2011. Coral reefs modify their seawater carbon chemistry – implications for impacts of ocean acidification. *Global Change Biology* 17:3655–3666.

Axelsson, L., and J. Uusitalo. 1988. Carbon acquisition strategies for marine macroalgae. *Marine Biology* 97:295–300.

Badger, M. R., T. J. Andrews, S. M. Whitney, M. Ludwig, D. C. Yellowlees, W. Leggat, and G. D. Price. 1998. The diversity and coevolution of Rubisco, plastids, pyrenoids, and chloroplast-based $CO_2$-concentrating mechanisms in algae. *Canadian Journal of Botany* 76:1052–1071.

Begley-Miller, D. R., A. L. Hipp, B. H. Brown, M. Hahn, and T. P. Rooney. 2014. White-tailed deer are a biotic filter during community assembly, reducing species and phylogenetic diversity. *AoB Plants* 6:plu030.

Björk, M., L. Axelsson, and S. Beer. 2004. Why is *Ulva intestinalis* the only macroalga inhabiting isolated rockpools along the Swedish Atlantic coast? *Marine Ecology Progress Series* 284:109–116.

Blomberg, S. P., T. Garland, and A. R. Ives. 2003. Testing for phylogenetic signal in comparative data: behavioral traits are more labile. *Evolution* 57:717–745.

Bracken, M. E. S., E. Jones, and S. L. Williams. 2011. Herbivores, tidal elevation, and species richness simultaneously mediate nitrate uptake by seaweed assemblages. *Ecology* 92:1083–1093.

Brawley, S. H., and L. E. Johnson. 1991. Survival of fucoid embryos in the intertidal zone depends upon developmental stage and microhabitat. *Journal of Phycology* 27:179–186.

Brewer, P. G., and J. C. Goldman. 1976. Alkalinity changes generated by phytoplankton growth. *Limnology and Oceanography* 21:108–117.

Burnham, K. P., and D. R. Anderson. 2002. Model selection and multimodel inference: a practical information-theoretic approach. *Springer Science & Business Media*.

Bustamante, R. H., G. M. Branch, and S. Eekhout. 1995. Maintenance of an exceptional intertidal grazer biomass in South Africa: subsidy by subtidal kelps. *Ecology* 76:2314–2329.

Cadotte, M. W., R. Dinnage, and D. Tilman. 2012. Phylogenetic diversity promotes ecosystem stability. *Ecology* 93:S223–S233.

Cadotte, M. W., and S. Y. Strauss. 2011. Phylogenetic patterns of colonization and extinction in experimentally assembled plant communities. *PLoS ONE* 6:e19363.

Campbell, J. E., and J. W. Fourqurean. 2013. Mechanisms of bicarbonate use influence the photosynthetic carbon dioxide sensitivity of tropical seagrasses. *Limnology and Oceanography* 58:839–848.

Cavender-Bares, J., D. D. Ackerly, D. A. Baum, and F. A. Bazzaz. 2004. Phylogenetic Overdispersion in Floridian Oak Communities. *The American Naturalist* 163:823–843.

Cavender-Bares, J., A. Keen, and B. Miles. 2006. Phylogenetic structure of Floridian plant communities depends on taxonomic and spatial scale. *Ecology* 87:109–122.

Cavender-Bares, J., and P. B. Reich. 2012. Shocks to the system: community assembly of the oak savanna in a 40-year fire frequency experiment. *Ecology* 93.

Chase, J. M. 2007. Drought Mediates the Importance of stochastic community assembly. *Proceedings of the National Academy of Sciences* 104:17430–17434.

Chin, N. K. M., M. T. Brown, and M. J. Heads. 1991. The biogeography of Lessoniaceae, with special reference to *Macrocystis* C. Agardh (Phaeophyta: Laminariales). *Hydrobiologia* 215:1–11.

Christin, P.-A., C. P. Osborne, D. S. Chatelet, J. T. Columbus, G. Besnard, T. R. Hodkinson, L.

M. Garrison, M. S. Vorontsova, and E. J. Edwards. 2013. Anatomical enablers and the evolution of $C_4$ photosynthesis in grasses. *Proceedings of the National Academy of Sciences* 110:1381–1386.

Connell, J. H. 1978. Diversity in tropical rain forests and coral reefs. *Science* 199:1302.

Connell, S. D., K. J. Kroeker, K. E. Fabricius, D. I. Kline, and B. D. Russell. 2013. The other ocean acidification problem: $CO_2$ as a resource among competitors for ecosystem dominance. *Philosophical Transactions of the Royal Society B: Biological Sciences* 368:20120442.

Cornwall, C. E., C. D. Hepburn, C. A. Pilditch, and C. L. Hurd. 2013. Concentration boundary layers around complex assemblages of macroalgae: implications for the effects of ocean acidification on understory coralline algae. *Limnology and Oceanography* 58:121–130.

Cornwall, C. E., C. D. Hepburn, D. Pritchard, K. I. Currie, C. M. McGraw, K. A. Hunter, and C. L. Hurd. 2012. Carbon-use strategies in macroalgae: differential responses to lowered pH and implications for ocean acidification. *Journal of Phycology* 48:137–144.

Cornwall, C. E., A. T. Revill, and C. L. Hurd. 2015. High prevalence of diffusive uptake of $CO_2$ by macroalgae in a temperate subtidal ecosystem. *Photosynthesis Research*:1–10.

Cuntz, M. 2011. Carbon cycle: A dent in carbon's gold standard. *Nature* 477:547–548.

Dayton, P. K. 1971. Competition, disturbance, and community organization: the provision and subsequent utilization of space in a rocky intertidal community. *Ecological Monographs* 41:351–389.

Dickson, A. G., and F. J. Millero. 1987. A comparison of the equilibrium constants for the dissociation of carbonic acid in seawater media. *Deep Sea Research Part A. Oceanographic Research Papers* 34:1733–1743.

Drummond, A. J., M. A. Suchard, D. Xie, and A. Rambaut. 2012. Bayesian phylogenetics with BEAUti and the BEAST 1.7. *Molecular Biology and Evolution* 29:1969–1973.

Duggins, D. O., and M. N. Dethier. 1985. Experimental studies of herbivory and algal competition in a low intertidal habitat. *Oecologia* 67:183–191.

Ehleringer, J. R. 1991. $^{13}C/^{12}C$ fractionation and its utility in terrestrial plant studies. *Carbon isotope techniques* 1:187.

Fabregas, J., C. Herrero, B. Cabezas, and J. Abalde. 1987. Growth and biochemical variability of the marine microalga *Chlorella stigmatophora* in batch cultures with different salinities and nutrient gradient concentration. *British Phycological Journal* 22:269–276.

Falkenberg, L. J., S. D. Connell, and B. D. Russell. 2013a. Disrupting the effects of synergies between stressors: improved water quality dampens the effects of future $CO_2$ on a marine habitat. *Journal of Applied Ecology* 50:51–58.

Falkenberg, L. J., B. D. Russell, and S. D. Connell. 2013b. Contrasting resource limitations of marine primary producers: implications for competitive interactions under enriched $CO_2$ and nutrient regimes. *Oecologia* 172:575–583.

Forrestel, E. J., M. J. Donoghue, and M. D. Smith. 2015. Functional differences between dominant grasses drive divergent responses to large herbivore loss in mesic savanna grasslands of North America and South Africa. *Journal of Ecology* 103:714–724.

Gabrielson, P. W., S. C. Lindstrom, and C. J. O'Kelly. 2012. Keys to the Seaweeds and Seagrasses of Southeast Alaska, British Columbia, Washington, and Oregon. First edition. PhycoID, Hillsborough, North Carolina.

Gerhold, P., J. F. Cahill, M. Winter, I. V. Bartish, and A. Prinzing. 2015. Phylogenetic patterns are not proxies of community assembly mechanisms (they are far better). *Functional Ecology* 29:600–614.

Gernhard, T. 2008. The conditioned reconstructed process. *Journal of Theoretical Biology* 253:769–778.

Giehl, E. L., and J. A. Jarenkow. 2015. Disturbance and stress gradients result in distinct taxonomic, functional and phylogenetic diversity patterns in a subtropical riparian tree community. *Journal of Vegetation Science* 26:889–901.

Giordano, M., J. Beardall, and J. A. Raven. 2005. $CO_2$ concentrating mechanisms in algae: mechanisms, environmental modulation, and evolution. *Annual Review of Plant Biology* 56:99–131.

Goldman, J. C., and P. G. Brewer. 1980. Effect of nitrogen source and growth rate on phytoplankton-mediated changes in alkalinity. *Limnology and Oceanography* 25:352–357.

Gómez, I., and P. Huovinen. 2012. Morpho-functionality of Carbon Metabolism in Seaweeds. Pages 25–46 *in* C. Wiencke and K. Bischof, editors. Seaweed Biology. Springer Berlin Heidelberg.

Graham, C. H., and P. V. A. Fine. 2008. Phylogenetic beta diversity: linking ecological and evolutionary processes across space in time. *Ecology Letters* 11:1265–1277.

Graham, C. H., J. L. Parra, C. Rahbek, and J. A. McGuire. 2009. Colloquium Papers:

Phylogenetic structure in tropical hummingbird communities. *Proceedings of the National Academy of Sciences* 106:19673–19678.

Gruber, N., and C. D. Keeling. 2001. An improved estimate of the isotopic air-sea disequilibrium of $CO_2$: implications for the oceanic uptake of anthropogenic $CO_2$. *Geophysical Research Letters* 28:555–558.

Gruber, N., and J. L. Sarmiento. 1997. Global patterns of marine nitrogen fixation and denitrification. *Global Biogeochemical Cycles* 11:235–266.

Guidone, M., C. S. Thornber, and E. Vincent. 2012. Snail grazing facilitates growth of two morphologically similar bloom-forming *Ulva* species through different mechanisms. *Journal of Ecology* 100:1105–1112.

Guiry, M. D., and G. M. Guiry. 2012. Algae Base. World-wide electronic publication, National University of Ireland, Galway. http://www.algaebase.org.

Haglund, K., Z. Ramazanov, M. Mtolera, and M. Pedersén. 1992. Role of external carbonic anhydrase in light-dependent alkalization by *Fucus serratus* L. and *Laminaria saccharina* (L.) Lamour. (Phaeophyta). *Planta* 188:1–6.

Harmon, L. J., B. Matthews, S. Des Roches, J. M. Chase, J. B. Shurin, and D. Schluter. 2009. Evolutionary diversification in stickleback affects ecosystem functioning. *Nature* 458:1167–1170.

Hector, A. 2011. Ecology: Diversity favours productivity. *Nature* 472:45–46.

Hellblom, F., and L. Axelsson. 2003. External $HCO_3^-$ dehydration maintained by acid zones in the plasma membrane is an important component of the photosynthetic carbon uptake in *Ruppia cirrhosa*. *Photosynthesis Research* 77:173–181.

Helmus, M. R., T. J. Bland, C. K. Williams, and A. R. Ives. 2007. Phylogenetic measures of biodiversity. *The American Naturalist* 169:E68–E83.

Helmus, M. R., W. (Bill) Keller, M. J. Paterson, N. D. Yan, C. H. Cannon, and J. A. Rusak. 2010. Communities contain closely related species during ecosystem disturbance. *Ecology Letters* 13:162–174.

Helmuth, B. S. T., and G. E. Hofmann. 2001. Microhabitats, thermal heterogeneity, and patterns of physiological stress in the rocky intertidal zone. *The Biological Bulletin* 201:374 –384.

Hepburn, C. D., D. W. Pritchard, C. E. Cornwall, R. J. McLeod, J. Beardall, J. A. Raven, and C. L. Hurd. 2011. Diversity of carbon use strategies in a kelp forest community: implications for a high $CO_2$ ocean. *Global Change Biology* 17:2488–2497.

Hernández-Ayon, J. M., A. Zirino, A. G. Dickson, T. Camiro-Vargas, and E. Valenzuela. 2007. Estimating the contribution of organic bases from microalgae to the titration alkalinity in coastal seawaters. *Limnology and Oceanography: Methods* 5:225–232.

Hoiss, B., J. Krauss, S. G. Potts, S. Roberts, and I. Steffan-Dewenter. 2012. Altitude acts as an environmental filter on phylogenetic composition, traits and diversity in bee communities. *Proceedings of the Royal Society of London B: Biological Sciences* 279:4447–4456.

Huelsenbeck, J. P., R. Nielsen, and J. P. Bollback. 2003. Stochastic mapping of morphological characters. *Systematic Biology* 52:131–158.

Hurd, C. L. 2000. Water motion, marine macroalgal physiology, and production. *Journal of Phycology* 36:453–472.

Hurd, C. L., C. E. Cornwall, K. Currie, C. D. Hepburn, C. M. McGraw, K. A. Hunter, and P. W. Boyd. 2011. Metabolically induced pH fluctuations by some coastal calcifiers exceed projected 22nd century ocean acidification: a mechanism for differential susceptibility? *Global Change Biology* 17:3254–3262.

Huston, M. 1979. A general hypothesis of species diversity. *American Naturalist* 81–101.

Johnson, L. E. 1992. Potential and peril of field experimentation: the use of copper to manipulate molluscan herbivores. *Journal of Experimental Marine Biology and Ecology* 160:251–262.

Kembel, S. W., and S. P. Hubbell. 2006. The phylogenetic structure of a Neotropical forest tree community. *Ecology* 87:S86–S99.

Kluge, J., and M. Kessler. 2011. Phylogenetic diversity, trait diversity and niches: species assembly of ferns along a tropical elevational gradient. *Journal of Biogeography* 38:394–405.

Kraft, N. J. B., and D. D. Ackerly. 2011. Functional trait and phylogenetic tests of community assembly across spatial scales in an Amazonian forest. *Ecological Monographs* 80:401–422.

Kraft, N. J. B., W. K. Cornwell, C. O. Webb, and D. D. Ackerly. 2007. Trait evolution, community assembly, and the phylogenetic structure of ecological communities. *The American Naturalist* 170:271–283.

Kroeker, K. J., R. L. Kordas, R. N. Crim, and G. G. Singh. 2010. Meta-analysis reveals negative yet variable effects of ocean acidification on marine organisms. *Ecology Letters* 13:1419–

1434.

Kroeker, K. J., F. Micheli, and M. C. Gambi. 2013. Ocean acidification causes ecosystem shifts via altered competitive interactions. *Nature Climate Change* 3:156–159.

Kübler, J. E., A. M. Johnston, and J. A. Raven. 1999. The effects of reduced and elevated $CO_2$ and O2 on the seaweed *Lomentaria articulata. Plant, Cell & Environment* 22:1303–1310.

Lapiedra, O., D. Sol, S. Carranza, and J. M. Beaulieu. 2013. Behavioural changes and the adaptive diversification of pigeons and doves. *Proceedings of the Royal Society of London B: Biological Sciences* 280:20122893.

Larkin, M. A., G. Blackshields, N. P. Brown, R. Chenna, P. A. McGettigan, H. McWilliam, F. Valentin, I. M. Wallace, A. Wilm, R. Lopez, and others. 2007. Clustal W and Clustal X version 2.0. *Bioinformatics* 23:2947–2948.

Larkum, A. W. D., E.-M. W. Koch, and M. Kühl. 2003. Diffusive boundary layers and photosynthesis of the epilithic algal community of coral reefs. *Marine Biology* 142:1073–1082.

Laubach, T., A. von Haeseler, and M. J. Lercher. 2012. TreeSnatcher plus: capturing phylogenetic trees from images. *BMC Bioinformatics* 13:110.

Leigh, E. G., R. T. Paine, J. F. Quinn, and T. H. Suchanek. 1987. Wave energy and intertidal productivity. *Proceedings of the National Academy of Sciences* 84:1314–1318.

Leonardos, N., B. Read, B. Thake, and J. R. Young. 2009. No mechanistic dependence of photosynthesis on calcification in the coccolithophorid *Emiliania Huxleyi* (haptophyta). *Journal of Phycology* 45:1046–1051.

Lindstrom, S. C., J. R. Hughey, and P. T. Martone. 2011. New, resurrected and redefined species of *Mastocarpus* (Phyllophoraceae, Rhodophyta) from the northeast Pacific. *Phycologia* 50:661–683.

Li, S., M. W. Cadotte, S. J. Meiners, Z. Hua, L. Jiang, and W. Shu. 2015. Species colonisation, not competitive exclusion, drives community overdispersion over long-term succession. *Ecology Letters* 18:964–973.

Litchman, E., P. de Tezanos Pinto, K. F. Edwards, C. A. Klausmeier, C. T. Kremer, and M. K. Thomas. 2015. Microbial giants: global biogeochemical impacts of phytoplankton in the past, present, and future. *Journal of* 103:1384-1396.

Litsios, G., L. Pellissier, F. Forest, C. Lexer, P. B. Pearman, N. E. Zimmermann, and N. Salamin. 2012. Trophic specialization influences the rate of environmental niche evolution in

damselfishes (Pomacentridae). *Proceedings of the Royal Society of London B: Biological Sciences* 279:3662–3669.

Littler, M. M., and D. S. Littler. 1980. The Evolution of thallus form and survival strategies in benthic marine macroalgae: field and laboratory tests of a functional form model. *The American Naturalist* 116:25–44.

Lobban, C., and P. Harrison. 1994. Seaweed Ecology and Physiology. Cambridge University Press.

Losos, J. B. 2008. Phylogenetic niche conservatism, phylogenetic signal and the relationship between phylogenetic relatedness and ecological similarity among species. *Ecology Letters* 11:995–1003.

Losos, J. B. 2011. Seeing the forest for the trees: the limitations of phylogenies in comparative biology. *The American Naturalist* 177:709–727.

Low-Décarie, E., G. F. Fussmann, and G. Bell. 2014. Aquatic primary production in a high-$CO_2$ world. *Trends in Ecology & Evolution* 29:223–232.

Lubchenco, J. 1983. *Littorina* and *Fucus*: effects of herbivores, substratum heterogeneity, and plant escapes during succession. *Ecology* 64:1116–1123.

Lubchenco, J., and S. D. Gaines. 1981. A unified approach to marine plant-herbivore interactions. i. populations and communities. *Annual Review of Ecology and Systematics* 12:405–437.

Maberly, S. C. 1990. Exogenous sources of inorganic carbon for photosynthesis by marine macroalgae. *Journal of Phycology* 26:439–449.

Maberly, S. C., J. A. Raven, and A. M. Johnston. 1992. Discrimination between $^{12}C$ and $^{13}C$ by marine plants. *Oecologia* 91:481–492.

MacArthur, R. H. 1965. Patterns of species diversity. *Biological Reviews* 40:510–533.

Machac, A., M. Janda, R. R. Dunn, and N. J. Sanders. 2011. Elevational gradients in phylogenetic structure of ant communities reveal the interplay of biotic and abiotic constraints on diversity. *Ecography* 34:364–371.

Maddison, W. ., and D. . Maddison. 2011. Mesquite: a modular system for evolutionary analysis. Version 2.75 http://mesquiteproject.org.

Marconi, M., M. Giordano, and J. A. Raven. 2011. Impact of taxonomy, geography, and depth on $\delta^{13}C$ and $\delta^{15}N$ variation in a large collection of macroalgae. *Journal of Phycology*

47:1023–1035.

McConnaughey, T. A., and J. F. Whelan. 1997. Calcification generates protons for nutrient and bicarbonate uptake. *Earth-Science Reviews* 42:95–117.

McCoy, S. J., and N. A. Kamenos. 2015. Coralline algae (Rhodophyta) in a changing world: integrating ecological, physiological, and geochemical responses to global change. *Journal of Phycology* 51:6–24.

McCoy, S. J., and C. A. Pfister. 2014. Historical comparisons reveal altered competitive interactions in a guild of crustose coralline algae. *Ecology Letters* 17:475–483.

McDevit, D. C., and G. W. Saunders. 2009. On the utility of DNA barcoding for species differentiation among brown macroalgae (Phaeophyceae) including a novel extraction protocol. *Phycological Research* 57:131–141.

Menge, B. A. 1976. Organization of the New England rocky intertidal community: role of predation, competition, and environmental heterogeneity. *Ecological Monographs* 46:355.

Mercado, J. M., F. L. Figueroa, F. Xauier Niell, and L. Axelsson. 1997. A new method for estimating external, carbonic anhydrase actmty in macroalgae. *Journal of Phycology* 33:999–1006.

Mercado, J. M., C. B. de los Santos, J. Lucas Pérez-Lloréns, and J. J. Vergara. 2009. Carbon isotopic fractionation in macroalgae from Cádiz Bay (Southern Spain): comparison with other bio-geographic regions. *Estuarine, Coastal and Shelf Science* 85:449–458.

Meyer, M., and H. Griffiths. 2013. Origins and diversity of eukaryotic $CO_2$-concentrating mechanisms: lessons for the future. *Journal of Experimental Botany* 64:769–786.

Middelboe, A. L., and P. J. Hansen. 2007. High pH in shallow-water macroalgal habitats. *Marine Ecology Progress Series* 338:107.

Mook, W. G., J. C. Bommerson, and W. H. Staverman. 1974. Carbon isotope fractionation between dissolved bicarbonate and gaseous carbon dioxide. *Earth and Planetary Science Letters* 22:169–176.

Morel, F., J. G. Hering, and F. Morel. 1993. Principles and applications of aquatic chemistry. Wiley, New York.

Moroney, J. V., N. Jungnick, R. J. DiMario, and D. J. Longstreth. 2013. Photorespiration and carbon concentrating mechanisms: two adaptations to high $O_2$, low $CO_2$ conditions. *Photosynthesis Research* 117:121–131.

Moulin, P., J. R. Andría, L. Axelsson, and J. M. Mercado. 2011. Different mechanisms of inorganic carbon acquisition in red macroalgae (Rhodophyta) revealed by the use of TRIS buffer. *Aquatic Botany* 95:31–38.

Murru, M., and C. D. Sandgren. 2004. Habitat matters for inorganic carbon acquisition in 38 species of red macroalgae (Rhodophyta) from Puget Sound, Washington, USA. *Journal of Phycology* 40:837–845.

Norden, N., S. G. Letcher, V. Boukili, N. G. Swenson, and R. Chazdon. 2012. Demographic drivers of successional changes in phylogenetic structure across life-history stages in plant communities. *Ecology*:S70–S82.

Oksanen, J., F. G. Blanchet, R. Kindt, P. Legendre, P. R. Minchin, R. B. O'Hara, G. L. Simpson, P. Solymos, M. H. H. Stevens, and H. Wagner. 2015. vegan: Community Ecology Package. R package version 2.0-10. 2013.

Orr, J. C., V. J. Fabry, O. Aumont, L. Bopp, S. C. Doney, R. A. Feely, A. Gnanadesikan, N. Gruber, A. Ishida, F. Joos, and others. 2005. Anthropogenic ocean acidification over the twenty-first century and its impact on calcifying organisms. *Nature* 437:681–686.

Padilla, D. K. 1989. Algal structure defenses: form and calcification in resistance to tropical limpets. *Ecology* 70:835–842.

Pagel, M. 1999. Inferring the historical patterns of biological evolution. *Nature* 401:877–884.

Paine, R. T. 1966. Endothermy in comb calorimetry. *Limnology and Oceanography* 11:126–129.

Paine, R. T. 1984. Ecological determinism in the competition for space: the Robert H. MacArthur award lecture. *Ecology* 65:1339–1348.

Paine, R. T., and S. A. Levin. 1981. Intertidal landscapes: disturbance and the dynamics of pattern. *Ecological Monographs* 51:145–178.

Paradis, E., B. Bolker, J. Claude, H. S. Cuong, R. Desper, B. Durand, J. Dutheil, O. Gascuel, C. Heibl, D. Lawson, V. Lefort, P. Legendre, J. Lemon, J. Nylander, R. Opgen-Rhein, A.-A. Popescu, K. Schliep, K. Strimmer, and D. de Vienne. 2014. ape: Analyses of Phylogenetics and Evolution.

Pfeil, B., A. Olsen, D. C. Bakker, S. Hankin, H. Koyuk, A. Kozyr, J. Malczyk, A. Manke, N. Metzl, C. L. Sabine, and others. 2012. A uniform, quality controlled Surface Ocean $CO_2$ Atlas (SOCAT). *Earth System Science Data Discussions* 5:735–780.

Pierrot, D. E. L., and D. W. R. Wallace. 2006. MS Excel Program Developed for $CO_2$ System

Calculations. ORNL/CDIAC-105a. Carbon Dioxide Information Analysis Center, Oak Ridge National Laboratory, U.S. Dept. of Energy, Oak Ridge, TN.

Posada, D., and K. A. Crandall. 1998. Modeltest: testing the model of DNA substitution. *Bioinformatics* 14:817–818.

Prasad, V., C. a. E. Strömberg, A. D. Leaché, B. Samant, R. Patnaik, L. Tang, D. M. Mohabey, S. Ge, and A. Sahni. 2011. Late Cretaceous origin of the rice tribe provides evidence for early diversification in Poaceae. *Nature Communications* 2:480.

Price, T. D., D. M. Hooper, C. D. Buchanan, U. S. Johansson, D. T. Tietze, P. Alström, U. Olsson, M. Ghosh-Harihar, F. Ishtiaq, S. K. Gupta, and others. 2014. Niche filling slows the diversification of Himalayan songbirds. *Nature* 509:222–225.

Rambaut, A., and A. J. Drummond. 2014. TreeAnnotator v2. 1.2. Edinburgh: University of Edinburgh, Institute of Evolutionary Biology.

Ratnasingham, S., and P. D. N. Hebert. 2007. BOLD: the barcode of life data system (www.barcodinglife.org). *Molecular Ecology Notes* 7:355–364.

Raven, J. 1997. Putting the C in phycology. *European Journal of Phycology* 32:319–333.

Raven, J. A., L. A. Ball, J. Beardall, M. Giordano, and S. C. Maberly. 2005. Algae lacking carbon-concentrating mechanisms. *Canadian Journal of Botany* 83:879–890.

Raven, J. A., and J. Beardall. 2014. $CO_2$ concentrating mechanisms and environmental change. *Aquatic Botany* 118:24–37.

Raven, J. A., J. Beardall, and M. Giordano. 2014. Energy costs of carbon dioxide concentrating mechanisms in aquatic organisms. *Photosynthesis Research* 121:111–124.

Raven, J. A., A. M. Johnston, J. E. Kübler, R. Korb, S. G. McInroy, L. L. Handley, C. M. Scrimgeour, D. I. Walker, J. Beardall, M. N. Clayton, M. Vanderklift, S. Fredriksen, and K. H. Dunton. 2002a. Seaweeds in cold seas: evolution and carbon acquisition. *Annals of Botany* 90:525 –536.

Raven, J. A., A. M. Johnston, J. E. Kübler, R. Korb, S. G. McInroy, L. L. Handley, C. M. Scrimgeour, D. I. Walker, J. Beardall, M. Vanderklift, S. Fredriksen, and K. H. Dunton. 2002b. Mechanistic interpretation of carbon isotope discrimination by marine macroalgae and seagrasses. *Functional Plant Biology* 29:355–378.

Reinfelder, J. R. 2011. Carbon concentrating mechanisms in eukaryotic marine phytoplankton. *Annual Review of Marine Science* 3:291–315.

Revell, L. J. 2012. phytools: an R package for phylogenetic comparative biology (and other things). *Methods in Ecology and Evolution* 3:217–223.

Roleda, M. Y., and C. L. Hurd. 2012. Seaweed Responses to Ocean Acidification. Pages 407–431 *in* C. Wiencke and K. Bischof, editors. Seaweed Biology. Springer Berlin Heidelberg.

Sabine, C. L., S. Hankin, H. Koyuk, D. C. Bakker, B. Pfeil, A. Olsen, N. Metzl, A. Kozyr, A. Fassbender, A. Manke, and others. 2012. Surface Ocean $CO_2$ Atlas (SOCAT) gridded data products. *Earth System Science Data Discussions* 5:781–804.

Sage, R. F., P.-A. Christin, and E. J. Edwards. 2011. The $C_4$ plant lineages of planet Earth. *Journal of Experimental Botany* 62:3155–3169.

Saunders, G. W., and T. E. Moore. 2013. Refinements for the amplification and sequencing of red algal DNA barcode and RedToL phylogenetic markers: a summary of current primers, profiles and strategies. *Algae* 28:31–43.

Schmittner, A., N. Gruber, A. C. Mix, R. M. Key, A. Tagliabue, and T. K. Westberry. 2013. Biology and air–sea gas exchange controls on the distribution of carbon isotope ratios ($\delta^{13}C$) in the ocean. *Biogeosciences* 10:5793–5816.

Silberfeld, T., J. W. Leigh, H. Verbruggen, C. Cruaud, B. de Reviers, and F. Rousseau. 2010. A multi-locus time-calibrated phylogeny of the brown algae (Heterokonta, Ochrophyta, Phaeophyceae): Investigating the evolutionary nature of the “brown algal crown radiation.” *Molecular Phylogenetics and Evolution* 56:659–674.

Silvertown, J. 2004. Plant coexistence and the niche. *Trends in Ecology & Evolution* 19:605–611.

Simberloff, D. S. 1970. Taxonomic Diversity of Island Biotas. *Evolution* 24:23–47.

Simpson, G. G. 1944. Tempo and mode in evolution. Columbia University Press.

Smith, M. A., W. Hallwachs, and D. H. Janzen. 2014. Diversity and phylogenetic community structure of ants along a Costa Rican elevational gradient. *Ecography* 37:720–731.

Sousa, W. P. 1979. Disturbance in marine intertidal boulder fields: the nonequilibrium maintenance of species diversity. *Ecology* 60:1225–1239.

Sousa, W. P. 1984. Intertidal mosaics: patch size, propagule availability, and spatially variable patterns of succession. *Ecology* 65:1918.

Steneck, R. S., and L. Watling. 1982. Feeding capabilities and limitation of herbivorous molluscs: a functional group approach. *Marine Biology* 68:299–319.

Stephenson, T. A., and A. Stephenson. 1972. Life Between Tidemarks on Rocky Shores. W.H. Freeman and Company, San Francisco.

Stepien, C. C. 2015. Impacts of geography, taxonomy and functional group on inorganic carbon use patterns in marine macrophytes. *Journal of Ecology* 103:1372–1383.

Stucky, B. J. 2012. SeqTrace: a graphical tool for rapidly processing DNA sequencing chromatograms. *Journal of Biomolecular Techniques: JBT* 23:90–93.

Surif, M. B., and J. A. Raven. 1989. Exogenous inorganic carbon sources for photosynthesis in seawater by members of the Fucales and the Laminariales (Phaeophyta): ecological and taxonomic implications. *Oecologia* 78:97–105.

Tilman, D. 1981. Resource competition and community structure. *Monographs in Population Biology* 17:1–296.

Truchot, J.-P., and A. Duhamel-Jouve. 1980. Oxygen and carbon dioxide in the marine intertidal environment: diurnal and tidal changes in rockpools. *Respiration Physiology* 39:241–254.

Verbruggen, H., C. A. Maggs, G. W. Saunders, L. Le Gall, H. Yoon, and O. De Clerck. 2010. Data mining approach identifies research priorities and data requirements for resolving the red algal tree of life. *BMC Evolutionary Biology* 10:16.

Verdú, M., and J. G. Pausas. 2007. Fire drives phylogenetic clustering in Mediterranean Basin woody plant communities. *Journal of Ecology* 95:1316–1323.

Webb, C. O., D. D. Ackerly, M. A. McPeek, and M. J. Donoghue. 2002. Phylogenies and community ecology. *Annual Review of Ecology and Systematics* 33:475–505.

Weiher, E., and P. A. Keddy. 1995. Assembly rules, null models, and trait dispersion: new questions from old patterns. *Oikos* 74:159–164.

Whittaker, R. H. 1960. Vegetation of the Siskiyou Mountains, Oregon and California. *Ecological Monographs* 30:279–338.

Wilbur, K. M., and N. G. Anderson. 1948. Electrometric and colorimetric determination of carbonic anhydrase. *Journal of Biological Chemistry* 176:147–154.

Wood, S. A., S. A. Lilley, D. R. Schiel, and J. B. Shurin. 2010. Organismal traits are more important than environment for species interactions in the intertidal zone. *Ecology Letters* 13:1160–1171.

Wootton, J. T. 1997. Estimates and tests of per capita interaction strength: diet, abundance, and impact of intertidally foraging birds. *Ecological Monographs* 67:45–64.

Wootton, J. T., and M. Emmerson. 2005. Measurement of interaction strength in nature. *Annual Review of Ecology, Evolution, and Systematics* 36:419–444.

Wootton, J. T., and J. D. Forester. 2013. Complex population dynamics in mussels arising from density-linked stochasticity. *PLOS ONE* 8:e75700.

Wootton, J. T., C. A. Pfister, and J. D. Forester. 2008. Dynamic patterns and ecological impacts of declining ocean pH in a high-resolution multi-year dataset. *Proceedings of the National Academy of Sciences* 105:18848 –18853.

Yessoufou, K., T. J. Davies, O. Maurin, M. Kuzmina, H. Schaefer, M. Bank, and V. Savolainen. 2013. Large herbivores favour species diversity but have mixed impacts on phylogenetic community structure in an African savanna ecosystem. *Journal of Ecology* 101:614–625.

Yoon, H. S., J. D. Hackett, C. Ciniglia, G. Pinto, and D. Bhattacharya. 2004. A molecular timeline for the origin of photosynthetic eukaryotes. *Molecular Biology and Evolution* 21:809–818.